Impact of silicon nutrition on barley plants under potassium deficiency or drought stress: Insight into transcriptional, hormonal and metabolic regulation

Dissertation
zur Erlangung des
Doktorgrades der Naturwissenschaften (Dr. rer. nat.)

der

Naturwissenschaftlichen Fakultät I
-Biowissenschaften-
der Martin-Luther-Universität
Halle-Wittenberg

Vorgelegt von

Frau Seyedeh Sara Beier
geb. Naseri Rad
geb. am 23.07.1985 in Iran, Ghazvin

begutachtet von

Prof. Dr. Nicolaus von Wirén (IPK, Gatersleben)
Prof. Dr. Edgar Peiter (Universität Halle-Wittenberg)
Prof. Dr. Klaus Dittert (Universität Göttingen)

verteidigt

am 26.01.2022
Halle (Saale), Germany

Dedicated:

To my beloved mom and dad,

who have always been great inspirations to me,

and taught me to go after my dreams!

Table of Contents

1 Summary **1**

2 Introduction **3**

2.1 Silicon in soil 3

2.2 Silicon transport in plants 3

2.3 Impact of silicon nutrition on plants 4

2.3.1 Protective role of silicon in salinity stress 5

2.3.2 Protective role of silicon under mineral elements toxicity 6

2.3.3 Protective role of silicon under mineral elements deficiency 6

2.3.4 Protective role of silicon under potassium deficiency 7

2.4 Potassium uptake and distribution in plants 8

2.5 Role of potassium in alleviating drought stress 10

2.6 Protective role of silicon under drought stress 12

2.7 Aim of present work 13

3 Materials and Methods **14**

3.1 Preparing monosilicic acid 14

3.2 Long-term potassium deficiency experiment 15

3.3 Short-term potassium starvation and rubidium flux measurements 15

3.4 Gibberellin experiment 16

3.5 Drought stress experiment 16

3.6 Relative water content 16

3.7 Chlorophyll measurements 16

3.8 Elemental analysis 17

3.9 Primary metabolite analysis 17

3.10 Soluble sugars and starch measurements 18

3.11 Free amino acids measurements 19

3.12 Phytohormone measurements 19

3.13 RNA isolation, cDNA synthesis and gene expression analysis 20

3.14 RNA sequencing and identification of differentially expressed genes 21

3.15 Statistical analysis 22

4 Results **23**

4.1 Impact of silicon application on plant growth under potassium deficiency 23

4.2 Impact of silicon application on the nutritional status of plants under potassium deficiency 24

4.3 Impact of silicon application on phytohormone homeostasis of plants under potassium deficiency 28

4.4 Impact of silicon application on metabolic changes of plants under potassium deficiency ... 34

4.5 Impact of silicon application on gene expression patterns of plants under potassium deficiency 40

4.6 Impact of silicon application on root uptake and root-to-shoot translocation of potassium in plants under potassium starvation 49

4.7 Effect of manipulated gibberellin biosynthesis on silicon-mediated mitigation of potassium deficiency 58

4.8 Impact of silicon application on plant growth under drought stress 62

4.9 Impact of silicon application on the nutritional status of plants under drought stress 64

4.10 Impact of silicon application on phytohormone homeostasis of plants under drought stress 67

5 Discussion 70

5.1 Silicon prevents long-term potassium deficiency responses by increasing internal potassium utilization and reconstituting hormonal and metabolite homeostasis 70

5.2 Silicon temporarily delays short-term potassium starvation responses by increasing internal potassium availability and *de novo* potassium uptake in roots 76

5.3 Silicon mediates drought tolerance by improving water content and reconstituting hormonal homeostasis 78

6 Conclusion 84

7 References 85

8 Annex 104

9 Abbreviations 109

10 Acknowledgements 111

11 Publications related to the submitted thesis 112

12 Curriculum Vitae 113

13 Declaration under oath / Eidesstattliche Erklärung 116

14 Declaration concerning criminal record and pending investigations / Erklärung über bestehende vorstrafen und anhängige Ermittlungsverfahren 117

1 Summary

Potassium (K) deficiency is one of the major abiotic stresses in agriculture that impairs plant growth and development. This problem relates to the essential role of K in many diverse processes in plants including photosynthesis, water balance, nutrient and assimilate transport, enzyme activation and stomatal regulation. Also, K provides osmotic adjustment and maintains cell turgor under conditions of water shortage. Low water availability under drought stress decreases total nutrient uptake and translocation in plants. In fact, both K deficiency and drought stress employ overlapping signaling pathways to induce adaptive responses, which indicates a tight connection between K deficiency and drought tolerance. Among the most sustainable approaches in crop protection and production is the application of silicon (Si), as beneficial element in plant nutrition, which has been shown to improve plant growth and increase tolerance to a wide range of biotic and abiotic stress conditions. Although previous studies have shown that Si supply can alleviate K deficiency and induce drought tolerance in a variety of plant species, processes underlying stress mitigation by Si have remained unclear. To elucidate the mechanistic role of Si in alleviating plants from low K stress, barley plants were subjected to long-term K deficiency or short-term K starvation in two separate hydroponic experiments in the presence or absence of Si. Physiological analyses revealed that under long-term low K conditions, Si nutrition improved adaptive responses through maintenance of higher chlorophyll concentrations and reconstituted hormonal homeostasis by increasing the level of growth-promoting hormones especially bioactive forms of cytokinins and gibberellins, while at the same time suppressing accumulation of stress-related hormones such as abscisic acid, salicylic acid and jasmonic acid. Moreover, Si improved phloem transport of sugars resulting in higher shoot and root biomass. However, the K nutritional status was hardly affected and except transcriptional upregulation of the vacuolar K exporter KCO1, most high- and low-affinity K transporters gene were downregulated by Si. These analyses showed that the main physiological target of Si-mediated stress mitigation was the shoot, as the K-deficient leaf transcriptome signature reverted back to adequate, while that of the root did not, and roots just profited from reconstituted metabolism and hormone homeostasis in the shoot. Under short-term K starvation, K uptake and re-/translocation processes were investigated using rubidium as a tracer for K transport processes. Nutrient measurements and gene expression analysis revealed that relative to the absence of Si, Si-supplied plants upregulated the root vacuolar K exporter KCO1 earlier, which temporary delayed induction of K transporter genes *HAK1* and *AKT1* and subsequent *de novo* K uptake for a few days and caused several-fold higher expression levels of K transporters as well as K uptake rates. At the same time, root K pools in Si-supplied plants became almost completely depleted, which was accompanied by higher root-to-shoot translocation rates of K and its tracer. Thus, these results indicated that Si application not only alters local K deficiency signaling in roots by modulating K transporter regulation but also enhances internal K mobilization from root-to-shoot under low K stress. To investigate the mechanistic role of Si in alleviating drought stress, barley plants were grown in soil and after suppling different doses of Si, they were subjected to drought stress. Nutrient

and phytohormone measurements in shoots of barley plants showed that only the highest Si supplementation level conferred drought tolerance and increased shoot biomass. This was mainly achieved via improved water content and reconstituted hormonal homeostasis in leaves, in particular by suppressed abscisic acid but increased cytokinins levels. However, Si hardly affected ion imbalances in shoot under drought stress. The observed prevention of growth retardation points to a general mode of action of Si under low K and drought stress, which may rely on an improved internal availability of limiting resources for the sake of improved photosynthesis and biomass gain primarily in the shoot. Altogether, this study reveals novel physiological processes and regulatory patterns conferred by Si under low K and drought stress, which can provide better understanding about the functions of Si and improve its application in plant production to foster sustainable agriculture.

2 Introduction

2.1 Silicon in soil

Silicon (Si) is the second most abundant element in the earth's crust after oxygen, with a mean share of 28.8 % (w/w) (Epstein, 1999). Depending on the soil fraction Si can occur in different forms (Sauer *et al.*, 2006). The majority of Si is fixed in the solid phase including crystalline forms such as silica (SiO_2) and silicate minerals (e.g., feldspar, mica, clay minerals), or amorphous forms such as phytoliths from plant residues (Farmer *et al.*, 2005; Řezanka and Sigler, 2008; Cornelis *et al.*, 2011). In the soil solution and below pH 9, Si occurs as an uncharged monomeric form, silicic acid (H_4SiO_4), which is weakly acidic and probably the only available form of Si for plant uptake (Weast *et al.*, 1983; Knight and Kinrade, 2001; Ma *et al.*, 2008). However, dissolved silicic acid in the soil solution can be adsorbed onto a variety of solid phases including clay particles, iron (Fe) or aluminum (Al) oxides/hydroxides and compete with other anions for sorption sites (Hansen *et al.*, 1994; Dietzel, 2002). Whereas most soils are abundant in Si, weathering and the mineral break-down release silicic acid (H_4SiO_4) leading to average concentrations of 0.1-0.6 mM in the soil solution (Knight and Kinrade, 2001). Therefore, plant-available Si is limited and depends on the type of soil minerals, environmental conditions, and long-term crop production, which actually withdraws substantial amounts of soluble Si (Datnoff *et al.*, 2001; Guntzer *et al.*, 2012).

2.2 Silicon transport in plants

All plants grown in soil will have some Si in their tissues. In particular graminaceous plant species, which generally accumulate Si to much higher levels than dicot species (Takahashi *et al.*, 1990), respond effectively to Si availability. Accordingly, higher plants have been classified as: (i) active Si accumulators with Si concentrations of 10-15% in their dry mass including wetland grasses, (ii) passive accumulators with Si concentrations of 1-3% in their dry mass like dryland grasses, and (iii) non-accumulators or Si-rejective plants with Si concentrations of <1% in their dry mass including dicots (Takahashi *et al.*, 1990; Ma and Takahashi, 2002). The differences in Si accumulation between species can be attributed to the different ability of their roots to take up Si. Basic mechanisms in Si acquisition and uptake into cells rely on Lsi1-type Si importers, belonging to nodulin 26-like intrinsic protein (NIP)-type water channels, which facilitate the passive transport of Si, and Lsi2-type exporters, belonging to a poorly characterized family of putative anion transporters (Ma and Yamaji, 2015). Polar localization of these two transporters at the endodermis, like in *Arabidopsis*, or at the exodermis and endodermis in some graminaceous species like rice allows building a concentration gradient that is most likely driven by the secondary active export of Si via a proposed anion/H^+ antiport at the proximal side of the cells, thus creating the main driving force for cellular Si export towards the vascular system (Ma and Yamaji, 2015). Notably in seminal roots of barley, HvLsi1 is localized in the plasma membrane on the distal side of epidermal and cortical cells (Chiba *et al.*, 2009), whereas HvLsi2 is exclusively expressed in the endodermis but there without polar localization (Mitani *et al.*, 2009). Such differences among graminaceous plant species in

Si transport pathways may reflect long-term adaptations to soil type and environment. After uptake by the roots via Lsi1 and Lsi2, Si is translocated to the shoot through the xylem. Lsi6, a homolog of Lsi1 in rice and barley, Lsi2 and its homolog Lsi3, are responsible for unloading Si from xylem sap into the nodes, whereas only Lsi6 is unloading Si into the leaves (Figure1; Ma and Yamaji, 2015; Yamaji *et al.*, 2015). Apart from these transporters, there are no other plant proteins identified to date that fulfil a biochemical function directly related to Si transport or metabolism through direct interaction with Si.

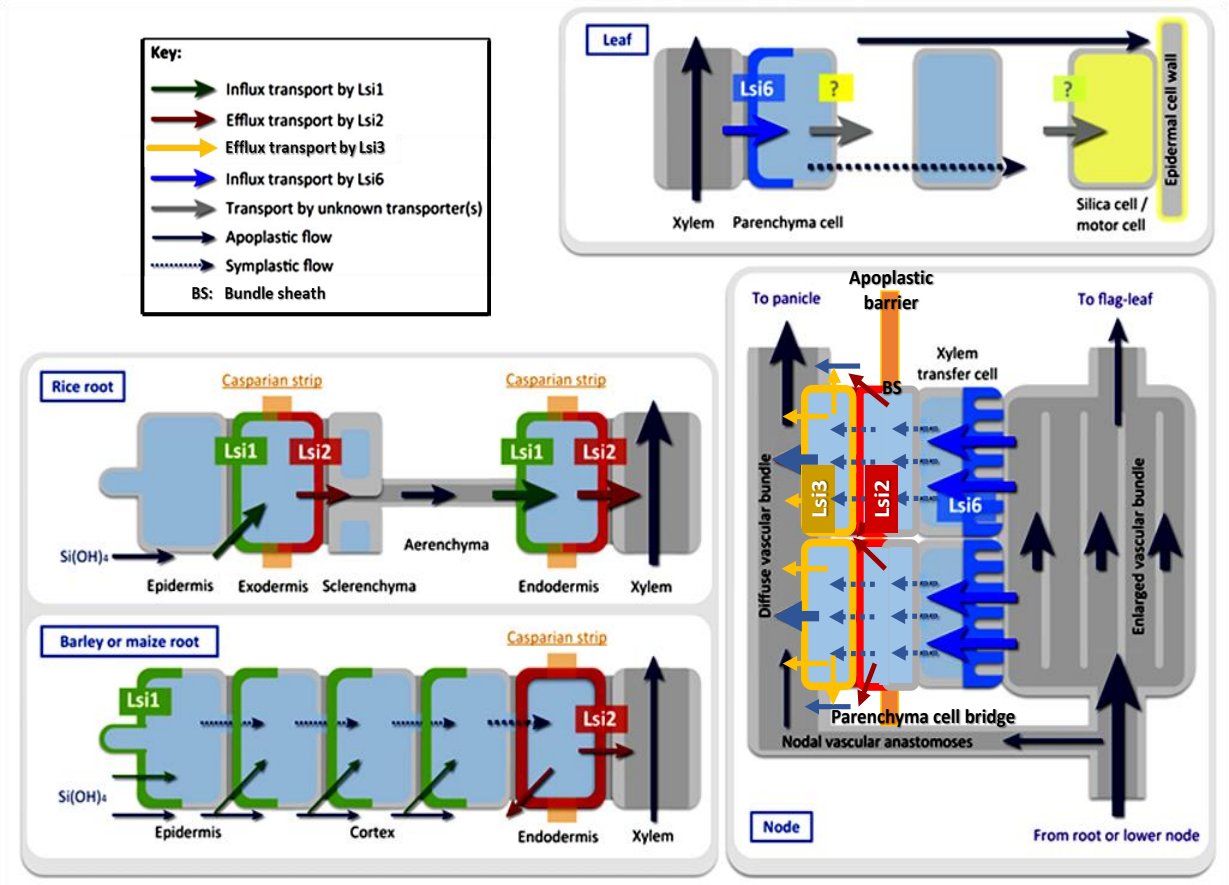

Figure 1. Proposed cooperated system of silicon (Si) transport for its uptake, xylem unloading, and distribution in plants. The work of Ma and Yamaji (2015) indicates that in rice roots, Si uptake is cooperatively mediated by Low Silicon 1 and 2 (Lsi1 and Lsi2), which are transport proteins localized at the distal and proximal side, respectively, of both exodermis and endodermis. By contrast, in barley and maize roots, Si uptake is also cooperatively mediated by Lsi1 and Lsi2, but localized at different cell layers. In leaves, Si in the xylem sap is unloaded by Lsi6. In nodes, Si in the xylem of enlarged vascular bundle is also unloaded by Lsi6, Lsi2 and Lsi3 localized at the parenchyma cell bridge. In barley, HvLsi2 is implicated in reloading Si to the xylem of the diffuse vascular bundle, but a similar transporter in rice has not been identified. Graph taken and modified from Ma and Yamaji (2015).

2.3 Impact of silicon nutrition on plants

Although Si is so abundant in the soil, it is not classified as an essential plant nutrient. For an element to be considered essential, three criteria must be met: (i) In the absence of this element plant must be unable to complete its lifecycle, (ii) the function of the element must not be replaceable by another element, and (iii) the element must be directly or indirectly

involved in plant metabolism (Arnon and Stout, 1939). Silicon has been shown to act as a beneficial nutrient that can promote plant growth in a variety of plant species and alleviate plants from certain biotic or abiotic stresses (Bélanger *et al.*, 2003; Flam-Shepherd *et al.*, 2018; Rémus-Borel *et al.*, 2009). Regarding the mode of action causing improvement under such a large variety of environmental stresses, Si has been suggested to protect plants through different scenarios.

2.3.1 Protective role of silicon in salinity stress

Salt stress is a major environmental limiting factor in plant growth and productivity (Hashemi *et al.*, 2010). In general, sodium (Na) enters roots passively, via non-selective cation channels and Na transporters, such as those of the HKT family that have high affinity for potassium (K) uptake (Leigh and Storey, 1993; Rubio *et al.*, 1995; Blumwald, 2000; Munns and Tester, 2008). Therefore, under high salt concentration, Na competes with K for influx into cells and alters the K/Na ratio (Niu *et al.*, 1995; Amtmann and Sanders, 1998; Blumwald, 2000). Consequently, higher intracellular Na levels change the ionic equilibrium, facilitate chloride (Cl) uptake, restrict the function of some enzymes (Niu *et al.*, 1995), and overproduce reactive oxygen species (ROS) (Flowers *et al.*, 1977; Greenway and Munns, 1980; Yeo, 1998). Interestingly, it was reported that Si affects transcript levels of membrane transporter genes under salt stress. For instance, Si decreased Na concentrations in the cytosol by enhanced activity of the plasma membrane Na^+/H^+-antiporter SOS1, the tonoplast Na^+/H^+-exchanger NHX1 or tonoplast-localized H^+-pyrophosphates, and enhanced K influx via K^+-H^+ symporters such as HAK1 in roots of barley (Liang *et al.*, 2005; 2006). Similarly, in sugarcane, Si reduced Na uptake and transport, and improved K concentrations in the shoot, which consequently raised the K/Na ratio of plants under salinity (Ashraf *et al.*, 2010).

It was reported that Si interacts with cell structures by increasing cell-wall binding of Na in salt-stressed wheat roots (Ahmad *et al.*, 1992; Saqib *et al.*, 2008), or in rice by deposition in the endodermis that restricts Na transport along the transpirational bypass route from root-to-shoot (Gong *et al.*, 2006). Likewise, Si stimulated lignin and suberin biosynthesis which form barriers to apoplastic Na transport in roots, correlating with higher salt tolerance in rice (Krishnamurthy *et al.*, 2011). It also has been suggested that Si mediates salt tolerance by reconstituting hormonal and metabolite homeostasis. Such a mode of action has been postulated, as Si stimulated the biosynthesis and accumulation of polyamines (e.g., putrescine, spermidine, and spermine) in salt-stressed sorghum plants (Yin *et al.*, 2016) to regulate K and Na transport, improve antioxidant capacity, and modify osmotic potentials (Kusano *et al.*, 2008; Alcázar *et al.*, 2010). Also, Si supply, in a dose- and time-dependent manner, alleviated salinity stress and decreased jasmonic acid (JA) levels but increased abscisic acid (ABA) concentrations via enhanced expression of ABA biosynthesis genes in rice (Kim *et al.*, 2014). Moreover, in a variety of salt-stressed plant species higher doses of Si increased endogenous bioactive gibberellins (GA) contents (Hwang *et al.*, 2007; Hamayun *et al.*, 2010; Lee *et al.*, 2010) or suppressed ethylene signaling (Yin *et al.*, 2016). However, the mechanism by which these changes occur is still unclear.

2.3.2 Protective role of silicon under mineral elements toxicity

Excessive levels of mineral elements can induce toxic effects, especially ROS formation, alter the metabolic activities and impair plant growth (Adriano, 2001). Silicon was reported to remediate mineral elements toxicity by decreasing the level of ROS via stimulating enzymatic ROS degradation and antioxidant production as brought about by enhanced ascorbate peroxidase, superoxide dismutase, and catalase activities under zinc (Zn) or manganese (Mn) toxicity in rice (Song *et al.*, 2011; Li *et al.*, 2012), lead (Pb) toxicity in cotton (Bharwana *et al.*, 2013), or boron (B) toxicity in wheat (Gunes *et al.*, 2007; Inal *et al.*, 2009). Silicon application also elevated activities of non-enzymatic antioxidants such as thiols to reduce the toxic effect of arsenic (As) in rice or induced exudation of low-molecular weight metabolites, like phenolic acids, to chelate and decrease Al absorption by maize roots (Kidd *et al.*, 2001; Tripathi *et al.*, 2013). Another proposed approach, by which Si alleviates an excess level of mineral elements in plants is via affecting nutrient uptake and translocation. In case of Zn or Mn toxicity, Si was reported to promote formation and co-localization of Zn-silicate in the cytoplasm or Mn-silicate in cell-wall, thus decreasing their mobilization and root-to-shoot translocation (Neumann and zur Nieden, 2001; Rogalla and Römheld, 2002; Che *et al.*, 2016). Likewise, it has been proposed that in rice plants treated with Si, suppression of transcript levels of membrane transporter genes for uptake and translocation of cadmium (Cd) or deposition of silica in the vicinity of the endodermis might be the possible mechanism by which Si can physically block the apoplastic bypass flow across the root and restrict the uptake of Cd (Shi *et al.*, 2005; Feng Shao *et al.*, 2017). Using the *lsi1* mutant in rice allowed showing that Si application reduced uptake and translocation of As due to the direct competition between Si and arsenite for the same influx transporter Lsi1 (Guo *et al.*, 2009). However, there is no further evidence explaining how Si alleviates mineral elements toxicities.

2.3.3 Protective role of silicon under mineral elements deficiency

Generally, plants suffering from mineral elements deficiencies show abnormalities with respect to their growth, development and productivity which makes them more susceptible to biotic and abiotic stresses (Marschner, 2012). A protective role of Si was reported against a variety of nutrient deficiencies and one of the common claims is that Si can influence the uptake capacity and root-to-shoot translocation rates in plants. For instance, Si application enhanced nitrogen (N) uptake by increasing the gene expression of high-affinity (*NRT2.1*) or low-affinity (*NRT1:1*) nitrate transporter in roots of N-starved rapeseed or N-deficient rice, respectively (Wu *et al.*, 2017; Haddad *et al.*, 2018). In an acid low-phosphorus (P) soil, Si supply upregulated the gene expression of the high-affinity P transporters *PHT1.1* and *PHT1.2* together with increased malate and citrate exudation, which led to enhanced P influx in roots of wheat plants (Kostic *et al.*, 2017). It has been proposed that the beneficial effect of Si on plant growth under P deficiency is attributed to enhanced availability of internal P through the decrease of excess Fe and Mn uptake (Ma, 2004). Also, Si application increased SO_4^{2-} uptake via increasing the expression of the SO_4^{2-} transporter gene *ST1;1* in roots of barley under combined sulfur (S) deficiency and osmotic stress (Maillard *et al.*, 2018). In iron-

deficient cucumber plants, Si supply increased the Fe pool in the root apoplast by enhanced accumulation of Fe-chelating compounds (e.g., organic acids and phenolics) together with upregulated genes involved in Fe(III) reduction (i.e., *HA1*, *FRO2*). In shoots, Si enhanced Fe re-mobilization from older to younger leaves via increased nicotianamine (NA) accumulation and upregulation of the transporter gene *YSL1* involved in phloem loading/unloading of the Fe-NA complex (Pavlovic *et al.*, 2013; 2016). Furthermore, it was reported that Si alleviates nutrient deficiency through altered metabolite and hormonal regulation, as it increased the levels of different forms of cytokinins (CK) and JA in maize plants under magnesium (Mg) deficiency. Silicon also enhanced the levels of polyamines and different amino acids such as gamma-aminobutyric-acid (GABA), serine and glycine, which overall contributed to Mg stress tolerance (Hosseini *et al.*, 2019). However, it has remained open whether Si directly or indirectly enhances the tolerance of plants to nutrient deficiencies.

2.3.4 Protective role of silicon under potassium deficiency

Among the most prominent nutrient deficiencies in agriculture is K deficiency, since plant's demand for K is high and K deficiency reduces plant growth, drought tolerance and crop resistance to pathogens (Liebersbach *et al.*, 2004; Pettigrew, 2008). These symptoms relate to the essential role of K in regulating enzyme activities, stabilizing membrane potentials or acting as osmotic substance affecting many diverse processes in plants, including photosynthesis, stomatal regulation, energy metabolism, protein synthesis, transport of sugars, water and nutrients (Amtmann *et al.*, 2008; Prajapati and Modi, 2012). Recent studies have reported that Si alleviates K deficiency by protecting cells from H_2O_2 accumulation and membrane lipid peroxidation through modulated activities of antioxidant enzymes in soybean (Miao *et al.*, 2010). Silicon also had positive effects on plant biomass and K concentration in leaves, stems and roots of soybean (Miao *et al.*, 2010). Furthermore, application of Si alleviated K deficiency-induced leaf chlorosis by decreasing the accumulation of putrescine in sorghum (Chen *et al.*, 2016a), or by delaying osmotic and K deficiency-induced leaf senescence via suppressing ABA biosynthesis genes and increasing the level of active cytokinins in barley (Hosseini *et al.*, 2017). At the same time, Si increased sugar transport from shoot-to-root that was impaired during K deficiency and enhanced root biomass in barley (Hosseini *et al.*, 2017). Another study in sorghum proposed that Si moderates K deficiency-induced plant dehydration via two strategies (Chen *et al.*, 2016b). On the one hand, Si enhanced the water conductivity by upregulating plasma-membrane intrinsic protein (PIP)-type aquaporin genes and by alleviating adverse effects of ROS on these transporters. On the other hand, Si increased root-to-shoot translocation of K by inducing the stelar K transporter gene *SKOR* in the xylem and by downregulating *HAK5* and *AKT1* genes in roots. Then, higher K concentrations in the xylem sap enhanced the osmotic gradient and hydraulic conductance. Despite such progress in the understanding Si-mediated responses at the physiological and biochemical levels, yet information on the mechanisms by which Si induces these responses is lacking.

2.4 Potassium uptake and distribution in plants

Root hairs contribute effectively to K uptake that primarily happens through the epidermis (Kochian and Lucas, 1983; Nieves-Cordones *et al.*, 2014). Influx of K into the root symplast is mainly mediated by K channels (e.g., AKT1 and KAT1), by carriers of the HAK/KUP family and by non-selective cyclic nucleotide gated channels (CNGC) (Hirsch *et al.*, 1998; Nieves-Cordones *et al.*, 2014; Li *et al.*, 2017). Then, K moves radially within the symplast using interconnecting plasmodesmata (PM) (Sanderson, 1983). Potassium can also cross the outer layers of the root via the apoplast but this pathway is blocked at the endodermis by the Casparian strip or the highly suberised structure of the endodermis which prevents uncontrolled water and nutrient delivery to the stelar tissues (Foster and Miklavcic, 2014). Later on, K release into the xylem occurs through the selective shaker-type K outward-rectifying channel SKOR, which is activated by membrane depolarization (Gaymard *et al.*, 1998; Gambale and Uozumi, 2006). A *skor* knockout mutant showed a reduced K content in shoot and xylem sap confirming its crucial role in K delivery from root-to-shoot (Gaymard *et al.*, 1998).

Phloem loading of K for recycling and sucrose loading is facilitated by another selective shaker-type K channel, called AKT2/3 (Deeken *et al.*, 2002). It was reported that AKT2/3 is expressed in the phloem of both source and sink tissues and that it can switch between inward- and non-rectifying states. This indicates that AKT2/3 is potentially able to mediate both, K influx and efflux and can be involved in both loading and unloading of phloem sap K in source and sink tissues, respectively (Lacombe *et al.*, 2000; Marten *et al.*, 1999). Generally, K is present in all cellular compartments of roots and shoots, while the majority of cellular K is deposited in the vacuole, where it is one of the main turgor providers (Hsiao and Lauchli, 1986). Potassium concentrations are maintained at 100-200 mM in the cytosol (Leigh and Wyn Jones, 1984), and chloroplasts (Schröppel-Meier and Kaiser, 1988), however, it varies between 10 to 200 mM in the vacuole (Hsiao and Lauchli, 1986). Potassium accumulation in the vacuole mainly occurs through the H^+-coupled antiporters, such as NHX, whereas vacuolar K release is either passive through TPK1-type channels (KCO1) under K deficiency, or active through H^+-coupled KUP/HAK transporters under K starvation (Walker *et al.*, 1996; Voelker *et al.*, 2006; Gobert *et al.*, 2007; Barragán *et al.*, 2012) (Figure 2).

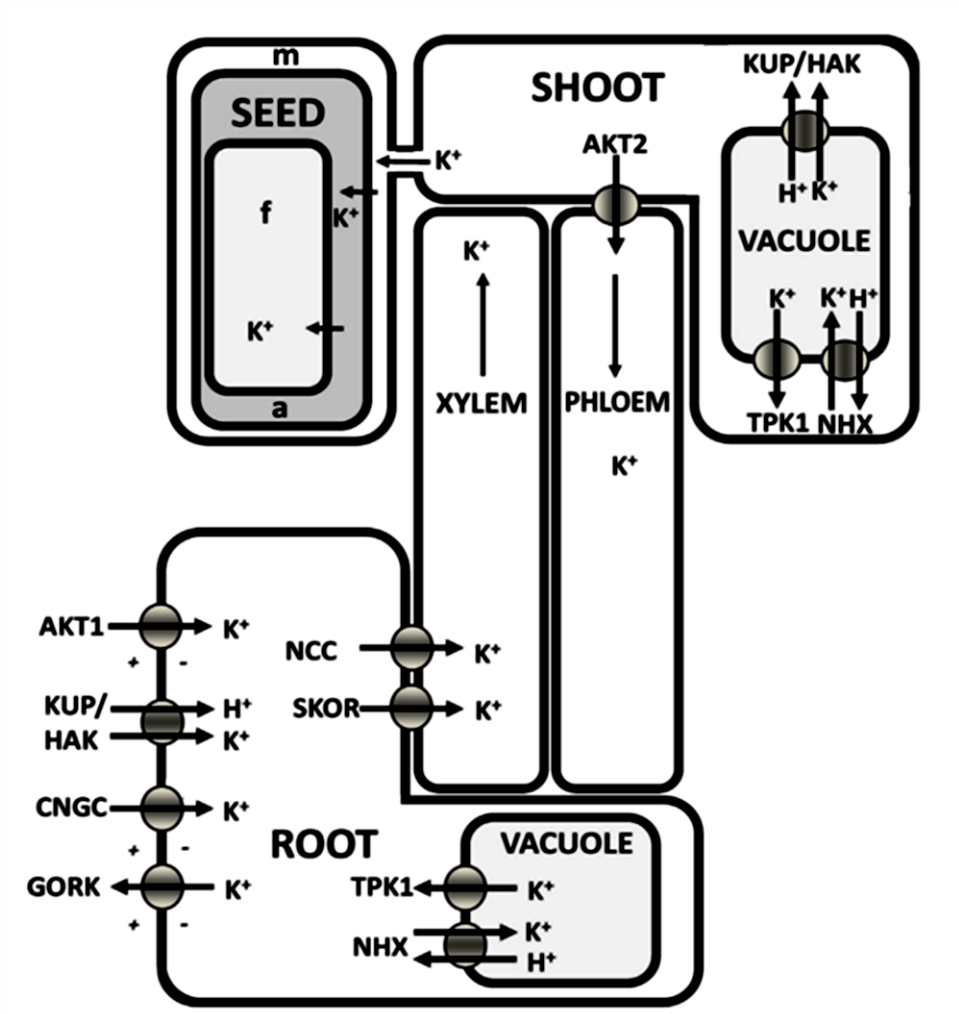

Figure 2. Proposed transport processes and proteins that are involved in K uptake, efflux and distribution in plants. At the external soil-root interface transport functions are shown for passive [AKT1 and CNGC (cyclic nucleotide gated channel)] and energized (KUP/HAK) K uptake and channel-mediated K release (guard cell outward-rectifying K channel; GORK); xylem loading mainly happens through K-selective (SKOR) and non-selective (NCC) cation channels. Phloem loading of K for recycling and/or sucrose loading may involve the AKT2 channel; vacuolar K accumulation is primarily driven by H^+-coupled antiporters such as NHX while vacuolar K release is either passive through TPK1-type channels (KCO1), or in K starvation conditions, active through H^+-coupled KUP/HAK transporters. Graph taken from Ahmad and Maathuis (2014).

2.5 Role of potassium in alleviating drought stress

Drought is one of the major stress factors limiting crop growth and production worldwide (Cruz de Carvalho, 2008). Under drought stress, an impairment of water uptake by roots results in hormonal, mostly ABA-controlled, chemical and hydraulic signaling towards shoots to close their stomata and prevent transpirational water loss which ultimately leads to a decrease in photosynthesis (Aroca *et al.*, 2012; Seiler *et al.*, 2014). Potassium, as an essential mineral element for plant growth, plays a pivotal role particularly in cell turgor, stomatal regulation and drought tolerance (Restrepo-Diaz *et al.*, 2008; Wei *et al.*, 2013; Cakmak, 2005). In fact, K increases the level of carbohydrates such as sugars and sugar alcohols via activating several enzymes in carbohydrate metabolism (e.g., starch synthase, pyruvate kinase, or phosphofructokinase) which provides osmotic adjustment and maintains cell turgor under conditions of water deficit (Seki *et al.*, 2007). Moreover, both K deficiency and drought stress induce a similar signaling pathway in plants (Figure 3). Under K deficiency enhanced ethylene biosynthesis triggers calcium (Ca) signaling via ROS overproduction which induces stomatal closure in leaves and promotes K uptake capacity by increasing K transporter activities in roots (e.g., AKT1 and HAK5) (Ashley *et al.*, 2006; Cheong *et al.*, 2007; Kim *et al.*, 2009; Kim *et al.*, 2010). Likewise, drought stress employs the same signal transduction chain provoking ROS production and Ca signaling via enhanced ABA biosynthesis, which also leads to the induction of K transporters and channels in roots and guard cells of leaves (Cheong *et al.*, 2007). By this way, drought stress additionally stimulates the induction of K deficiency responses to maintain transpiration and carbon assimilation under water shortage. It was reported that barley lines with a higher K nutritional status in flag leaf promoted ABA degradation and delayed drought-induced leaf senescence, which overall contributed to drought tolerance (Hosseini *et al.*, 2016). Also, an *AKT1*-overexpressing rice line showed less sensitivity to osmotic and drought stress by increased levels of K, especially in the root, confirming the crucial role of K in osmotic and drought stress tolerance (Ahmad *et al.*, 2016).

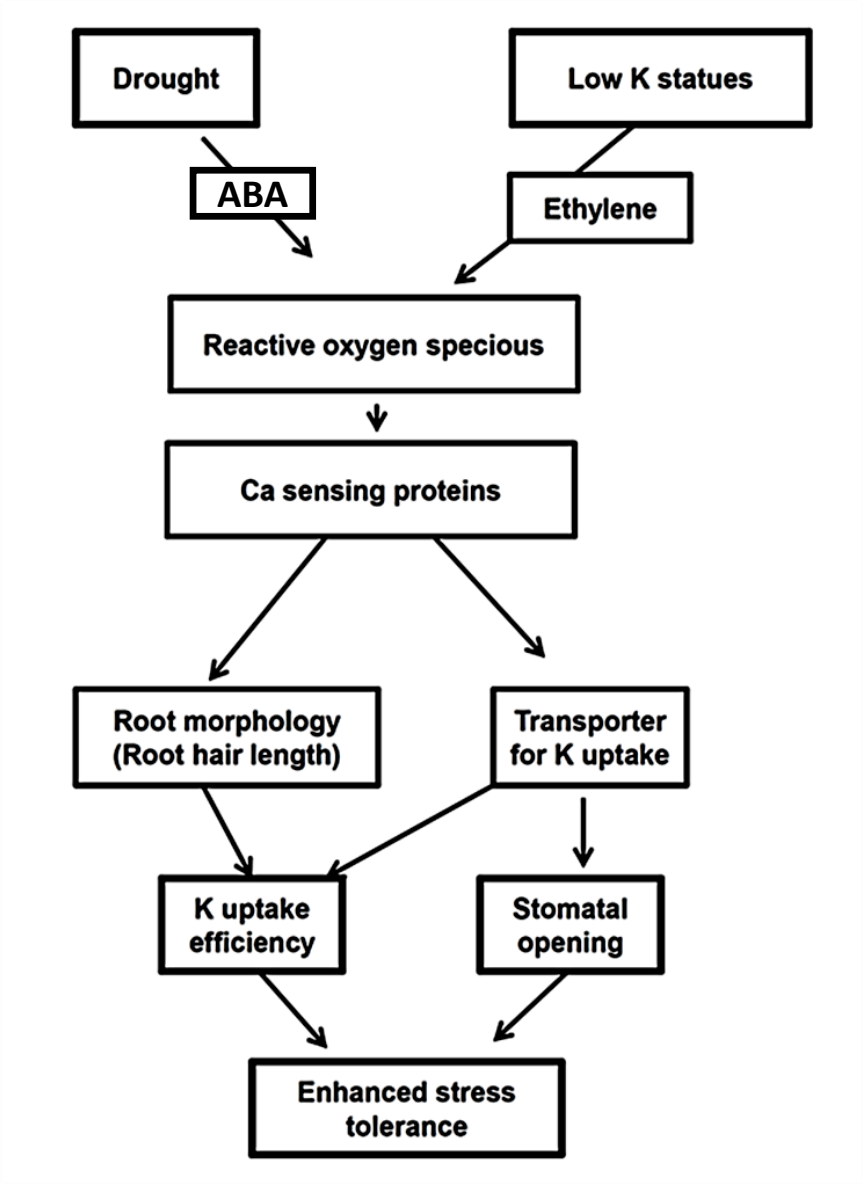

Figure 3. Proposed common signaling pathway induced by drought and a low K nutritional status of plants in the regulation of K uptake and drought stress tolerance. The work of Cheong and his colleagues (2007) indicates that K deficiency and drought employ the same signaling pathway for the induction of physiological and morphological responses. Drought induces ABA which leads to the generation of ROS, while under K deficiency ethylene formation enhances ROS levels. Then, ROS trigger Ca fluxes which lead to an enhanced K uptake capacity in roots as well as to an improved regulation of guard cells in leaves. Graph taken and modified from Cheong et al. (2007).

2.6 Protective role of silicon under drought stress

Among the abiotic stresses targeted by Si nutrition, Si-supplied plants were also reported to better tolerate drought stress (Shi *et al.*, 2016). So far, a long series of experiments spanning from hydroponically-grown plants to test mainly Si-dependent osmotic stress responses, or soil-grown plants in the greenhouse or on the field have provided compelling evidence for the reliable action of Si increasing drought tolerance. Thereby, Si has been supplied in different forms, ranging from purified mono-silicic acid to nano-sized, hydrophilic and pyrogenic Si dioxide, indicating that many different forms of Si and application procedures can be effective in drought stress alleviation (Haghighi *et al.*, 2013; Cao *et al.*, 2017). Regarding the mode of Si action, different mechanisms have been proposed, which strongly depend on the type of measures and analyses that have been conducted. A meta-analysis conducted on Si-related studies showed that in many cases Si increased photosynthesis and net carbon (C) assimilation rates, and decreased oxidative stress markers, which did not necessarily correlate with increasing antioxidant production (Cooke and Leishman, 2016). However, in tomato, Si mitigated drought-induced oxidative stress by activating antioxidant enzymes and decreasing malondialdehyde concentrations (Shi *et al.*, 2014).

Besides enhancing antioxidant defence capacity, Si application affects transpiration and water content under drought or osmotic stress, but this effect can vary largely and depends on species, stress intensity and environmental conditions (Coskun *et al.*, 2016). For example, in rice, Si decreased the transpiration rate by approx. 30% via deposition beneath the cuticle of leaves forming a Si-cuticle double layer (Ma *et al.*, 2001). By contrast, in sorghum, Si increased transpiration rate, root and whole-plant hydraulic conductance, leaf water content, and stomatal conductance via increased expression of PIP-type aquaporins under osmotic stress (Liu *et al.*, 2014; 2015). Increased root hydraulic conductance and water transport may also be attributed to Si-induced reductions in oxidative stress and membrane damage, or to adjustment of the cell's osmotic potential through increased osmolyte accumulation such as proline, soluble sugars, and inorganic ions (Pei *et al.*, 2010; Sonobe *et al.*, 2010; Ming *et al.*, 2012; Liu *et al.*, 2014; Shi *et al.*, 2016). In tall fescue, Si deposition on guard cells was reported to increase stomatal sensitivity by modulating K efflux thereby decreasing stomatal conductance (Vandegeer *et al.*, 2020).

Although many of these reported plant responses belong to those typically regulated by the major drought stress-related phytohormone ABA, there are only few reports that investigated a direct relation between Si, ABA and other hormones under drought stress. For instance, Si application either increased or decreased shoot ABA levels in wheat plants subjected to a polyethylene glycol (PEG) treatment (Xu *et al.*, 2017). Also, Si nutrition decreased ABA levels via suppressing ABA biosynthesis genes in shoots of barley under combined osmotic stress and K deficiency or osmotic stress and S deficiency (Hosseini *et al.*, 2017; Maillard *et al.*, 2018). Thus, there is currently not enough understanding whether and to what extent the Si-induced drought stress responses in plants depend on ABA biosynthesis or signalling.

2.7 Aim of present work

So far, several reports have provided strong evidence that Si application can increase the tolerance to K deficiency or drought stress. However, all previous studies are based on correlative evidence and do not provide a mechanistic understanding of the underlying processes or even the sequence of processes leading to stress mitigation by Si. Although some progress has been made in the understanding of components involved in Si-mediated tolerance at the physiological and biochemical level, yet information on the molecular aspect is still lacking. Since transcriptome analysis is an important approach that can help elucidate the regulatory mechanisms of Si action in plants, it was also employed here to provide a basis for dissecting the whole picture of Si-mediated processes that provide tolerance to potassium deficiency or drought stress. Thus, the present thesis addresses the following main questions:

- By which physiological processes can Si supply alleviate plants from K deficiency and drought stress?
- What are the molecular mechanisms by which Si nutrition mitigates K deficiency and enhances drought tolerance?

To address these questions, barley was chosen as the target plant because as a graminaceous species it benefits well from Si supply and some Si transport mechanisms in barley have already been characterized (Ma and Yamaji, 2015). The first chapter describes a hydroponic experiment with wild-type barley subjected to K deficiency in the presence or absence of Si to analyze the longer-term impact of Si nutrition on physiological and molecular responses to K deprivation. Here, a special emphasis was laid on the nutritional traits, phytohormone analyses and on a transcriptome study to uncover genes involved in the molecular mechanisms promoted by Si. The subsequent chapter describes a rubidium (Rb) uptake experiment, which was designed to assess how Si regulates the K uptake capacity of roots and the root-to-shoot translocation as well as the underlying K transporters under K starvation. As evidence was found for a role of gibberellins in Si-mediated alleviation of K deficiency, a further experiment was conducted with GA_{20} oxidase-defective barley lines. The last part addresses the role of Si in drought tolerance. Here, a soil experiment was performed with wild-type barley subjected to drought stress in the presence or absence of Si to investigate the impact of Si nutrition on nutrient and hormone homeostasis under water shortage. The final discussion emphasizes beneficial aspects of Si nutrition on both, K deficiency and drought stress.

3 Materials and Methods

3.1 Preparing monosilicic acid

Monosilicic acid (H_2SiO_4), was freshly prepared according to Sonobe et al. (2009) by passing sodium metasilicate nonahydrate ($Na_2O_3Si.9H_2O$; Sigma, Germany) solution through a column filled with a cation-exchange resin. 80 g of amberlite IR120 hydrogen form (Sigma, Germany) was weighted and loaded into the chromatography column. Since amberlite is a gel-type acidic cation exchange resin, it was washed several times with de-ionized water (Milli-Q® Reference System, Merck, Germany) until the pH reached to 6.5-7. Afterwards, 25 g of Na_2SiO_3 was diluted in 900 mL de-ionized (Milli-Q) water and added to the resin. When Na_2SiO_3 was slowly passed through the resin and the eluate was collected, the column was rinsed twice with 100 mL of de-ionized (Milli-Q) water (Figure 4). At the end, the monosilicic acid and sodium concentration were measured by Inductively Coupled Plasma-Optical Emission Spectroscopy technique (ICP-OES; iCAP 7400 duo OES Spectrometer; Thermo Fisher Scientific) and stored in plastic containers at 4°C.

Figure 4. Preparing monosilicic acid (H_2SiO_4) from sodium metasilicate nonahydrate ($Na_2O_3Si.9H_2O$) by column chromatography. The column was filled with amberlite that adsorbed sodium through the cation exchange process.

3.2 Long-term potassium deficiency experiment

Barley seeds (*Hordeum vulgare* L.), variety Irina, were germinated on vermiculite for three days in the dark and additional four days under light conditions. Thereafter, uniform seedlings (of 10 ± 0.5 cm height) were selected and transferred to 5 L plastic pots in a climate-controlled growth chamber that was set to a 16/8 h day/night cycle at a day/night temperature of 20/18°C with 65% relative humidity. Plants were divided into two batches: (i) K-sufficient plants were grown in a full nutrient solution: $Ca(NO_3)_2$ 2 mM, K_2SO_4 2 mM, $MgSO_4$ 0.5 mM, $NH_4H_2PO_4$ 0.5 mM, $CaCl_2$ 0.5 mM, H_3BO_3 0.001 mM, $MnSO_4$ 0.0025 mM, $ZnSO_4$ 0.0005 mM, $CuSO_4$ 0.0002 mM, $(NH_4)_6Mo_7O_{24}$ 0.00001 mM and Fe-EDTA 0.1 mM, while (ii) K-deficient plants were grown in the same solution but with a lower concentration of 0.04 mM K_2SO_4. In Si treatment of the long-term K-deficiency experiment, monosilicic acid was supplied to the culture solution at a concentration of 1.78 mM from the beginning of hydroponic culture. The nutrient solution was buffered to pH 5.9 and renewed every 2 days and continuously aerated. After 24 days, roots and the last fully expanded leaves of eight independent biological replicates, each consisting of three plants from the same treatment, were separately harvested and immediately frozen in liquid nitrogen and stored at −80°C for further analyses. Sixteen independent samples from each treatment were harvested, eight for dry weight (DW) and the other eight for chlorophyll measurements.

3.3 Short-term potassium starvation and rubidium flux measurements

Seed germination and growth conditions were as described above. After seven days of germination, plants were subjected to three nutrient regimes for a period of 12 days: (i) K-sufficient nutrient solution without monosilicic acid, (ii) K-free nutrient solution without or (iii) K-free nutrient solution with 1.78 mM monosilicic acid. For Rb influx measurements, 6 plants from each treatment were transferred for 1 min to $CaSO_4$ in order to stabilize the apoplastic ionic environment, followed by incubation in 1 mM RbCl for 10 min, and transferred again for 1 min to 1 mM $CaSO_4$ to wash-out Rb from the root apoplast. Afterwards, the shoots and roots of six independent samples from each treatment were harvested separately, immediately frozen in liquid nitrogen and stored at −80°C for nutrient and gene expression analyses. Another six independent samples from each treatment were harvested for DW measurements. Root influx was calculated using the following equation:

$$Root\ influx = \frac{\frac{(A \times C) + (B \times D)}{C}}{10\ (min)}$$

$$Root - to - shoot\ translocation\ of\ Rb\ = \frac{\frac{(B \times D)}{C}}{10\ (min)}$$

where A is Rb concentration in root, B is Rb concentration in shoot, C is root dry weight, and D is shoot dry weight.

3.4 Gibberellin experiment

Seeds of barley wild-type, variety Golden Promise, and of three independent *GA_{20}-oxidase2* mutated lines were germinated and grown as described before. The *GA_{20}-oxidase2* gene was knocked out in transgenic lines by a CRISPR/Cas9 approach (Jochen Kumlehn, IPK, pers. comm.). Then, plants were grown in K-free nutrient solution either in the absence or presence of monosilicic acid for 14 days. Afterwards, the shoots and roots of five independent plants from each treatment were separately harvested and immediately frozen in liquid nitrogen and stored at −80°C for nutrient and hormonal analyses. Another five plants from each treatment were harvested for DW measurements.

3.5 Drought stress experiment

Seeds of barley wild-type, variety Irina, were germinated as described before. Thereafter, seedlings were transferred to 5 L plastic pots containing 50% sand and 50% peat-based growth substrate (Substrate 2, Klasmann Deilmann GmbH, Germany) in a greenhouse that was illuminated in a 16/8 h day/night cycle at a day/night temperature of 20/15°C with 60% relative humidity and sufficient water. Plants were divided into five batches and every 7 days supplied with: (i) 0 mg/5L pot (0 mL), (ii) 250 mg/5L pot (115 mL), (iii) 500 mg/5L pot (230 mL), (iv) 750 mg/5L pot (345 mL), or (v) 1000 mg/5L pot (461 mL) of monosilicic acid for 3 weeks by maintaining the same water content in the substrate. Thereafter, plants in each Si treatment were divided into two further batches and (i) continued to remain well-watered, or (ii) subjected to drought stress for 2 more weeks. During the drought-stress treatment, the soil moisture content was monitored every day using the moisture meter (Delta T Devices Ltd., England). After 35 days, the last fully expanded leaves of eight independent biological replicates were separately harvested and immediately frozen in liquid nitrogen and stored at −80°C for further analyses. Eight independent shoot samples from each treatment were harvested for DW, relative water content (RWC), and chlorophyll determination.

3.6 Relative water content

The Relative water content (RWC) was determined in the last fully expanded leaves. The fresh weight (FW) of the last fully expanded leaves was recorded immediately after harvest and floated in a petri dish containing distilled water and the petri dish was kept at 4°C overnight. The turgid weight (TW) was recorded the next day after gently wiping the sample with tissue paper to remove the water adhering to the sample. Finally, the leaves were oven-dried at 65°C for 24 h and DW were recorded. The RWC was calculated using the formula RWC (%) = [(FW-DW) / (TW-DW)] x 100.

3.7 Chlorophyll measurements

Chlorophyll concentrations were determined in the last fully expanded leaves following the protocol of Porra *et al.* (1989). 30 mg of fresh flag leaf material were incubated at 4°C for 48 h in N,N'-dimethyl formamide (Merck). The samples were centrifuged at 14000 rpm for 2 min

and the absorbance at 647 nm and 664 nm was determined in a photometer (BIO-TEC, UVLKONxl, Germany). Then, total chlorophyll concentrations were calculated using the formula described by Porra *et al.* (1989).

3.8 Elemental analysis

The shoot and root samples were dried at 65°C for 72 h, ground and digested with 2 mL of concentrated HNO_3 (67-69%, Bernd Kraft, Germany) in polytetrafluoroethylene vials in a pressurized microwave digestion system (UltraCLAVE IV; MLS GmbH, Leutkirch, Germany). Digested samples were transferred to Greiner centrifuge tubes and diluted with de-ionized (Milli-Q) water to a final volume of 15 mL. Then, elemental analysis was performed by ICP-OES. Rubidium concentration was measured by Inductively Coupled Plasma-Mass Spectrometry (ICP-MS; ELEMENT-2, Thermo Fisher Scientific). For silicon determination, 25 mg of dry ground leaf or root material was weighted into 15 mL centrifuge tubes (Greiner Bio-One GmbH, Germany). The samples were prepared according to the method of Guntzer *et al.* (2010) with minor modifications. Briefly, 0.1 M tiron solution was prepared by weighing 33.2 g of tiron into a plastic container, adding 800 mL ultra-pure water, and buffering at pH 10.5 by 10 M NaOH solution. Then 8 mL of 0.1 M tiron solution were added to each sample including blanks (empty tubes). All samples were placed in a water bath under horizontal shaking at 85°C for 1 h. To ensure complete silicon extraction, samples were let for additional 4 h in a Minitron incubator shaker (Infors-HT, Germany) at 65°C and 300 rpm. The sample tubes were then cooled and 7 mL 30% H_2O_2 were added to destroy tiron. Afterwards samples were shaken at 85°C in a water bath until they became colorless. Before analysis, samples were centrifuged (5810 R Centrifuge, Eppendorf, Germany) for 10 min at 25°C and 4000 rpm. Supernatants were transferred to clean tubes. Silicon concentration was measured by ICP-OES. For sample introduction, a 4DX prepFAST auto-dilution system (ESI Elemental Service & Instruments GmbH, Mainz, Germany) was coupled to the ICP-OES. The light emitted at 251.6 nm wavelength was measured to determine Si concentrations using an external calibration curve. Yttrium was used as internal standard.

3.9 Primary metabolite analysis

Extraction of primary metabolites was carried out essentially as described in Ghaffari *et al.* (2016). Briefly, 100 mg of frozen shoots and roots of barley plants were mixed with 1 mL extraction buffer containing chloroform/methanol in a ratio of 1:1 (V/V) and shaken at 4°C for 20 min. After adding 300 µL HPLC-grade water, samples were centrifuged at 14000 rpm at 4°C for 10 minutes and the supernatant transferred to a new Eppendorf tube and dried in a speed vac (Christ RVC2-33IR, Germany) for 2 h at 35°C. The pellet was re-suspended in 300 µL HPLC-grade water and used immediately for the identification and quantification of desired compounds by ion chromatography coupled to mass spectrometry (IC-MS-MS). The IC-MS-MS instrumentation consisted of a Dionex ICS 5000 (Thermofisher, Dreieich, Germany) coupled with a 6490 triple quad MS-MS (Agilent, Waldbronn, Germany). Anionic compounds were separated on a 250×2 mm AS11-HC column (Thermofisher/Dionex) connected to a 10×2

mm AG 11-HC guard column (Dionex) and an ATC-1 anion trap column. The gradient was produced with H_2O (buffer A; HPLC-grade water) and KOH which was generated by an EGCIII KOH eluent generator cartridge. The column was equilibrated with a mixture of buffer A (96%) and 4% KOH at a flow rate of 0.38 mL min^{-1} and heated to 37°C during the measurement. The gradient was produced by changes of KOH concentrations as follows: 0–4 min: 4%; 4–15 min: 15%; 15–25 min: 25%; 25–28 min: 50%; 28–31 min: 80% and 31-40 min: 4%. Electron spray ionization (ESI)-MS/MS parameters were set as follows: gas temperature 350°C, drying gas flow rate 12 l min^{-1}, nebulizer pressure 35 psi, capillary voltage ± 3.5 kV. The fragmentor voltage and collision energy were optimized for each compound individually by tuning standards with a defined concentration. Primary metabolites were detected in the negative ion mode using multiple reactions monitoring (MRM). The data were extracted using the MassHunter software version B.03.01 (Agilent Technologies, Waldbronn, Germany). ^{13}C-pyruvate was used to normalize the data and added to each sample as internal standard before analysis.

3.10 Soluble sugars and starch measurements

Soluble sugars and starch were determined according to Ahkami *et al.* (2009). 50 mg frozen fully expanded leaves and roots material was homogenized in liquid nitrogen, dissolved in 0.75 mL 80% (v/v) ethanol and incubated at 80°C for 60 min. Crude extracts were centrifuged at 14,000 rpm at 4°C for 5 min and the upper phase was concentrated in a speed vacuum concentrator (Christ, RVC 2-33 IR, Germany) at 45°C for 120-180 min. The pellet was re-suspended in 0.3 mL HPLC-grade water and shaken for 15 min at 4°C before the measurement. Then, soluble sugars, glucose (Glc), fructose (Fru) and sucrose (Suc) were determined sequentially with a microplate reader. Next, 10-20 µL samples were added to 280 to 290 µL buffer containing 100 mM imidazol-HCl, pH 6.9, 5 mM $MgCl_2$, 2 mM NAD and 1 mM ATP. Prior to baseline recording, 1 µL Glc6P-dehydrogenase (diluted 1:1, 1-2 units in the same buffer) was added to each sample. Baseline was recorded for 10 to 15 min followed by the addition of 1 µL hexokinase (diluted 1:2, 0.75-1.5 units) to measure glucose. After reaching the maximum OD, 1 µL phosphoglucoisomerase (diluted 1:3, 0.35-0.7 units) was added to measure fructose and finally 1-2 µL fructosidase (or invertase 10 mg/50 µL buffer, ca. 60 units) was added to measure sucrose. For starch determination, the remaining pellet from soluble sugars extraction was washed twice with pure ethanol. The supernatant was discarded after centrifugation (2 min, 14000 rpm) and pellets were dried for 30 min under a hood or in a speed vac for 15 min. Subsequently, 200 µL 0.2 N KOH were added to the pellets, mixed thoroughly and incubated overnight at 4°C to break the starch chain into small pieces. Next day, another 200 µL 0.2 N KOH was added to each sample before it was incubated at 95°C for 60 min. After cooling down the samples, they were neutralized by 70 µL of 1 N acetic acid. Supernatant was digested by adding 50 µL of a buffer containing 7 U/mg amyloglucosidase in 50 mM NaAc, pH 5.2 to 50 µL of sample and incubated together over night at 37°C or alternatively for 5 h at 55°C. Produced glucose was measured as described by Hajirezaei *et al.* (2000).

3.11 Free amino acids measurements

Free amino acids were extracted as described for sugars and starch analysis. To detect primary and secondary amino acids, the fluorescing reagent AQC (6-aminoquinolyl-N-hydroxy-succinimidylcarbamate) was used. AQC was dissolved in 3 mg mL^{-1} of acetonitrile and incubated at 55°C for 10 min. 10 µL of sugar extracts were derivatized in a cocktail containing 10 µL of the fluorescing reagent AQC and 80 µL 0.2 M boric acid buffer (pH 8.8) in a final volume of 100 µL. The solution was incubated at 55°C for 10 min. Separation of soluble amino acids was performed on a newly developed UPLC-based method using ultra pressure reversed phase chromatography (UPLC; AcQuity H-Class, Waters GmbH, Eschborn, Germany). The UPLC system consisted of a quaternary solvent manager, a sample manager-FTN, a column manager and a fluorescent detector (PDA eλ Detector). The separation was carried out on a C18 reversed phase column (ACCQ Tag Ultra C18, 1.7 µm, 2.1x100 mm) with a flow rate of 0.7 mL min^{-1} and duration of 10.2 min. The column was heated at 50°C during the whole run. The detection wavelengths were 266 nm for excitation and 473 nm for emission. The gradient was accomplished with four solutions prepared from two different buffers purchased from Waters GmbH (eluent A concentrate and eluent B for amino acid analysis, Waters GmbH Germany). Eluent A was pure concentrate, eluent B was a mixture of 90% LCMS water (Geyer GmbH, Germany) and 10% eluent B concentrate, eluent C was pure concentrate (eluent B for amino acid analysis) and eluent D was LCMS water (Th. Geyer GmbH & Co. KG, Germany). The column was equilibrated with eluent A (10%) and eluent C (90%) for at least 30 min. The gradient was produced as follows: 0 min 10% A and 90% C / 0.29 min 9.9% A and 90.1% C / 5.49 min 9% A, 80% B and 11% C / 7.1 min 8% A, 15.6% B, 57.9% C and 18.5% D / 7.3 min 8% A, 15.6% B, 57.9% C and 18.5% D / 7.69% 7.8% A, 70.9% C and 21.3% D / 7.99 min 4% A, 36.3% C and 59.7% D / 8.68 min 10% A, 90% C / 10.2 min 10% A and 90% C. Chromatograms were recorded and quantification was carried out using the software program Empower Pro.

3.12 Phytohormone measurements

For phytohormone analysis, separately harvested shoots and roots were ground in liquid nitrogen. Samples of ca. 30 mg (fresh weight) were weighed into 2 mL safe lock tubes (Eppendorf AG, Germany) and kept at -80°C until analysis. Empty tubes were used as blanks. Before extraction, two 3 mm ceria-stabilized zirconium oxide beads were placed into each tube. The samples were extracted and purified as described in Šimura *et al.* (2018) with minor modifications. For phytohormone extraction 1 mL ice-cold 50% aqueous (v/v) ACN (Th. Geyer GmbH & Co. KG, Germany) containing the internal standards (OlChemim s.r.o, Czech Republic) was added to each tube. Samples were homogenized in a MM 301 vibration mill (Retsch GmbH, Germany) operating at a frequency of 27 Hz for 5 min and afterward sonicated for 3 min at 4°C using a Sonorex ultrasonic bath (BANDELIN electronic GmbH, Germany). Samples were subsequently extracted using a Reax 32 overhead shaker (Heidolph Instruments GmbH, Germany) for at least 30 min. After centrifuging for 10 min at 14000 rpm and 4°C (CT 15 RE centrifuge, Himac, Japan), the supernatant was transferred to clean Eppendorf tubes. All samples were purified using Oasis PRIME HLB RP (1 cc per 30 mg),

polymer-based SPE cartridges (Waters Co., USA). After loading the supernatant, the flow-through fraction was collected in a clean tube. The cartridge was then rinsed with 1 mL 30% (v/v) ACN, and this fraction was collected in the same tube as the flow-through fraction. After this single-step SPE, the samples were evaporated to dryness at 45°C in a RVC 2-33 IR vacuum concentrator (Martin Christ GmbH, Germany) and stored at −20°C until analysis. For UHPLC-ESI-MS-MS analysis, the samples were dissolved in 50 µL of 30% ACN (v/v) and transferred to insert-equipped vials. The absolute quantification of targeted phytohormones was performed as described in Eggert and von Wirén (2017). 10 µL of purified extracts were injected into an Acquity Ultra-performance LC system coupled with a Xevo TQ mass spectrometer (Waters, USA). The targeted analytes were separated on an Acquity UPLC® BEH C18 1.7 µm, 2.1 × 100 mm column coupled to a VanGuard pre-column BEH C18 1.7 µm, 2.1 × 5 mm. The column temperature was set to 40°C. The autosampler temperature was set to 4°C. The mobile UPLC phase consisted of a gradient of MeOH (Th. Geyer GmbH & Co. KG, Germany) with 0.1% (v/v) formic acid (Biosolve Chimie, France) (A) and 0.1% (v/v) aqueous formic acid (B), flowing at 0.4 mL min^{-1}. A 10-points external calibration curve was used for quantification. MassLynx software (version 4.1; Waters) was used to control the instrument and for data acquisition. MS data were processed by using TargetLynx V4.1 SCN 904.

Gibberellin baseline separation was achieved on a reversed phase Acquity UPLC® HSS T3 column (100 Å, 2.1 × 150 mm, 1.8 µm, Waters) using a gradient elution of A (Water, 0.1% FA) and B (MeOH, 0.1% FA) as follows: 0–0,3 min, 10% B; 0.3–0.7 min, 10% to 30% B; 0.7–2 min, 30% to 50% B; 2–4 min, 50% to 60% B; 4–8 min, 60% to 80% B; 8–9.5 min, 80% to 99% B; 9.5–10.4 min, 99% B. To preserve the integrity of the column, a guard column (130 Å, 2.1 × 5 mm, 1.8 µm, Waters) was also used. The column temperature was set at 45°C and the flow rate at 0.3 mL min^{-1}. The injection volume was 5 µL. The UHPLC system was coupled to Q Exactive Plus Mass Spectrometer (San Jose, CA, USA) equipped with a HESI source operating in negative ion mode. Source values were set as follow: Spray voltage 2.5 kV; capillary temperature 255°C; S-lens RF level 40; aux gas heater temp 320°C; sheath gas flow rate 47; aux gas flow rate 11. For spectra acquisition a Full MS/dd-MS^2 experiment was performed. Resolution in full scan mode was set as 70000. For MS/MS experiments resolution 17,500 and NCE 40V were used. MS data were acquired and processed by Trace Finder Software (v. 4.1, Thermo Scientific, San Jose, CA, USA). A 12-points curve was prepared from mixed standards solutions in the range of 0.5 to 1000 nM. To generate the calibration curve, the peak area on the extracted ion chromatogram (XIC) of the deprotonated molecule ion [M-H]- was measured. A least-square linear regression was used to best fit the linearity curve. The identification of compounds found in extracts was based on comparison of their retention time, high resolution m/z spectrum and isotope pattern with standards. Additionally, generated MS^2 spectra were searched in a custom spectral library for confirmation of compound identification.

3.13 RNA isolation, cDNA synthesis and gene expression analysis

Total RNA was extracted from 100 mg frozen and ground shoot or root materials using the NucleoSpin RNA Kit according to the manufacturer's protocol (Macherey-Nagel, Germany).

Samples were treated with DNase to remove all potential DNA contamination. RNA quality was determined using NanoDrop™ 2000c spectrophotometry (Thermo Scientific™). 2 µg of total RNA was used for cDNA synthesis using the RevertAid First Strand cDNA Synthesis Kit of Thermo Scientific and oligo(dT) primers. The primers for qPCR were designed using the primer3 software and were synthesized by Metabion (Germany); for details refer to Annex Table 1. The following criteria were considered: Tm=60 ± 1°C, 18–25 bp length, close to the 3'-end if possible, GC content between 40% and 60% to generate unique, short PCR products between 60 bp and 150 bp. The cDNA samples were used to study gene expression levels by quantitative real-time PCR (CFX384 TouchTM, Bio-Rad) using the iQ SYBR Green Supermix (Bio-Rad Laboratories, Hercules, CA, USA). The reaction was carried out in optical 384-well plates, each reaction well containing 5 µL of Power SYBR Green mastermix reagent, 2 µL of cDNA, 0.9 µL of each gene-specific primer and 1.2 µL distilled water in a final volume of 10 µL. The following standard thermal profile was used for all PCR reactions: one activation cycle for 3 min at 95°C; 40 amplification cycles with 15 sec at 95°C followed by 30 sec 58/60°C (depending on the primer used); one melting curve cycle from 65°C to 95°C in 5 sec (0.5°C increment). Recorded C_t values were exported from the Bio-Rad CFX Manager Software (Version 3.1, Bio-Rad Laboratories) and used for the calculation of PCR amplification efficiency and normalization factors using *CYCLOPHILIN* (*CYP*) and *UBIQUITIN* (*UBI*) as reference genes. The PCR amplification efficiency was calculated according to (Bustin *et al.*, 2009) and only experiments with an efficiency between 90% to 110% were included. Normalization factors were calculated using geNORM (Vandesompele *et al.*, 2002). Gene expression levels were expressed as fold-changes from using the following equation:

$$Fold\ change = \frac{\left(\frac{2^{-C_t GOI}}{NF}\right)_{target\ sample}}{\left(\frac{2^{-C_t GOI}}{NF}\right)_{reference\ sample}}$$

where NF is the calculated normalization factor, C_t is the cycle threshold, and GOI is the investigated gene of interest.

3.14 RNA sequencing and identification of differentially expressed genes

For library construction, total RNA of 3 replicates from each treatment was isolated and sent for mRNA enrichment, cDNA synthesis and sequencing on an Illumina HiSeq 2500 on a v4 platform for 2×100 bp paired-end reads with 17 million reads in total (Eurofins, Germany). Then, sequencing data were processed with the latest version of the Salmon software (Patro *et al.*, 2017). To obtain clean data, raw reads were trimmed by removing empty reads, adaptor sequences and low-quality bases at the 3'-end. Then, all the clean reads were considered for further analysis. High-confidence genes of the barley transcriptome (Mascher *et al.*, 2017) were used as reference to map the sequencing data. Differential expression of genes was analyzed with the latest version of DESeq2 software (Love *et al.*, 2014). To identify differentially expressed genes (DEGs) in different treatments, expression levels of each gene

were calculated by quantifying the number of reads. Our experiment followed a factorial treatment structure consisting of two factors, potassium and silicon, yielding four treatments. To compare the expression ratio of genes among treatments, we conducted simple effects analysis and examined the difference between groups within one level of one of the independent variables, K or Si. The Salmon software tool was used to convert raw sequencing data into counts (Patro *et al.*, 2017). Then, we compared the expression ratio in response to K deficiency (-K-Si versus +K-Si), or the effect of Si in K-sufficient (+K+Si versus +K-Si) or K-deficient (-K+Si versus -K-Si) roots or the last fully expanded leaves with DESeq2 Library in R (Anders and Huber, 2010). Finally, The Barley Genome Explorer (BARLEX) (Colmsee *et al.,* 2015) and the National Center for Biotechnology Information (NCBI) databases were used for functional annotation of each single gene ID.

3.15 Statistical analysis

All data are presented as mean ± standard error (SE) (Williams and Abdi, 2010). In the K deficiency experiment, data were subjected to factorial treatment analysis using the least significant difference (LSD) to calculate confidence intervals for pairwise comparisons between factor levels. In other experiments, data were analyzed by one-way ANOVA and post-hoc Tukey's test using the R software (de Mendiburu and de Mendiburu, 2019).

4 Results

4.1 Impact of silicon application on plant growth under potassium deficiency

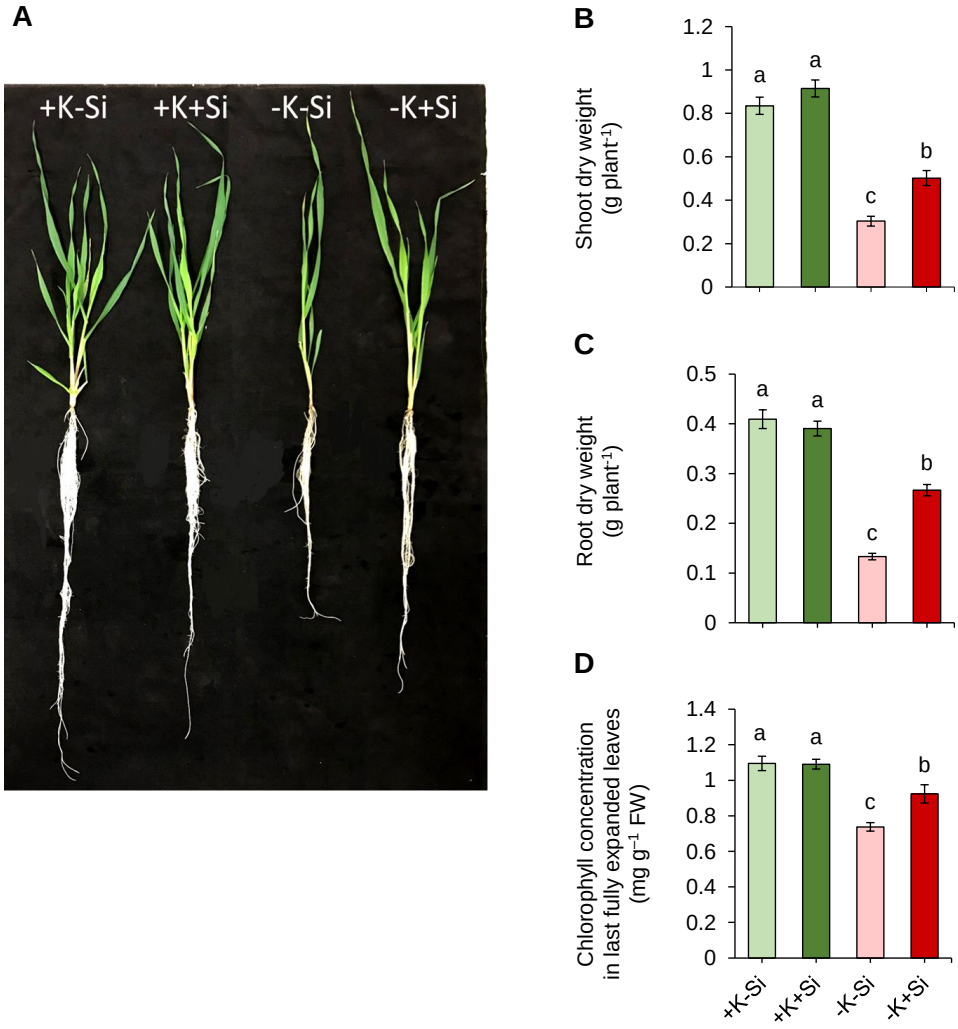

Figure 5. Influence of Si supply on phenotype, shoot and root dry weights and chlorophyll concentrations of barley plants grown under adequate or low K supply. (A) Appearance of shoots and roots, (B) shoot dry weights, (C) root dry weights and (D) chlorophyll concentrations in the last fully expanded leaf. After 7 days of germination, plants were grown under either adequate (2 mM) or low (0.04 mM) K for 24 days in the absence or presence of 1.78 mM Si. Bars indicate means ± SE. Different letters denote significant differences among treatments according to LSD test ($p < 0.05$; $n = 8$).

To investigate whether and how Si can alleviate K deficiency in barley, hydroponically-grown barley plants were subjected to adequate or low K supply for 24 days in the absence or presence of Si. In the absence of Si, continuous low supply of K suppressed the formation of tillers and new leaves while roots grew much shorter (Figure 5A). This expressed in two- to three-fold lower shoot and root biomass (Figure 5B, C). In the presence of Si, plant growth recovered and shoot and root biomass of K-deficient plants increased by 66 and 100%, respectively (Figure 5A-C). In contrast, in K-sufficient plants Si supply caused only a small, non-significant increase in shoot biomass (Figure 5B). Since K deficiency leads also to chlorosis and inhibits photosynthesis (Marschner, 2012), chlorophyll concentrations were determined in fully expanded leaves, which declined by 32% under low K stress. In the presence of Si,

however, such a strong decline of chlorophyll concentrations was prevented, whereas under ample K supply Si had no impact (Figure 5D). These results show that Si application substantially restores growth and increases biomass in K-deficient plants while its impact on growth remains negligible under adequate K nutrition.

4.2 Impact of silicon application on the nutritional status of plants under potassium deficiency

To investigate how Si nutrition affects the plant nutrient status under K deficiency, concentrations of all nutrients were determined in fully expanded leaves and roots by ICP-OES. As expected, Si application led to considerable Si accumulation in leaf and root tissues (Figure 6A, B). In K-sufficient plants, Si concentrations were around 7 mg g^{-1} in shoots or roots, while they were 1-1.5 mg g^{-1} lower under K deficiency, which may result from lower transpiration (Wang *et al.*, 2013). Under low K supply, K concentrations decreased below 1% in both tissues, which is indicative of K deficiency in barley (Bergmann, 1992), despite the absence of chlorosis in leaves (Figure 5A; 6C, D). Silicon application to low K plants increased leaf K concentrations significantly but rather marginally, while root concentrations remained similar (Figure 6C, D). These results suggested that Si did not necessarily improve the K nutritional status of the plants but rather translated K efficiently into biomass.
In both tissues, lower K concentrations in K-deficient plants were accompanied by an increase in the concentrations of Mg, Ca and Na (Figure 7A-F). This reflects a typical response of plants to K deficiency, which compensates for lower K uptake by enhanced uptake of other cations (Marschner, 2012). While these elevated levels of Mg and Ca remained unaffected by Si supply, Na concentrations increased in both tissues after Si application (Figure 7A-F), but remained far below a growth-inhibitory level (Marschner, 2012). Concentrations of other macroelements, including P and S in both tissues and N in roots, increased only slightly under K deficiency, while the nutritional status of these elements remained unaffected by Si supply (Figure 7G-J; 8A, B). Among the metal micronutrients, changes in Fe and Zn levels were moderate and considered less relevant, with the exception of Mn, which was preferentially translocated to shoots under low K supply and accumulated more under Si application (Figure 8C-H). Carbon concentrations in leaves and roots remained unaffected by Si application but slightly increased in K-deficient plants, probably due to the lack of K in the dry biomass (Figure 8I, J). Taken together, Si application did neither revert the nutritional status of K-deficient plants nor the K deficiency responses related to the ion uptake balance. Instead, the higher Na levels of Si-supplied plants exclusively under K deficiency suggest that K uptake systems, some of which are permeable to Na (Leigh and Storey, 1993; Rubio *et al.*, 1995), were even induced. To assess whether applying Si affects ion balance in Hoagland solutions, macro- and micronutrients were determined in culture solutions under all treatments by ICP-OES (Annex Figure 1). Silicon was provided at a concentration of 1.78 mM from a H_2SiO_3 stock solution prepared through the chromatography column (Figure 1). Concentration of all nutrients remained rather stable after Si application in the culture solutions, and only Si level increased. The major source of Na was Fe(III)-EDTA while the amount of Na that was introduced into the nutrient solution by Si was negligible.

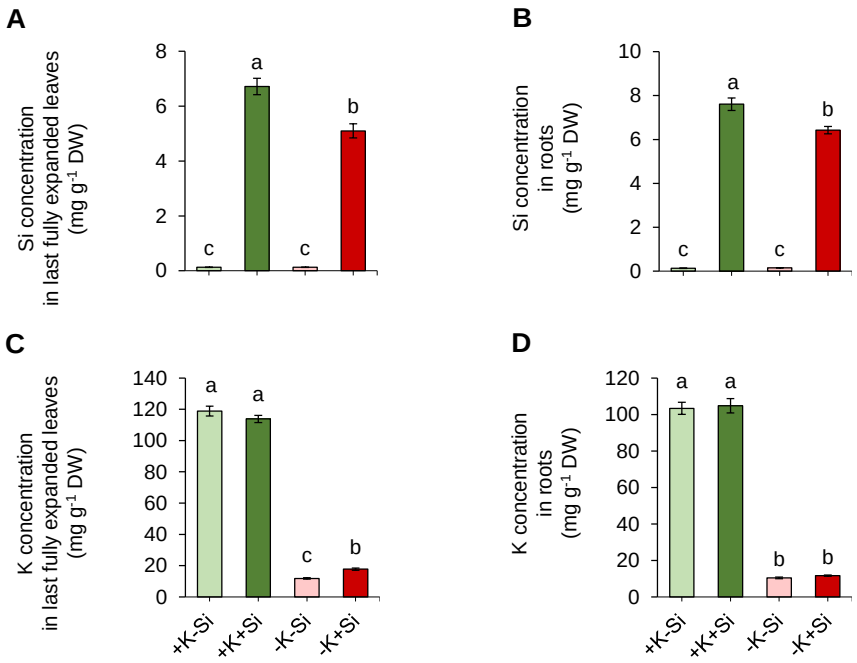

Figure 6. Influence of Si supply on Si and K concentrations in leaves and roots of barley plants grown under adequate or low K supply. (A-D) Concentrations of silicon (Si; A, B), and potassium (K; C, D) in leaves (A, C) or in roots (B, D). After 7 days of germination, plants were grown under either adequate (2 mM) or low (0.04 mM) K for 24 days in the absence or presence of 1.78 mM Si. Leaf analysis is based on the last fully expanded leaf. Bars indicate means ± SE. Different letters denote significant differences among treatments according to LSD test ($p < 0.05$; $n = 8$).

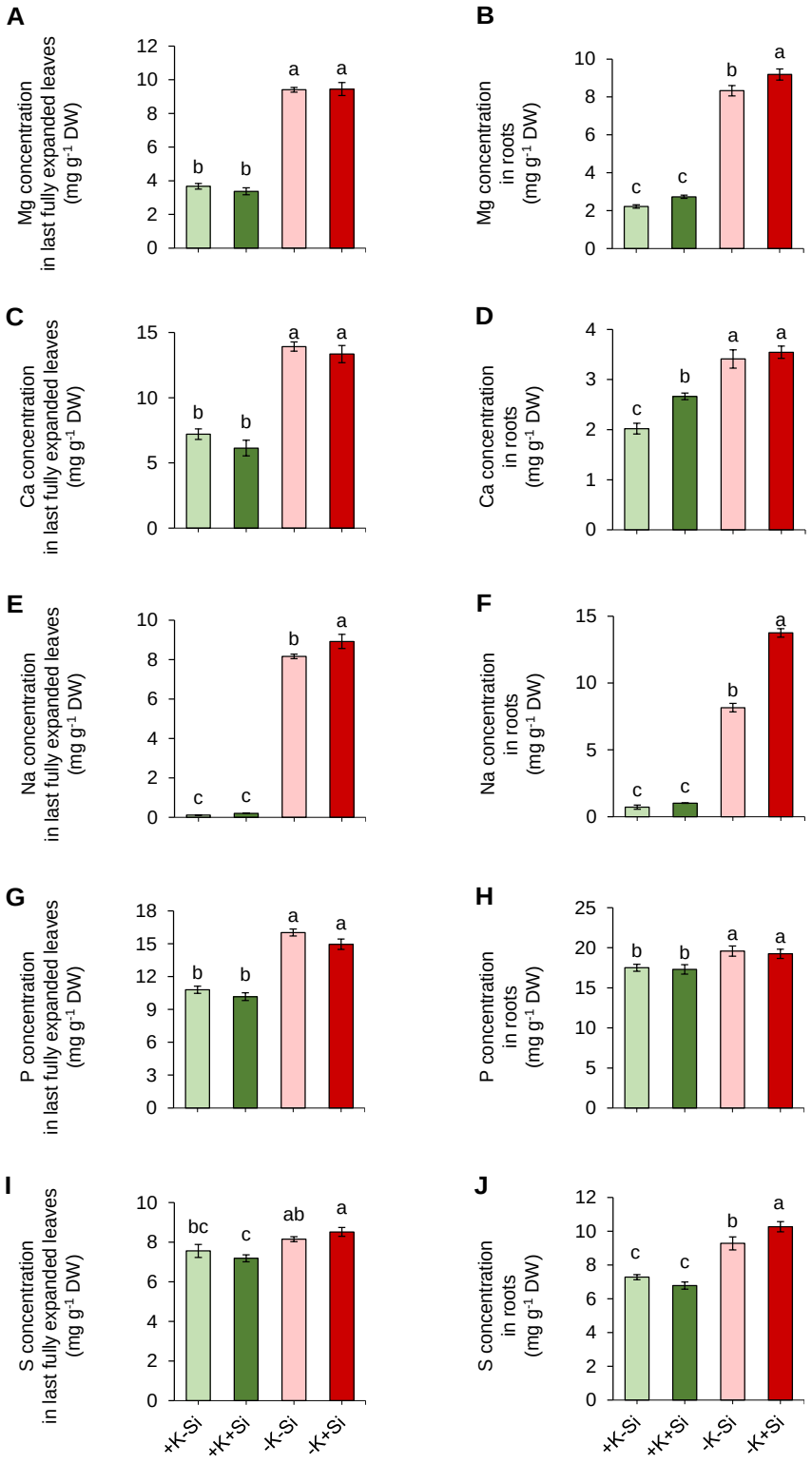

Figure 7. Influence of Si supply on Mg, Ca, Na, P and S concentrations in leaves and roots of barley plants grown under adequate or low K supply. (A-J) Concentrations of magnesium (Mg; A, B), calcium (Ca; C, D), sodium (Na; E, F), phosphorus (P; G, H), and sulfur (S; I, J) in leaves (A, C, E, G, I) or in roots (B, D, F, H, J). After 7 days of germination, plants were grown under either adequate (2 mM) or low (0.04 mM) K for 24 days in the absence or presence of 1.78 mM Si. Leaf analysis is based on the last fully expanded leaf. Bars indicate means ± SE. Different letters denote significant differences among treatments according to LSD test ($p < 0.05$; $n = 8$).

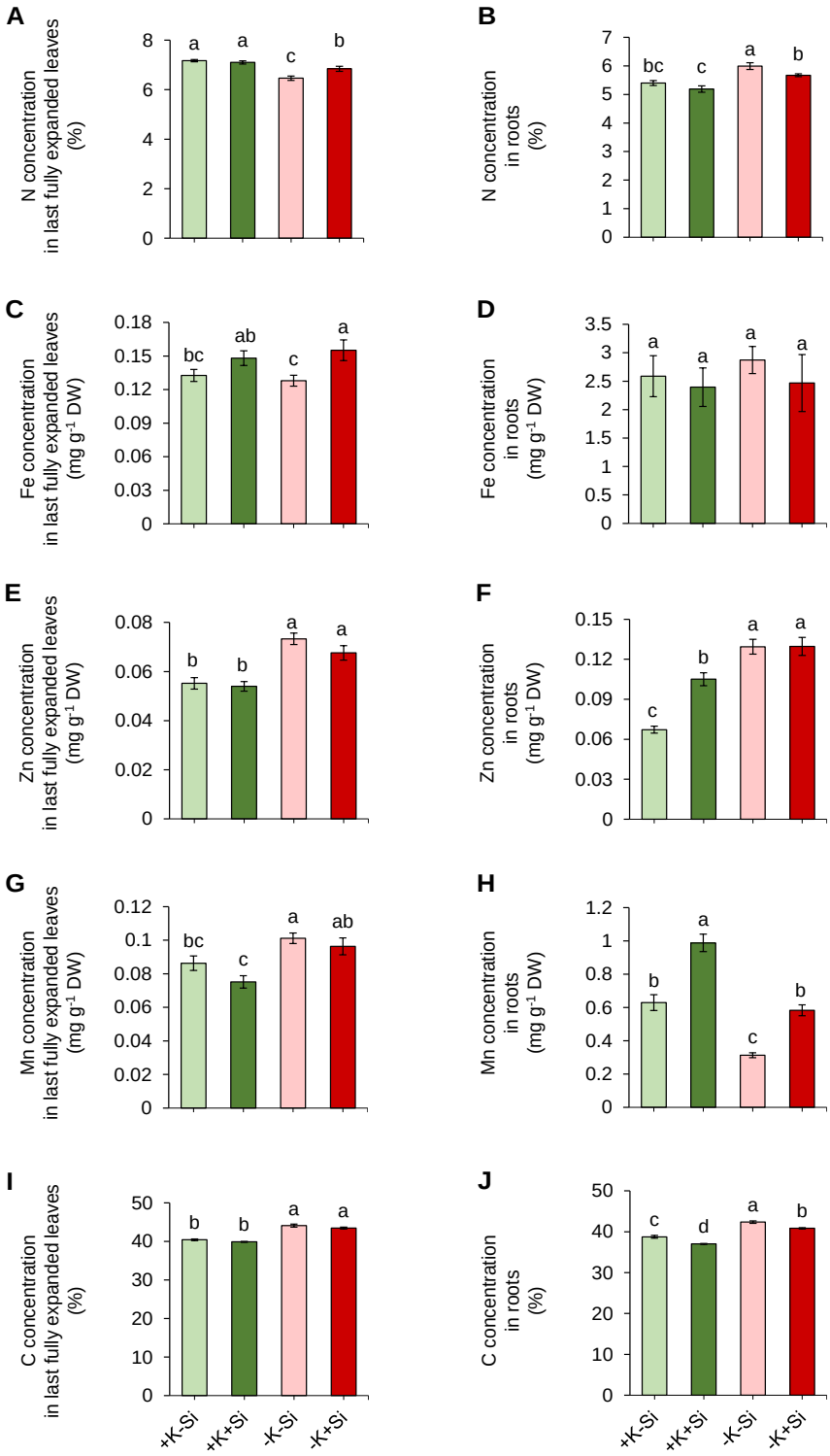

Figure 8. Influence of Si supply on N, Fe, Zn, Mn and C concentrations in leaves and roots of barley plants grown under adequate or low K supply. (A-J) Concentrations of nitrogen (N; A, B), iron (Fe; C, D), zinc (Zn; E, F), manganese (Mn; G, H), and carbon (C; I, J) in leaves (A, C, E, G, I) or in roots (B, D, F, H, J). After 7 days of germination, plants were grown under either adequate (2 mM) or low (0.04 mM) K for 24 days in the absence or presence of 1.78 mM Si. Leaf analysis is based on the last fully expanded leaf. Bars indicate means ± SE. Different letters denote significant differences among treatments according to LSD test ($p < 0.05$; $n = 8$).

4.3 Impact of silicon application on phytohormone homeostasis of plants under potassium deficiency

To assess the impact of Si on phytohormone homeostasis under K deficiency, phytohormones were profiled in fully expanded leaves and roots. In both tissues, the concentrations of ABA and its degradation products phaseic acid (PA) and dehydro-phaseic acid (DPA) as well as of its conjugate ABA-glucose ester (ABAGlc) in leaves increased as a typical plant response to K deficiency (Figure 9A-H) (Hosseini *et al.*, 2016). While leaf and root ABA levels remained more or less unaffected by Si supply, the leaf levels of inactivated ABA forms, which exceeded that of ABA by far, were significantly lower upon Si application, suggesting lower ABA synthesis and turnover during the stress treatment (Figure 9A-H). Moreover, the levels of two further stress-related hormones, i.e., salicylic acid (SA) and JA incl. its bioactive conjugate with isoleucine (JA-Ile), increased under low K, however, to a lesser extent in the presence of Si (Figure 10A-F). In roots, a comparable increase under K deficiency was only observed for SA, on which Si had little impact (Figure 10A-F). These findings suggest that in the presence of Si in particular the leaves of K-deficient plants are less affected by low K stress. Since cytokinins play a major role in abiotic stress responses (Ha *et al.*, 2012; Nam *et al.*, 2012), different cytokinins forms were also analyzed. In all treatments, the leaf concentrations of trans-zeatin (tZ), probably the most bioactive cytokinin form in shoots, and other, less active cytokinin forms were hardly or only very slightly affected. In contrast, root concentrations of trans-zeatin riboside (tZR) and isopentenyl adenine riboside (IPR) decreased under K deficiency in favour of cis-zeatin riboside (cZR) (Figure 11A-H). This conversion towards the weaker active species cZR (Heyl *et al.*, 2006) was prevented in the presence of Si (Figure 11A-H).
Auxin (IAA) levels in leaves remained quite constant across all treatments, whereas they increased slightly in roots of K-deficient plants and even further with Si supply (Figure 12A, B). This trend was evident in the two inactivated forms, indole-3-acetic acid methyl ester (IAAMe) and 2-oxindole-3-acetic acid (oxIAA), which increased in both tissues under K deficiency, while only IAAMe levels in leaves remained suppressed by Si (Figure 12C-F). Among the detected gibberellins, leaf and root concentrations of gibberellins precursors, like GA_{53} and GA_{19}, or of two downstream products of GA_{20}-oxidase, GA_{44} and GA_9, remained quite stable or slightly decreased under low K but did not respond to Si (Figure 13A-H). Leaf levels of the bioactive form GA_3 increased after Si supply irrespective of K conditions. In turn, concentrations of GA_8, a degradation product of the highly bioactive GA_1, increased under K deficiency in leaves but not in the presence of Si (Figure 13G-L). In total, the stress-related phytohormones ABA, SA and JA increased under K deficiency in leaves together with their downstream conjugates or metabolites, whereas with the exception of ABA, Si nutrition prevented this increase. Among the growth-promoting hormones, bioactive GA_3 increased after Si supply in leaves, while K deficiency-dependent accumulation of the deactivated species GA_8 was prevented by Si. Such effects of Si on hormone levels were weaker or even absent in roots, except for a slight Si-mediated increase in IAA.

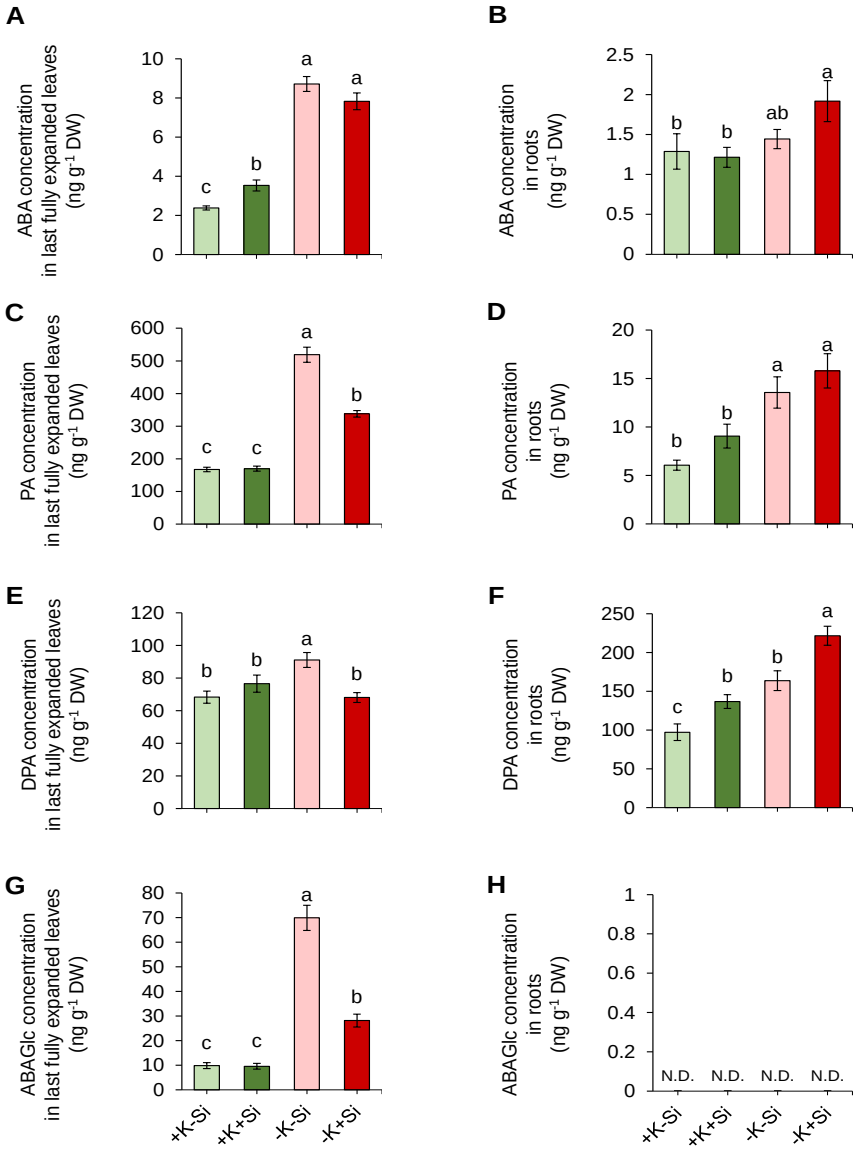

Figure 9. Influence of Si supply on concentrations of ABA, PA, DPA and ABAGlc in leaves and roots of barley plants grown under adequate or low K supply. (A-H) Concentrations of abscisic acid (ABA; A, B), phaseic acid (PA; C, D), dihydrophaseic acid (DPA; E, F), and abscisic acid glucose ester (ABAGlc; G, H) in leaves (A, C, E, G) or in roots (B, D, F, H). After 7 days of germination, plants were grown under either adequate (2 mM) or low (0.04 mM) K for 24 days in the absence or presence of 1.78 mM Si. Leaf analysis is based on the last fully expanded leaf. Bars indicate means ± SE. Different letters denote significant differences among treatments according to LSD test ($p < 0.05$; $n = 8$).

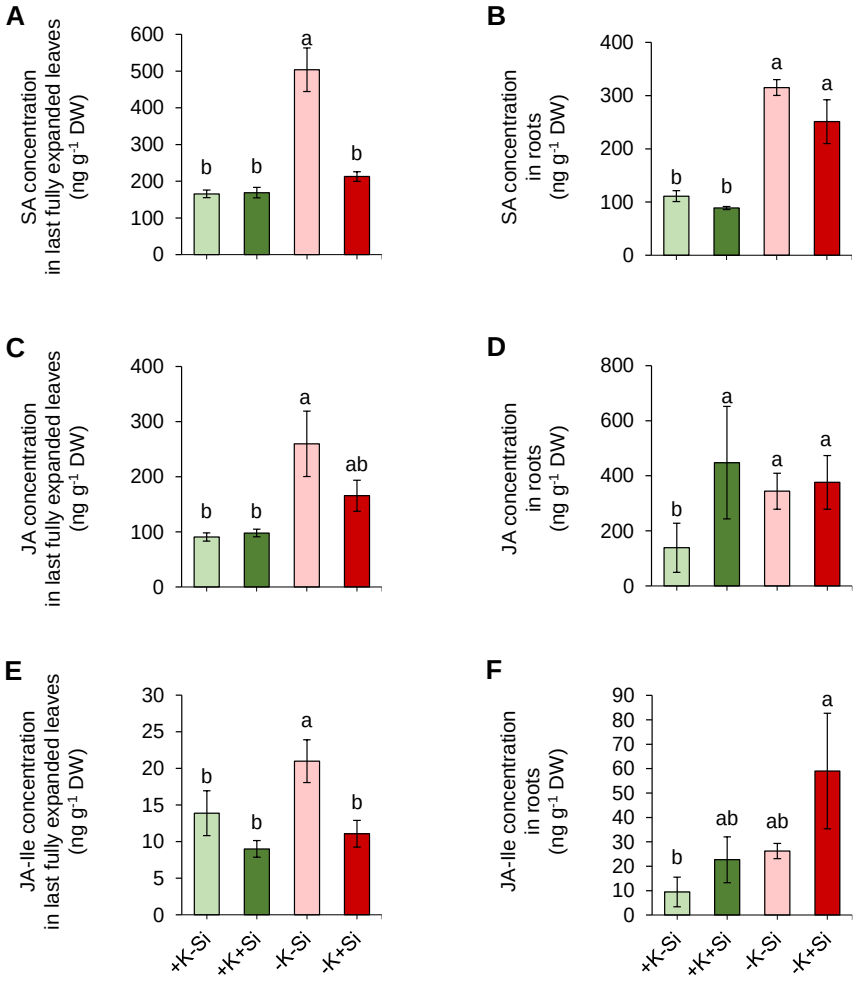

Figure 10. Influence of Si supply on concentrations of SA, JA, and JA-Ile in leaves and roots of barley plants grown under adequate or low K supply. (A-F) Concentrations of salicylic acid (SA; A, B), jasmonic acid (JA; C, D), and jasmonoyl isoleucine (JA-Ile; E, F) in leaves (A, C, E) or in roots (B, D, F). After 7 days of germination, plants were grown under either adequate (2 mM) or low (0.04 mM) K for 24 days in the absence or presence of 1.78 mM Si. Leaf analysis is based on the last fully expanded leaf. Bars indicate means ± SE. Different letters denote significant differences among treatments according to LSD test ($p < 0.05$; $n = 8$).

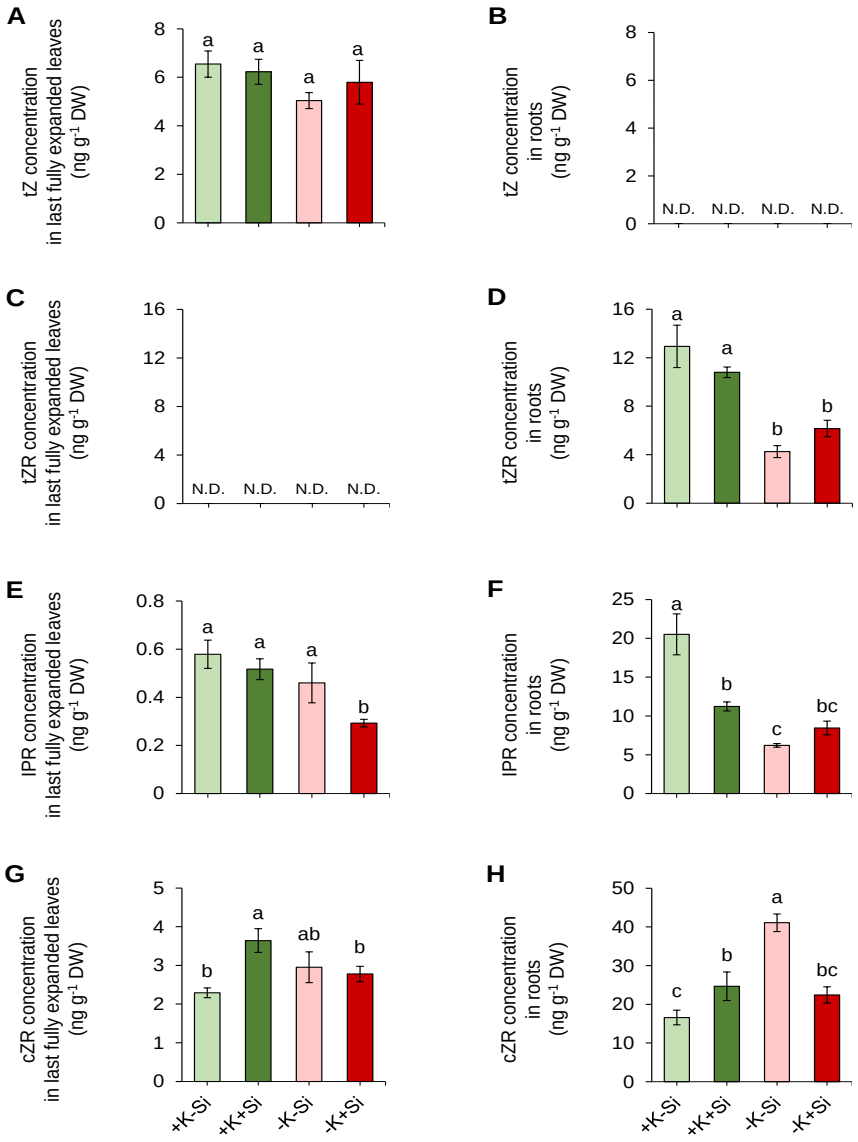

Figure 11. Influence of Si supply on concentrations of tZ, tZR, IPR, and cZR in leaves and roots of barley plants grown under adequate or low K supply. (A-H) Concentrations of trans-zeatin (tZ; A, B), trans-zeatin-riboside (tZR; C, D), isopentenyl adenine riboside (IPR; E, F), and cis-zeatin riboside (cZR; G, H) in leaves (A, C, E, G) or in roots (B, D, F, H). After 7 days of germination, plants were grown under either adequate (2 mM) or low (0.04 mM) K for 24 days in the absence or presence of 1.78 mM Si. Leaf analysis is based on the last fully expanded leaf. Bars indicate means ± SE. Different letters denote significant differences among treatments according to LSD test ($p < 0.05$; $n = 8$).

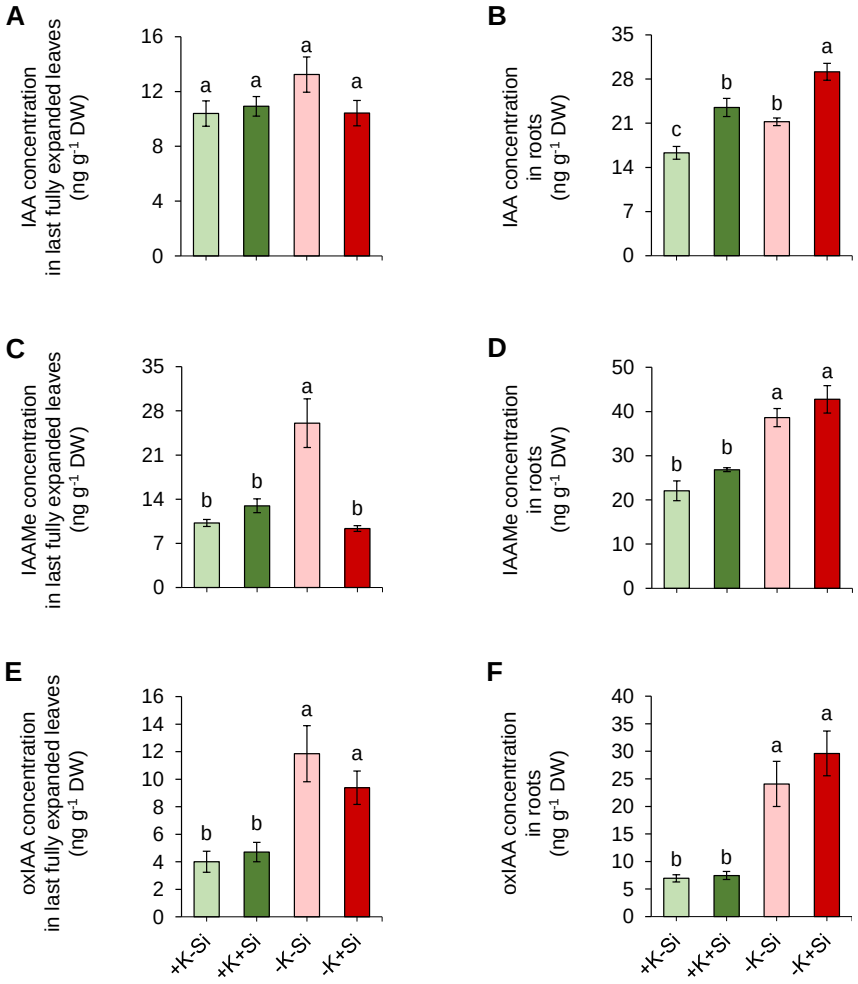

Figure 12. Influence of Si supply on concentrations of IAA, IAAMe, and oxIAA in leaves and roots of barley plants grown under adequate or low K supply. (A-F) Concentrations of indole-3-acetic acid (IAA; A, B), indole-3-acetic acid methyl ester (IAAMe; C, D), and 2-oxoindole-3-acetic acid (oxIAA; E, F) in leaves (A, C, E) or in roots (B, D, F). After 7 days of germination, plants were grown under either adequate (2 mM) or low (0.04 mM) K for 24 days in the absence or presence of 1.78 mM Si. Leaf analysis is based on the last fully expanded leaf. Bars indicate means ± SE. Different letters denote significant differences among treatments according to LSD test ($p < 0.05$; $n = 8$).

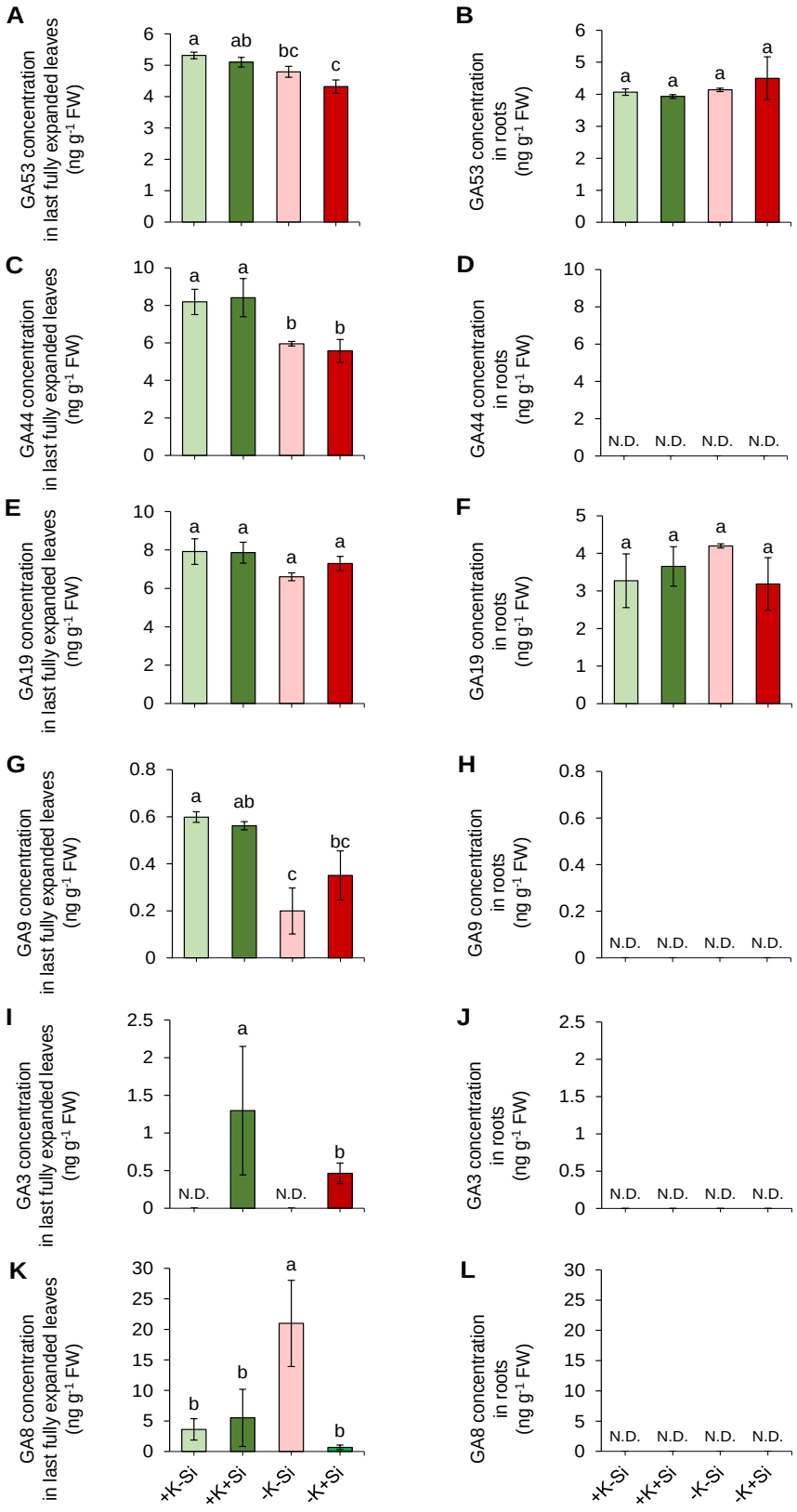

Figure 13. Influence of Si supply on concentrations of GA53, GA44, GA19, GA9, GA3 and GA8 in leaves and roots of barley plants grown under adequate or low K supply. (A-L) Concentrations of gibberellin-53 (GA53; A, B), gibberellin-44 (GA44; C, D), gibberellin-19 (GA19; E, F), gibberellin-9 (GA9; G, H), gibberellin-3 (GA3; I, J) and gibberellin-8 (GA8; K, L) in leaves (A, C, E, G, I, K) or in roots (B, D, F, H, J, L). After 7 days of germination, plants were grown under either adequate (2 mM) or low (0.04 mM) K for 24 days in the absence or presence of 1.78 mM Si. Leaf analysis is based on the last fully expanded leaf. Bars indicate means ± SE. Different letters denote significant differences among treatments according to LSD test ($p < 0.05$; n = 8).

4.4 Impact of silicon application on metabolic changes of plants under potassium deficiency

To investigate whether Si alleviates the accumulation of sugars in leaves as a consequence of inhibited phloem loading, which is a typical symptom of K deficiency (Cakmak, 1994), primary C and N metabolites were analysed by IC-MS-MS. Indeed, several downstream products of the Calvin cycle accumulated under K deficiency in leaves, in particular sucrose, glucose and fructose, but also phosphorylated sugars and energy carriers such as sucrose-6-phosphate (Suc-6-P), glucose-1-phosphate (Glc-1-P), trehalose-6-phosphate (Tre-6-P), and uridine diphosphate glucose (UDP-Glc), UDP, uridine monophosphate (UMP) as well as glucuronic acid (GlcA) (Figure 14; 16A, C, E, G, I; 17A, C). By contrast, starch and its precursors remained unaffected (Figure 14). While 3-phosphoglycerate (3PGA) remained unchanged, higher levels of acetyl-CoA suggested lower C turn-over in the tricarboxylic acid (TCA) cycle, which expressed in lower levels of fumarate and in trend of 2-oxoglutarate (Figure 14; 17E). With regard to the major amino acids, K deficiency led to accumulation of the diamines glutamine and asparagine at the cost of glutamate and aspartate, and further increased most other amino acids including the stress-responsive ones, proline and GABA (Figure 14; 18A, C). Not all of these changes were mitigated by Si in plants. In particular Suc, Suc-6-P, Glc and Fru concentrations decreased moderately as well as those of glucuronic acid and acetyl-CoA (Figure 14; 17C, E). The other phosphorylated sugars or energy carriers remained mostly unaffected by Si. However, Si efficiently prevented excess accumulation of di-aminated and stress-responsive amino acids and restored levels of glutamate and asparate (Figure 14). Thus, Si hardly altered the levels of energy-carrying metabolites but mostly prevented excess sugar and amino acid accumulation in K-deficient leaves, which may be indicative for a partial relieve of inhibited phloem loading activity.

In K-deficient roots, carbohydrate metabolism was less affected than expected. Concentrations of Suc and Glc as well as of phosphorylated sugars were hardly lower under K deficiency, only Glc-1-P levels showed a prominent decrease (Figure 15; 16D). Levels of Fru and glucuronic acid even increased (Figure 15; 17D). A lack of carbohydrates in K-deficient roots became evident rather by lower levels of 2-oxoglutarate, glutamate and aspartate in favour of higher levels of diamines, and most other amino acids, except for the stress-responsive ones, proline and GABA (Figure 15; 18B, D). Remarkable changes conferred by Si related to elevated levels of Suc, Glc and Fru, which even exceeded those of K-supplied roots (Figure 15). By contrast, phosphorylated metabolites, TCA cycle intermediates and most of the abundant amino acids were not or only slightly altered by Si (Figure 15-18). Thus, apart from restored amino acid levels, Si did not mitigate K deficiency-induced metabolic changes in roots.

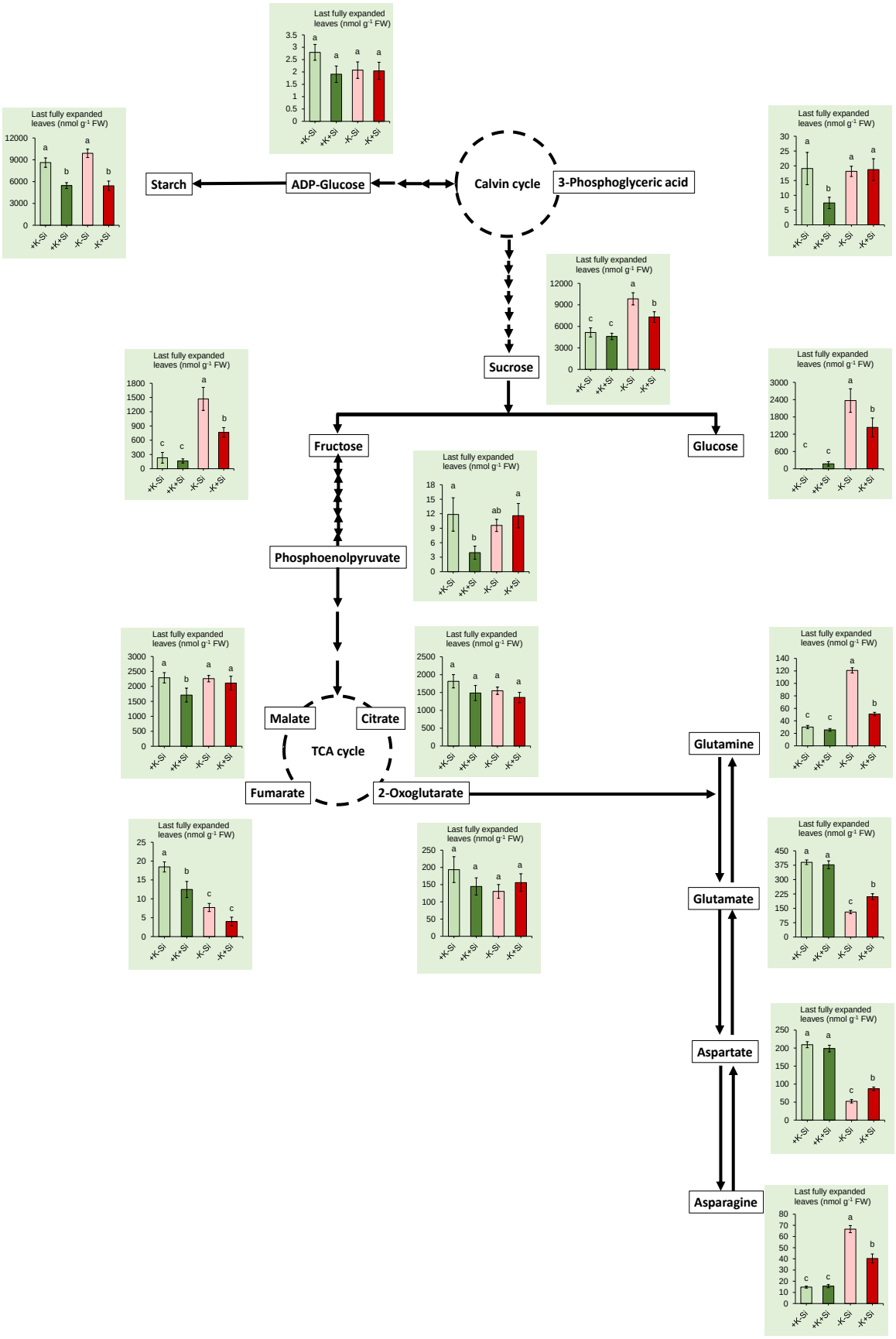

Figure 14. Metabolite profile in leaves of barley plants grown under adequate or low K supply in the presence or absence of Si. Concentrations of starch, sugars, sugar alcohols, organic acids and amino acids in leaves. After 7 days of germination, plants were grown under either adequate (2 mM) or low (0.04 mM) K for 24 days in the absence or presence of 1.78 mM Si. Leaf analysis is based on the last fully expanded leaf. Bars indicate means ± SE. Different letters denote significant differences among treatments according to LSD test ($p < 0.05$; $n = 8$).

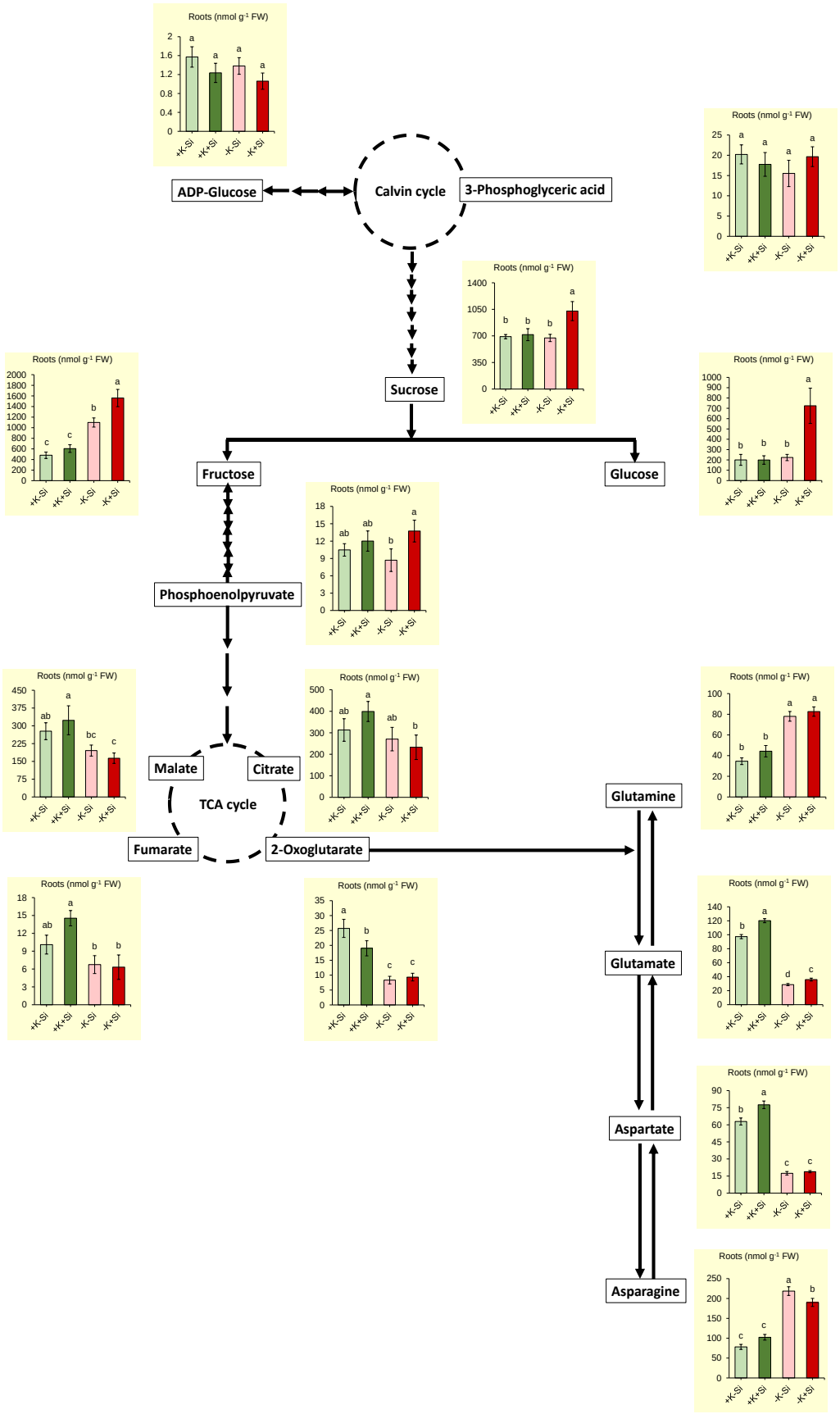

Figure 15. Metabolite profile in roots of barley plants grown under adequate or low K supply in the presence or absence of Si. Concentrations of sugars, sugar alcohols, organic acids and amino acids in roots. After 7 days of germination, plants were grown under either adequate (2 mM) or low (0.04 mM) K for 24 days in the absence or presence of 1.78 mM Si. Bars indicate means ± SE. Different letters denote significant differences among treatments according to LSD test ($p < 0.05$; n = 8).

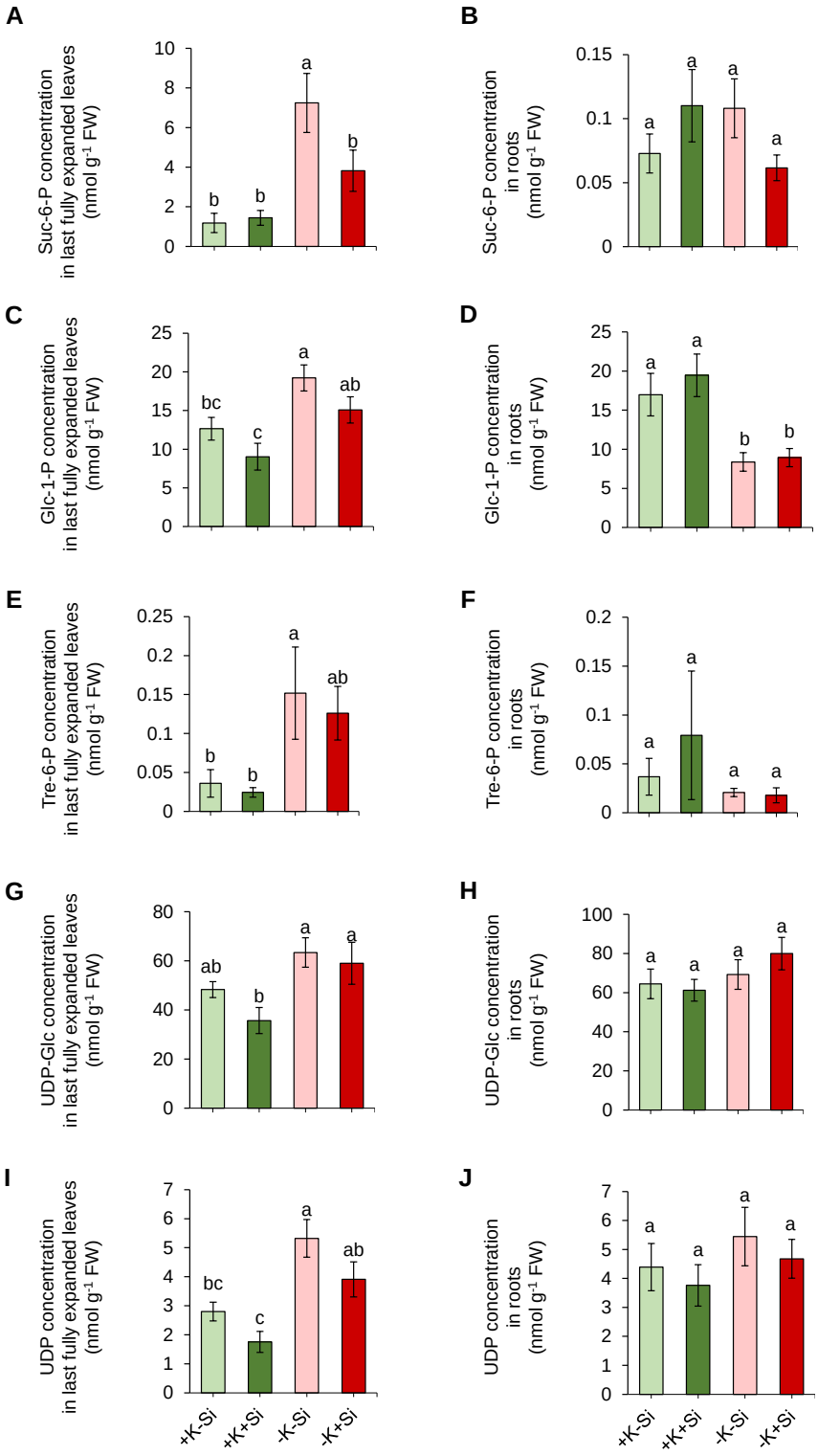

Figure 16. Influence of Si supply on concentrations of phosphorylated metabolites in leaves and roots of barley plants grown under adequate or low K supply. (A-J) Concentrations of sucrose-6-phosphate (Suc-6-P; A, B), Glucose-1-phosphate (Glc-1-P; C, D), trehalose-6-phosphate (Tre-6-P; E, F), uridine diphosphate glucose (UDP-Glc; G, H), and uridine diphosphate (UDP; I, J) in leaves (A, C, E, G, I) or in roots (B, D, F, H, J). After 7 days of germination, plants were grown under either adequate (2 mM) or low (0.04 mM) K for 24 days in the absence or presence of 1.78 mM Si. Leaf analysis is based on the last fully expanded leaf. Bars indicate means ± SE. Different letters denote significant differences among treatments according to LSD test ($p < 0.05$; $n = 8$).

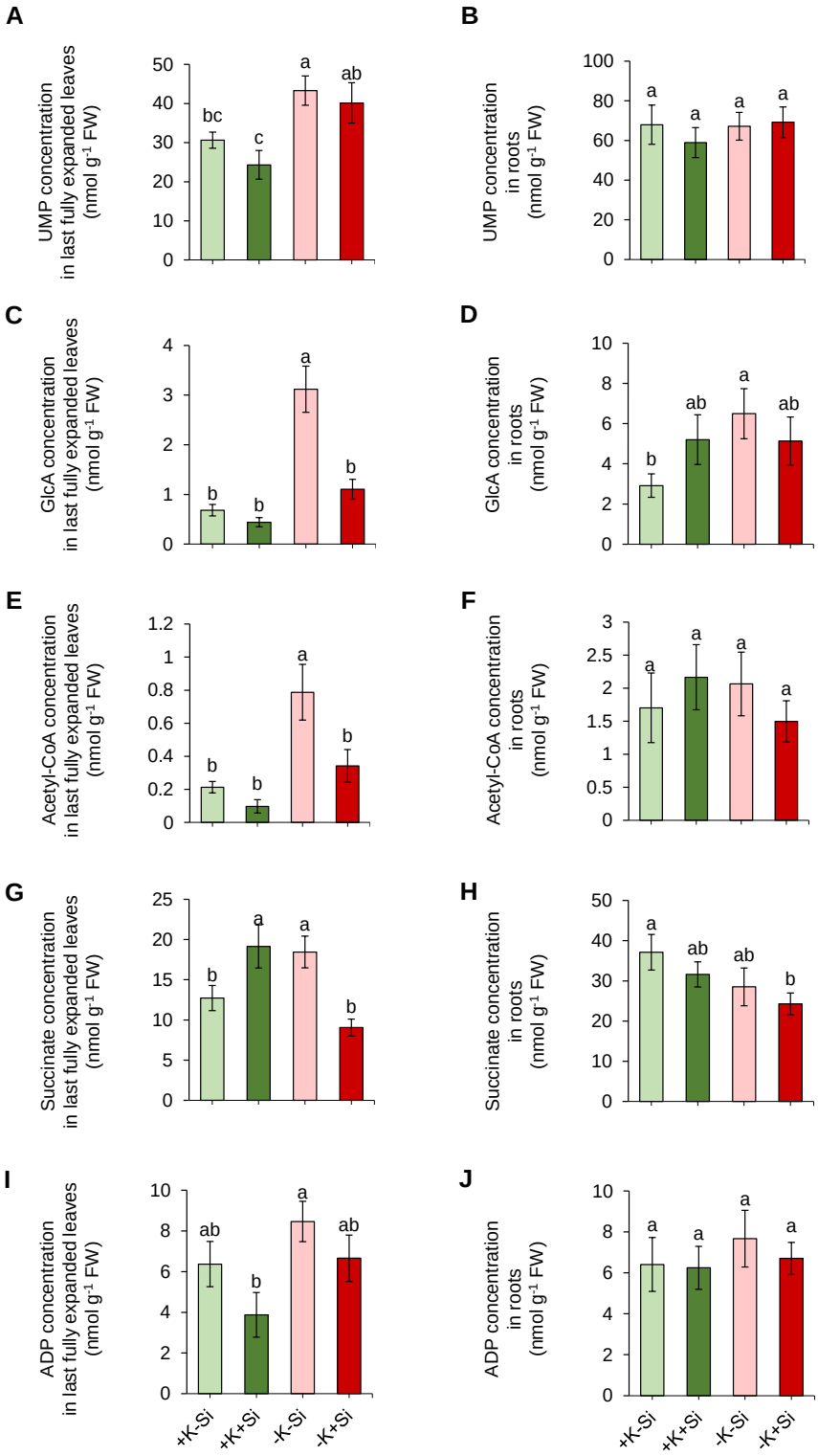

Figure 17. Influence of Si supply on concentrations of primary metabolites in leaves and roots of barley plants grown under adequate or low K supply. (A-J) Concentrations of uridine monophosphate (UMP; A, B), glucuronic acid (GlcA; C, D), acetyl coenzyme A (Acetyl-CoA; E, F), succinate (G, H), and adenosine diphosphate (ADP; I, J) in leaves (A, C, E, G, I) or in roots (B, D, F, H, J). After 7 days of germination, plants were grown under either adequate (2 mM) or low (0.04 mM) K for 24 days in the absence or presence of 1.78 mM Si. Leaf analysis is based on the last fully expanded leaf. Bars indicate means ± SE. Different letters denote significant differences among treatments according to LSD test ($p < 0.05$; $n = 8$).

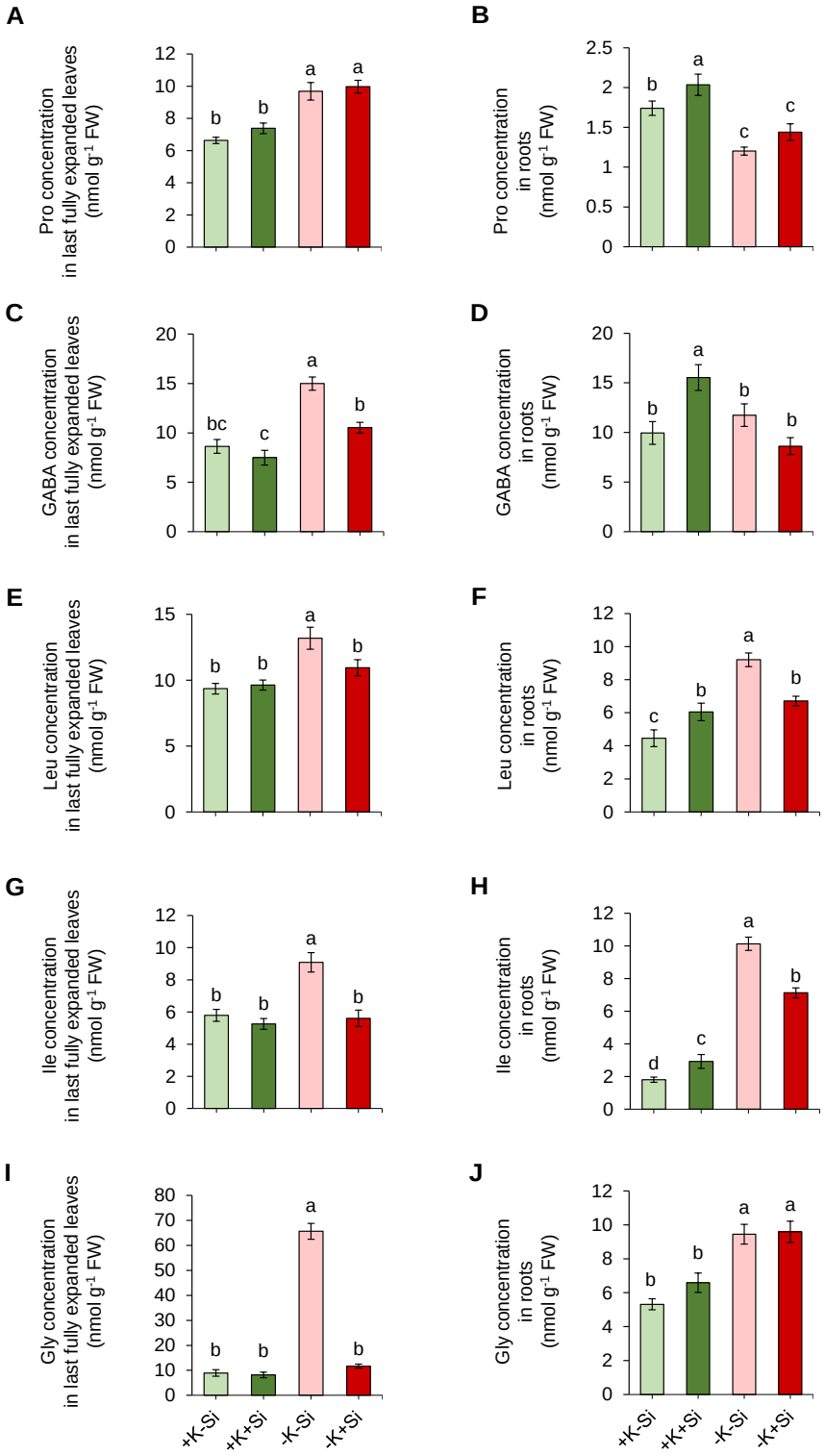

Figure 18. Influence of Si supply on concentrations of amino acids in leaves and roots of barley plants grown under adequate or low K supply. (A-J) Concentrations of proline (Pro; A, B), gamma aminobutyric acid (GABA; C, D), leucine (Leu; E, F), isoleucine (Ile; G, H), and glycine (Gly; I, J) in leaves (A, C, E, G, I) or in roots (B, D, F, H, J). After 7 days of germination, plants were grown under either adequate (2 mM) or low (0.04 mM) K for 24 days in the absence or presence of 1.78 mM Si. Leaf analysis is based on the last fully expanded leaf. Bars indicate means ± SE. Different letters denote significant differences among treatments according to LSD test ($p < 0.05$; $n = 8$).

4.5 Impact of silicon application on gene expression patterns of plants under potassium deficiency

To assess the impact of Si nutrition on transcriptome changes in plants under K deficiency, total RNA was extracted from fully expanded leaves and roots and subjected to RNA-Seq analysis. Before calculating differential gene expression, normalized data were subjected to principal component analysis (PCA), which indicated prominent changes among the four treatments (Figure 19A, B). In both tissues, K-dependent transcriptome changes separated clearly along PC1, which explained 87% and 63% of the variance in leaves and roots, respectively, indicating a significant qualitative shift in the transcriptome signature under K deficiency. Supplementation of Si separated the transcriptomes of K-sufficient and K-deficient plants at smaller variance along PC2, revealing that plants of both K regimes responded to the presence of Si in a similar direction. However, in K-deficient leaves, Si supply provoked transcriptome changes to approach those of K-sufficient leaves by decreasing variance along PC1. This was not the case in roots, suggesting that Si-mediated mitigation of K deficiency relates primarily to leaves.

Using simple effect analyses, the hypothesis was tested whether Si just reverts the transcriptional response to K deficiency. In leaves, 2211 genes altered their expression levels significantly either under K deficiency or under Si supply to K-deficient plants. In roots, the corresponding number was with 481 genes much lower (Figure 19C, D). The resulting gene list showed that approx. one-third of the leaf-expressed genes were upregulated when Si was supplied to K-deficient plants, while in roots almost half of the genes were upregulated. Most interestingly, in either tissue the large majority of genes showed a reverted expression pattern to that of K deficiency, indicating that Si prevented or reverted the K deficiency response. When K-sufficient plants were supplied with Si, the number of de-regulated genes was much lower, supporting the notion that Si targets primarily stress-responsive genes. Subsequent analysis of Gene Ontology (GO) terms was limited by the relatively small number of genes differentially expressed under Si supply, especially in roots, and mostly yielded less specified terms. In shoots, biological processes that were upregulated under K deficiency were associated with cation transport, but this term disappeared when assessing the Si effect on K-deficient plants (Table 1). Instead, in leaves and roots, terms related to cell wall metabolism dominated the response of K-deficient plants to Si. Altogether, the GO term analysis suggests that typical K deficiency responses have been replaced by general growth-related processes under Si supply.

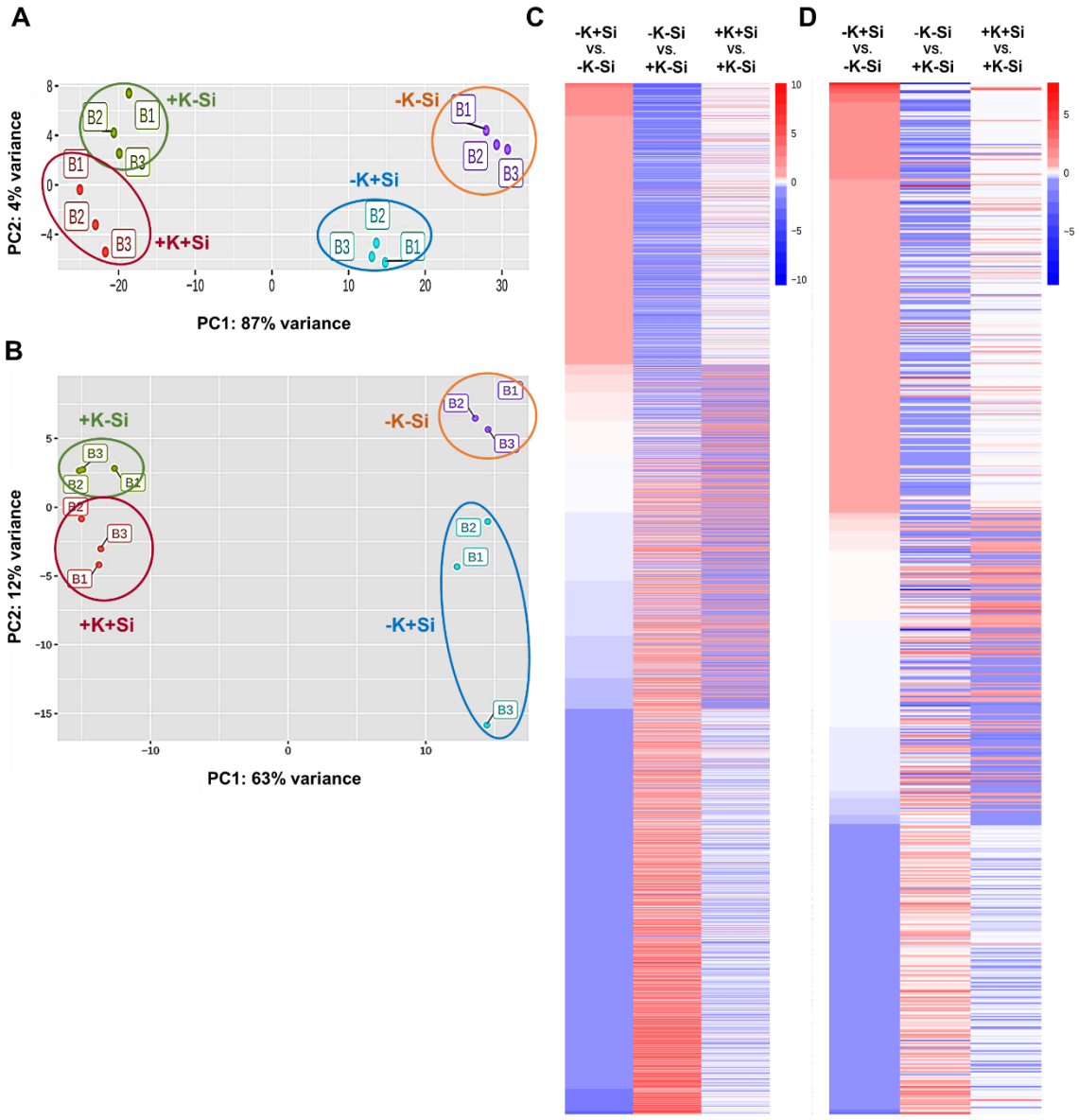

Figure 19. Changes in gene expression patterns of leaves and roots of barley plants as affected by K or Si supply. Principal component analysis (PCA) reflecting changes in transcript abundance in (A) the last fully expanded leaves or (B) roots in response to Si supply under adequate or low K supply. (C-D) Heatmap of relative gene expression changes in the last fully expanded leaves (C) or roots (D). In either tissue, genes were grouped according to their transcript abundance (i) after Si supply under K deficiency (-K+Si vs. -K-Si), (ii) under low K in the absence of Si (-K-Si vs. +K-Si), or (iii) after Si supply under adequate K nutrition (+K+Si vs. +K-Si). Genes were selected if their fold-change of expression was > 0.5 and significantly altered at a false discovery rate (FDR) of < 0.05%, either in first or second group.

Table 1. Enrichment of Gene Ontology (GO) terms in genes expressed in the last fully expanded leaves and roots of barley plants grown under adequate or low K supply in the absence or presence of Si. Gene Ontology identification numbers (GO.ID) represent changes in the abundance of transcripts that are significantly involved in known biological processes (BP), cellular components (CC), or molecular functions (MF) with p-value < 0.05%.

GO.ID	Term	Ontology Class	p-value					
			-K-Si vs. +K-Si	-K+Si vs. -K-Si	+K+Si vs. -K-Si	-K-Si vs. +K-Si	-K+Si vs. -K-Si	+K+Si vs. +K-Si
			Leaves			Roots		
GO:0006310	DNA recombination	BP				0.014		
GO:0010498	Proteasomal protein catabolic process	BP				0.025		
GO:0043161	Proteasome-mediated ubiquitin-dependent protein catabolic process	BP				0.025		
GO:0048193	Golgi vesicle transport	BP				0.025		
GO:0010467	Gene expression	BP				0.027		
GO:0090304	Nucleic acid metabolic process	BP				0.036		
GO:0043170	Macromolecule metabolic process	BP				0.046		
GO:0030163	Protein catabolic process	BP					0.010	
GO:0006508	Proteolysis	BP					0.023	
GO:0042545	Cell wall modification	BP					0.028	
GO:1901565	Organonitrogen compound catabolic process	BP					0.030	
GO:0006511	Ubiquitin-dependent protein catabolic process	BP					0.045	
GO:0019941	Modification-dependent protein catabolic process	BP					0.045	
GO:0043632	Modification-dependent macromolecule catabolic process	BP					0.045	
GO:0031109	Microtubule polymerization or depolymerization	BP	0.021					
GO:0006119	Oxidative phosphorylation	BP						0.007
GO:0015980	Energy derivation by oxidation of organic compounds	BP						0.007
GO:0022900	Electron transport chain	BP						0.007
GO:0022904	Respiratory electron transport chain	BP						0.007
GO:0042773	ATP synthesis coupled electron transport	BP						0.007
GO:0045333	Cellular respiration	BP						0.007
GO:0046034	ATP metabolic process	BP						0.014
GO:0006091	Generation of precursor metabolites and energy	BP						0.028
GO:0009126	Purine nucleoside monophosphate metabolic process	BP	0.005					
GO:0009127	Purine nucleoside monophosphate biosynthetic process	BP	0.005					
GO:0009167	Purine ribonucleoside monophosphate metabolic process	BP	0.005					
GO:0009168	Purine ribonucleoside monophosphate biosynthetic process	BP	0.005					
GO:0006366	Transcription by RNA polymerase II	BP	0.008					
GO:0006188	IMP biosynthetic process	BP	0.010					
GO:0007205	Protein kinase c-activating G protein-coupled receptor signaling pathway	BP	0.010					
GO:0046040	IMP metabolic process	BP	0.010					
GO:0006189	'De novo' IMP biosynthetic process	BP	0.021					
GO:0006476	Protein deacetylation	BP	0.021					
GO:0016575	Histone deacetylation	BP	0.021					
GO:0031110	Regulation of microtubule polymerization or depolymerization	BP	0.021					
GO:0032886	Regulation of microtubule-based process	BP	0.021					
GO:0035601	Protein deacylation	BP	0.021					
GO:0050801	Ion homeostasis	BP	0.021					
GO:0055080	Cation homeostasis	BP	0.021					
GO:0070507	Regulation of microtubule cytoskeleton organization	BP	0.021					
GO:0098732	Macromolecule deacylation	BP	0.021					
GO:0098771	Inorganic ion homeostasis	BP	0.021					
GO:0009123	Nucleoside monophosphate metabolic process	BP	0.021					
GO:0009124	Nucleoside monophosphate biosynthetic process	BP	0.021					
GO:0009156	Ribonucleoside monophosphate biosynthetic process	BP	0.021					
GO:0009161	Ribonucleoside monophosphate metabolic process	BP	0.021					
GO:0071805	Potassium ion transmembrane transport	BP	0.023					
GO:0006289	Nucleotide-excision repair	BP	0.041					
GO:0042026	Protein refolding	BP	0.041					
GO:0007020	Microtubule nucleation	BP	0.045					
GO:0007050	Cell cycle arrest	BP	0.045					
GO:0010968	Regulation of microtubule nucleation	BP	0.045					
GO:0031112	Positive regulation of microtubule polymerization or depolymerization	BP	0.045					
GO:0031113	Regulation of microtubule polymerization	BP	0.045					
GO:0031116	Positive regulation of microtubule polymerization	BP	0.045					
GO:0046785	Microtubule polymerization	BP	0.045					
GO:0090063	Positive regulation of microtubule nucleation	BP	0.045					
GO:0016310	Phosphorylation	BP		0.020				
GO:0042546	Cell wall biogenesis	BP		0.003				
GO:0044036	Cell wall macromolecule metabolic process	BP		0.004				
GO:0071554	Cell wall organization or biogenesis	BP		0.007				
GO:0006081	Cellular aldehyde metabolic process	BP		0.007				

Continue of table 1.

GO.ID	Term	Ontology Class	p-value					
			-K-Si vs. +K-Si	-K+Si vs. -K-Si	+K+Si vs. +K-Si	-K-Si vs. +K-Si	-K+Si vs. -K-Si	+K+Si vs. +K-Si
			Leaves			Roots		
GO:0010383	Cell wall polysaccharide metabolic process	BP		0.016				
GO:0010410	Hemicellulose metabolic process	BP		0.016				
GO:0006793	Phosphorus metabolic process	BP		0.019				
GO:0006796	Phosphate-containing compound metabolic process	BP		0.019				
GO:0006468	Protein phosphorylation	BP		0.027				
GO:0006002	Fructose 6-phosphate metabolic process	BP		0.043				
GO:0042822	Pyridoxal phosphate metabolic process	BP		0.043				
GO:0042823	Pyridoxal phosphate biosynthetic process	BP		0.043				
GO:0046184	Aldehyde biosynthetic process	BP		0.043				
GO:0006464	Cellular protein modification process	BP		0.045				
GO:0036211	Protein modification process	BP		0.045				
GO:0072524	Pyridine-containing compound metabolic process	BP		0.047				
GO:0072525	Pyridine-containing compound biosynthetic process	BP		0.047				
GO:0008152	Metabolic process	BP		0.049				
GO:0009432	SOS response	BP			0.008			
GO:0009991	Response to extracellular stimulus	BP			0.008			
GO:0031668	Cellular response to extracellular stimulus	BP			0.008			
GO:0071496	Cellular response to external stimulus	BP			0.008			
GO:0006725	Cellular aromatic compound metabolic process	BP			0.009			
GO:1901360	Organic cyclic compound metabolic process	BP			0.012			
GO:0006558	L-phenylalanine metabolic process	BP			0.023			
GO:0006739	NADP metabolic process	BP			0.023			
GO:1902221	Erythrose 4-phosphate/phosphoenolpyruvate family amino acid metabolic process	BP			0.023			
GO:0006139	Nucleobase-containing compound metabolic process	BP			0.024			
GO:0046483	Heterocycle metabolic process	BP			0.028			
GO:0006259	DNA metabolic process	BP			0.030			
GO:0019438	Aromatic compound biosynthetic process	BP			0.044			
GO:0009605	Response to external stimulus	BP			0.044			
GO:0034404	Nucleobase-containing small molecule biosynthetic process	BP			0.044			
GO:0015935	Small ribosomal subunit	CC				0.031		
GO:1990904	Ribonucleoprotein complex	CC				0.005		
GO:0005783	Endoplasmic reticulum	CC				0.028		
GO:0032993	Protein-DNA complex	CC					0.011	
GO:0000785	Chromatin	CC					0.011	
GO:0000786	Nucleosome	CC					0.011	
GO:0030312	External encapsulating structure	CC					0.025	
GO:0044815	DNA packaging complex	CC					0.011	
GO:0005694	Chromosome	CC					0.014	
GO:0005618	Cell wall	CC					0.025	
GO:0016591	RNA polymerase II, holoenzyme	CC	0.023					
GO:0005819	Spindle	CC	0.025					
GO:0033180	Proton-transporting v-type atpase, V1 domain	CC	0.025					
GO:0009507	Chloroplast	CC		0.012				
GO:0009536	Plastid	CC		0.012				
GO:0048475	Coated membrane	CC		0.034				
GO:0005737	Cytoplasm	CC		0.014				
GO:0030117	Membrane coat	CC		0.034				
GO:0003677	DNA binding	MF			0.042		0.014	
GO:0003676	Nucleic acid binding	MF				0.009	0.033	
GO:0070008	Serine-type exopeptidase activity	MF				0.007		
GO:0008238	Exopeptidase activity	MF				0.014		
GO:0043565	Sequence-specific DNA binding	MF				0.013		
GO:0004180	Carboxypeptidase activity	MF				0.013		
GO:0004185	Serine-type carboxypeptidase activity	MF				0.013		
GO:0004713	Protein tyrosine kinase activity	MF				0.024		
GO:0097159	Organic cyclic compound binding	MF				0.016		
GO:1901363	Heterocyclic compound binding	MF				0.016		
GO:0003684	Damaged DNA binding	MF				0.024		
GO:0140101	Catalytic activity, acting on a tRNA	MF				0.038		
GO:0004252	Serine-type endopeptidase activity	MF					0.002	
GO:0004175	Endopeptidase activity	MF					0.009	
GO:0017171	Serine hydrolase activity	MF					0.037	
GO:0030599	Pectinesterase activity	MF					0.036	
GO:0052689	Carboxylic ester hydrolase activity	MF					0.036	
GO:0008236	Serine-type peptidase activity	MF					0.037	
GO:0046982	Protein heterodimerization activity	MF					0.045	

Continue of table 1.

GO.ID	Term	Ontology Class	p-value					
			-K-Si vs. +K-Si	-K+Si vs. -K-Si	+K+Si vs. +K-Si	-K-Si vs. +K-Si	-K+Si vs. -K-Si	+K+Si vs. +K-Si
			Leaves			Roots		
GO:0008270	Zinc ion binding	MF						0.009
GO:0046914	Transition metal ion binding	MF						0.029
GO:0003954	NADH dehydrogenase activity	MF						0.031
GO:0008137	NADH dehydrogenase (ubiquinone) activity	MF						0.031
GO:0016655	Oxidoreductase activity, acting on NAD(P)H, quinone or similar compound as acceptor	MF						0.031
GO:0050136	NADH dehydrogenase (quinone) activity	MF						0.031
GO:0016651	Oxidoreductase activity, acting on NAD(P)H	MF						0.046
GO:0016810	Hydrolase activity, acting on carbon-nitrogen (but not peptide) bonds	MF	0.010					
GO:0001882	Nucleoside binding	MF	0.028					
GO:0008047	Enzyme activator activity	MF	0.000					
GO:0030695	GTPase regulator activity	MF	0.000					
GO:0060589	Nucleoside-triphosphatase regulator activity	MF	0.002					
GO:0005096	Gtpase activator activity	MF	0.003					
GO:0004143	Diacylglycerol kinase activity	MF	0.011					
GO:0003924	GTPase activity	MF	0.011					
GO:0008641	Ubiquitin-like modifier activating enzyme activity	MF	0.012					
GO:0016877	Ligase activity, forming carbon-sulfur bonds	MF	0.017					
GO:0004407	Histone deacetylase activity	MF	0.023					
GO:0016717	Oxidoreductase activity, acting on paired donors, with oxidation of a pair of donors resulting in th...	MF	0.023					
GO:0016813	Hydrolase activity, acting on carbon-nitrogen (but not peptide) bonds, in linear amidines	MF	0.023					
GO:0019213	Deacetylase activity	MF	0.023					
GO:0033558	Protein deacetylase activity	MF	0.023					
GO:0004518	Nuclease activity	MF	0.024					
GO:0004519	Endonuclease activity	MF	0.027					
GO:0016763	Transferase activity, transferring pentosyl groups	MF		0.005				
GO:0001883	Purine nucleoside binding	MF	0.028					
GO:0005525	GTP binding	MF	0.028					
GO:0032549	Ribonucleoside binding	MF	0.028					
GO:0032550	Purine ribonucleoside binding	MF	0.028					
GO:0032561	Guanyl ribonucleotide binding	MF	0.028					
GO:0004540	Ribonuclease activity	MF	0.029					
GO:0019001	Guanyl nucleotide binding	MF	0.035					
GO:0003746	Translation elongation factor activity	MF	0.037					
GO:0030234	Enzyme regulator activity	MF	0.039					
GO:0044769	Atpase activity, coupled to transmembrane movement of ions, rotational mechanism	MF	0.046					
GO:0046961	Proton-transporting atpase activity, rotational mechanism	MF	0.046					
GO:0004860	Protein kinase inhibitor activity	MF	0.049					
GO:0004861	Cyclin-dependent protein serine/threonine kinase inhibitor activity	MF	0.049					
GO:0017176	Phosphatidylinositol n-acetylglucosaminyltransferase activity	MF	0.049					
GO:0019210	Kinase inhibitor activity	MF	0.049					
GO:0030291	Protein serine/threonine kinase inhibitor activity	MF	0.049					
GO:0033218	Amide binding	MF		0.017				
GO:0016740	Transferase activity	MF		0.001				
GO:0072341	Modified amino acid binding	MF		0.017				
GO:0003824	Catalytic activity	MF		0.017				
GO:0016773	Phosphotransferase activity, alcohol group as acceptor	MF		0.032				
GO:0016757	Transferase activity, transferring glycosyl groups	MF		0.045				
GO:0003872	6-phosphofructokinase activity	MF		0.046				
GO:0003950	NAD+ ADP-ribosyltransferase activity	MF		0.046				
GO:0004470	Malic enzyme activity	MF		0.046				
GO:0004471	Malate dehydrogenase (decarboxylating) (NAD+) activity	MF		0.046				
GO:0004527	Exonuclease activity	MF		0.046				
GO:0008443	Phosphofructokinase activity	MF		0.046				
GO:0046912	Transferase activity, transferring acyl groups, acyl groups converted into alkyl on transfer	MF		0.046				
GO:0003697	Single-stranded DNA binding	MF			0.001			
GO:0008094	DNA-dependent atpase activity	MF			0.011			
GO:0005507	Copper ion binding	MF			0.041			
GO:0009982	Pseudouridine synthase activity	MF			0.041			
GO:0003700	DNA-binding transcription factor activity	MF			0.048			

Based on the observation that the K deficiency-dependent GO term “cation transport” disappeared in the presence of Si (Table 1), expression changes of the genes encoding K and Si transport proteins were verified by qPCR. In fully expanded leaves, transcript levels of the Si importer *Lsi1* were upregulated by Si, whereas they were repressed under K deficiency (Table 2A). qPCR analysis confirmed this mode of regulation also for the Si exporter *Lsi2* (Figure 20A, B). Transcriptome analysis identified a couple of genes that were strongly upregulated by Si supply in K-deficient plants, including *KCO1*, which encodes a tonoplast outward-rectifying K channel, the two high-affinity K transporters *HAK8* and *HAK2,* and the K-selective inward-rectifying channel *AKT2* (Boscari *et al.*, 2009; Feng *et al.*, 2020). With respect to their downregulation under K deficiency (-K-Si vs. +K-Si), Si largely reverted their transcriptional regulation. Conversely, the K deficiency-induced high-affinity K transporter *HAK1* (Santa-María *et al.*, 1997) and two paralogs were repressed by the Si treatment. qPCR analysis confirmed that in leaves *HAK1*, together with the inward-rectifying K channel *AKT1*, were downregulated upon Si supply to K-deficient plants while *AKT2* and in particular *KCO1* were upregulated (Figure 21A-F). Another group of genes that showed a highly significant transcriptional response to K and Si relates to gibberellins-dependent processes (Table 2A). Upregulation by Si application was observed for *GA_{20}-oxidase2* that plays a key role in gibberellins biosynthesis, and other genes that are involved in gibberellins catabolism, like *GA_2-oxidase*, or in gibberellins signaling, like *RGA1* encoding a DELLA-type repressor of the gibberellins signaling pathway, *CBF1*, a cold-responsive transcription factor suppressing gibberellins biosynthesis through enhanced expression of DELLA genes, and *PIF4*, a light-regulated transcription factor targeted by DELLA proteins. However, *GA_2-oxidase3*, which is involved in gibberellins catabolism, and *WRKY12*, a transcription factor regulating gibberellins-related genes, were downregulated under low K condition after Si supply (Table 2A). All of these genes showed an opposite transcriptional regulation in the absence of Si (Table 2A).

A small group of upregulated genes by Si under K deficiency relates to ethylene-dependent processes, such as *ACO3*, which oxidates 1-aminocyclopropane-1-carboxylic acid (ACC) and converts it into ethylene, and *RAP2-7*, that plays an important role in the ethylene signaling pathway. Both genes showed an opposite transcriptional regulation under low K condition (Table 2A). Also, *JAR1*, which catalyzes the synthesis of jasmonate-amino acid conjugates like JA-Ile, showed a similar expression pattern under low K and Si treatments (Table 2A). Taken together, several genes involved in gibberellins, ethylene and JA metabolism or signaling and most likely some of their upstream regulators significantly reverted their K deficiency response after Si supply, or Si simply prevented their response to K deficiency.

Regarding transcriptional changes in roots, upon Si supply to K-deficient roots, *Lsi1* was downregulated along with *Lsi2* and *Lsi6* (Figure 20D-F; Table 2B), suggesting their suppression in the presence of Si. However, *Lsi1* was upregulated under K deficiency (Figure 20D). Similar as in shoots, Si supply upregulated transcript levels of *KCO1* as well as a poorly characterized voltage-gated potassium channel subunit beta in roots under K deficiency (Table 2B). Whereas, all major genes involve in root K uptake, i.e., *HAK1*, *HAK4*, *AKT1*, also *AKT2* that likely relates to K re-translocation, and the xylem loader *SKOR*, which are upregulated under

low K condition, were suppressed by Si in K-deficient roots (Figure 21G-K; Table 2B). The transcript levels of gibberellins- and ethylene-related genes i.e., *CBF1*, *ACO1* and *ACC* were strongly increased after Si application (Table 2B). Altogether, the impact of Si supplementation on transcriptional regulation of K transporters was much stronger in K-deficient than in K-sufficient plants, and transcript levels of several of the K transporters were reverted when Si was supplemented to K-deficient plants, indicating a profound impact of Si on K transport processes in roots and shoots.

Table 2. Relative expression changes of genes with confirmed or putative functions in response to K or Si. Fold-change and adjusted (adj.) p-value for genes expressed in (A) the last fully expanded leaves or (B) roots of barley. Genes are grouped according to their transcript abundance under Si supply under low K (-K+Si vs. -K-Si) and compared to their abundance under low K versus adequate K in the absence of Si (-K-Si vs. +K-Si); VGSU = voltage-gated subunit beta. Heatmap represents fold-change of up- (red) or downregulation (blue).

A Last fully expanded leaves

Gene ID	Annotation	-K+Si vs. -K-Si	adj. p-value	-K-Si vs. +K-Si	adj. p-value
HORVU6Hr1G075850	Si transporter (Lsi1)	0.70	1.6E-02	-1.62	4.8E-09
HORVU5Hr1G095550	K channel (KCO1-like)	1.21	9.3E-08	-0.99	6.1E-06
HORVU5Hr1G095590	K channel (KCO1-like)	1.14	2.7E-07	-1.42	1.0E-11
HORVU5Hr1G095540	K channel (KCO1)	1.02	6.7E-08	-0.61	1.1E-03
HORVU4Hr1G049320	K transporter (HAK8)	0.44	2.6E-02	-1.39	1.8E-15
HORVU2Hr1G020220	K transporter (HAK2)	0.32	6.3E-03	-0.27	1.7E-02
HORVU1Hr1G065250	K channel (AKT2)	0.29	4.6E-03		7.8E-01
HORVU5Hr1G059200	K transporter (HAK23)	-0.46	9.2E-05	0.88	2.4E-15
HORVU2Hr1G071570	K transporter (HAK1)	-0.71	2.1E-03	2.06	9.5E-19
HORVU3Hr1G096860	K transporter (HAK5)	-0.88	3.8E-04	4.67	2.1E-75
HORVU6Hr1G073510	K transporter (HAK16)	-1.18	4.2E-09	2.52	9.6E-33
HORVU1Hr1G063780	GA20-oxidase 2	5.22	7.1E-04	-7.00	3.2E-06
HORVU2Hr1G090030	GA2-oxidase	3.82	2.8E-03	-2.69	1.2E-02
HORVU2Hr1G032420	DELLA protein (RGA1)	3.40	1.5E-04	-6.06	3.2E-13
HORVU0Hr1G016540	Transcription factor (CBF1)	3.35	1.0E-05	-3.81	9.0E-08
HORVU5Hr1G011780	Transcription factor (PIF4)	1.78	3.6E-12	-1.02	4.2E-05
HORVU3Hr1G072810	GA2-oxidase 3	-0.72	1.7E-02	2.13	3.8E-11
HORVU2Hr1G001780	Transcription factor (WRKY12)	-1.24	5.2E-07	3.16	1.7E-30
HORVU5Hr1G067490	ACO3	1.71	2.7E-26	-3.03	3.3E-88
HORVU1Hr1G011800	Transcription factor (RAP2-7)	1.68	7.8E-32	-1.66	5.5E-33
HORVU1Hr1G092890	JAR1	1.75	8.5E-17	-1.46	6.8E-13

B Roots

HORVU3Hr1G110530	Si transporter (Lsi2)	-0.58	1.4E-02		3.9E-01
HORVU5Hr1G095540	K channel (KCO1)	0.74	5.7E-03		8.0E-01
HORVU5Hr1G095590	K channel (KCO1-like)	0.62	3.3E-03		3.3E-01
HORVU6Hr1G091250	K channel (VGSU)	0.35	1.2E-02	-0.74	2.1E-09
HORVU4Hr1G079150	K transporter (HAK1)	-0.52	6.0E-04	4.13	3.0E-18
HORVU2Hr1G099810	K transporter (HAK15)	-0.64	1.4E-03	0.71	1.5E-04
HORVU0Hr1G016540	Transcription factor (CBF1)	3.90	1.1E-04		2.3E-01
HORVU2Hr1G004200	ACO1	5.91	3.7E-04		9.5E-01
HORVU4Hr1G009800	ACC synthase (ACS1)	2.33	6.8E-03		5.1E-01

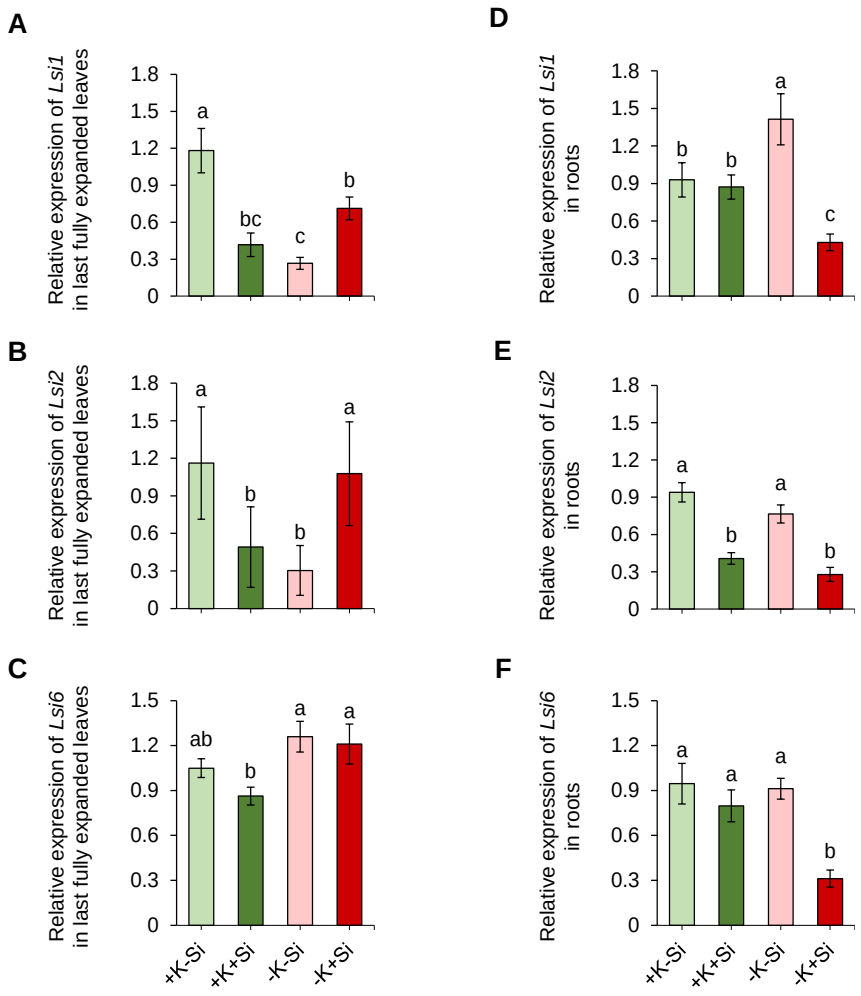

Figure 20. Influence of Si supply on relative expression of Si transporter genes in leaves or roots of barley plants grown under adequate or low K supply. (A-F) Relative mRNA levels of the influx Si transporter *Lsi1* (A, D), efflux Si transporter *Lsi2* (B, E), and inter-vascular Si transporter *Lsi6* (C, F) in leaves (A-C), or in roots (D-F). After 7 days of germination, plants were grown under either adequate (2 mM) or low (0.04 mM) K for 24 days in the absence or presence of 1.78 mM Si. Gene expression was assessed by quantitative real-time PCR analysis and normalized to *UBI* and *CYP*. Leaf analysis is based on the last fully expanded leaf. Bars indicate means ± SE. Different letters denote significant differences among treatments according to LSD test ($p < 0.05$; $n = 8$).

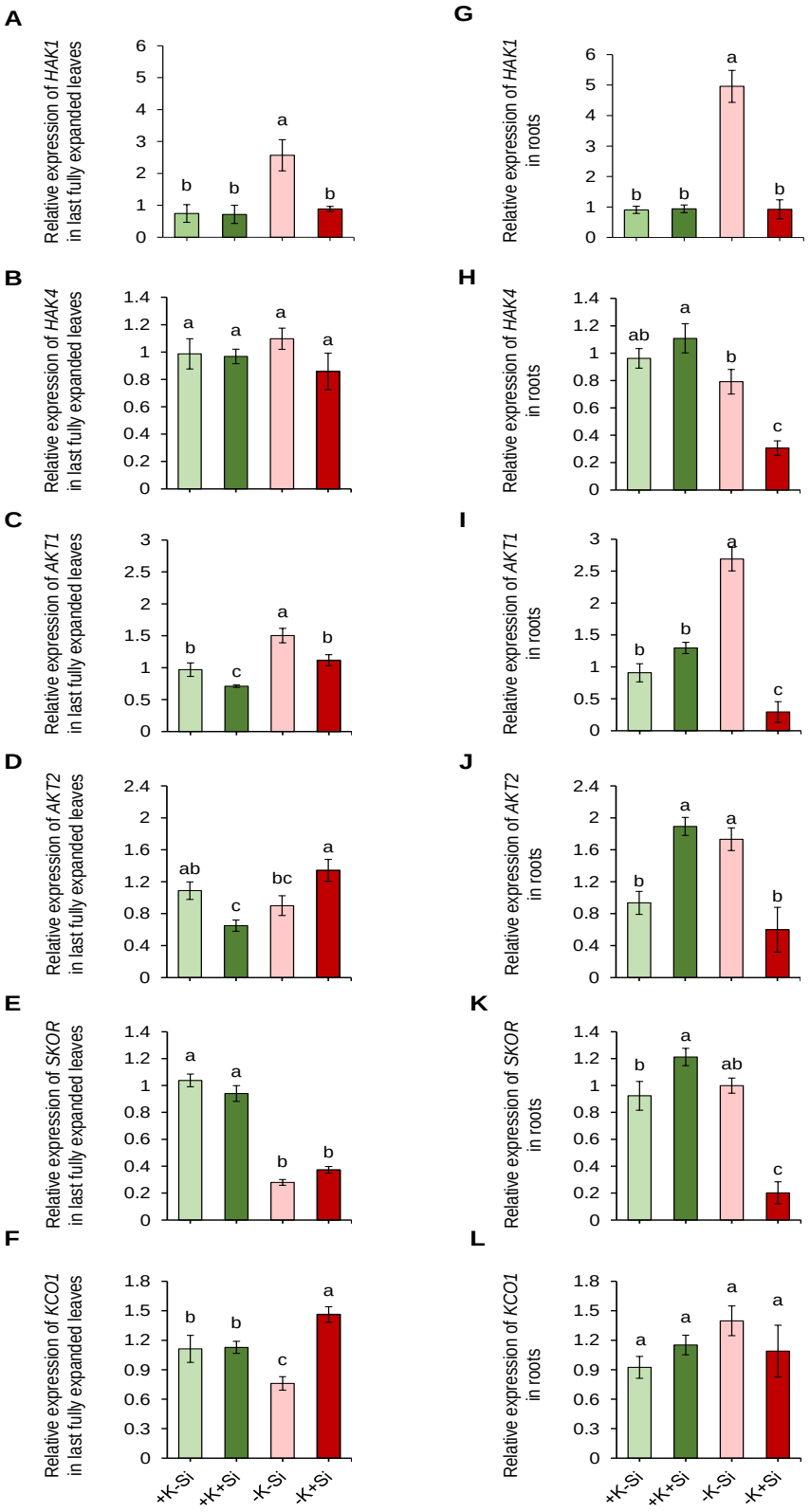

Figure 21. Influence of Si supply on relative expression of K transporter genes in leaves or roots of barley plants grown under adequate or low K supply. (A-L) Relative mRNA levels of the high-affinity K transporter *HAK1* (A, G), *HAK4* (B, H), inward-rectifying K channel *AKT1* (C, I), K-selective channel *AKT2* (D, J), stelar outward-rectifying K channel *SKOR* (E, K), and tonoplast outward-rectifying K channel *KCO1* (F, L) in leaves (A-F), or in roots (G-L). After 7 days of germination, plants were grown under either adequate (2 mM) or low (0.04 mM) K for 24 days in the absence or presence of 1.78 mM Si. Gene expression was assessed by quantitative real-time PCR analysis and normalized to *UBI* and *CYP*. Leaf analysis is based on the last fully expanded leaf. Bars indicate means ± SE. Different letters denote significant differences among treatments according to LSD test ($p < 0.05$; $n = 8$).

4.6 Impact of silicon application on root uptake and root-to-shoot translocation of potassium in plants under potassium starvation

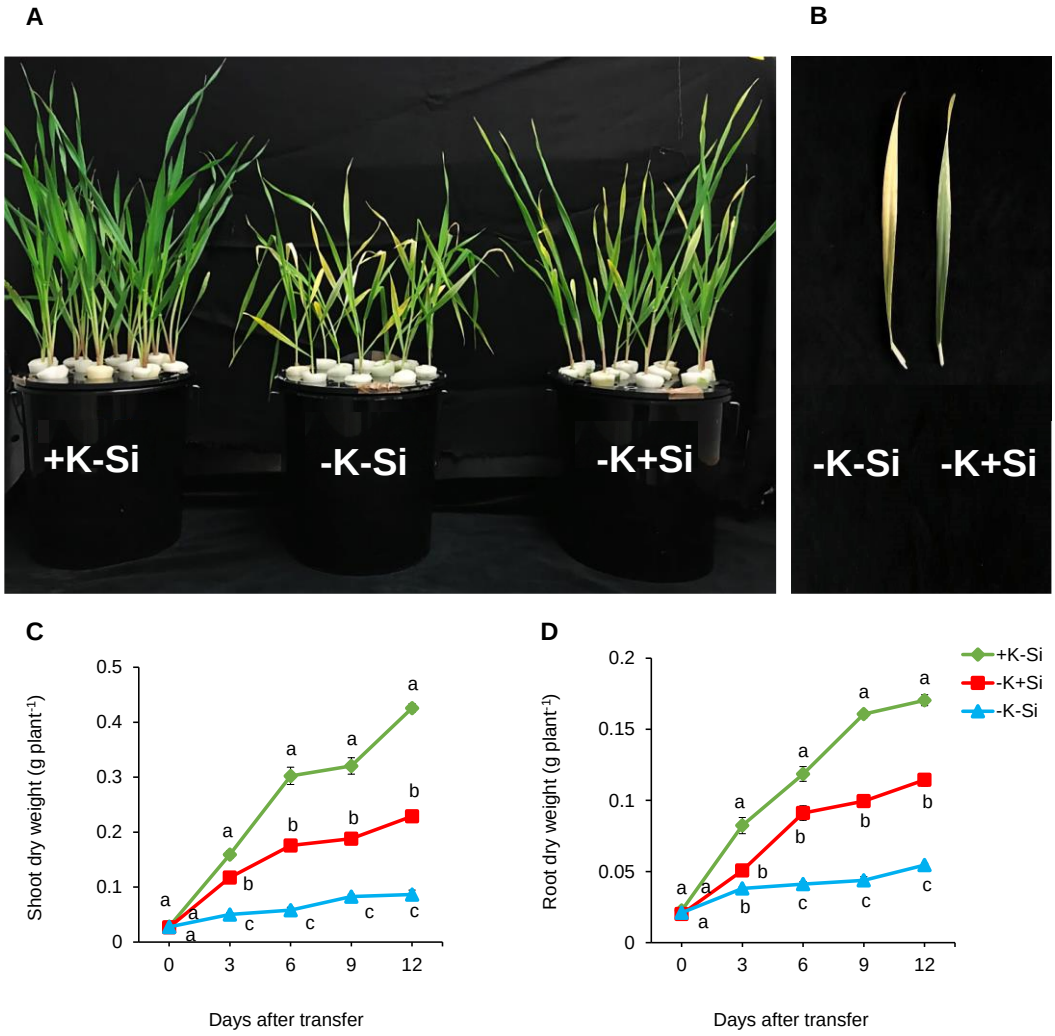

Figure 22. Influence of Si supply on visual appearance as well as shoot and root dry weights of barley plants grown with adequate or without K supply. (A, B) Visual appearance of shoots and of individual source leaves after 12 days of treatments. (C) Shoot dry weights and (D) root dry weights of plants. After 7 days of germination, plants were grown under continuous supply of adequate (2 mM) K or in K-free nutrient solution for 12 days either in the absence or presence of 1.78 mM Si. Symbols indicate means ± SE. Different letters denote significant differences among treatments according to one-way ANOVA and post-hoc Tukey's test ($p < 0.05$; $n = 6$).

Since the first experiment reflected the long-term impact of Si on K-deficient plants (Figure 5), the hypothesis whether there is an immediate effect of Si on the regulation of K uptake and translocation was investigated by conducting short-term K influx measurements using Rb as a tracer for K transport processes. After 7 days of germination, plants were transferred to a K-free solution in the presence or absence of Si, and sampled at five time points between 0 to 12 days after transfer. While biomass increase immediately slowed down under K starvation, successive harvesting showed that the simultaneous presence of Si increased shoot and root growth rates by two- to three-fold in K-starved plants, going along with weaker K starvation-induced chlorosis and necrosis in leaves (Figure 22A-C). To address the question of whether Si can influence K transport activity in roots and subsequent root-to-shoot

translocation, elemental analysis of roots and shoots was performed using ICP-MS. Continuous growth of plants under adequate K supply and in the absence of Si resulted in poor Si enrichment in root and shoot tissues, which originated from initial seed content and was diluted by biomass gain (Figure 23A; 24A). Meanwhile, K concentrations slightly increased, from 60 to approx. 75 mg g^{-1} in roots or from 48 to approx. 60 mg g^{-1} in shoots (Figure 23B; 24B). As consequence of increasing plant biomass (Figure 22C, D), K contents sharply increased from 1.4 to approx. 13 mg $plant^{-1}$ in roots, and 25 mg $plant^{-1}$ in shoots during the growth period of 12 days (Figure 23C; 24C). During this monitored time, the short-term influx of Rb in roots as well as the translocation rate of this tracer from roots-to-shoots, decreased from a rather low level to almost zero (Figure 23D; 24D), reflecting high K saturation in these plants. When K was withheld from the nutrient solution, Si levels remained low and largely unaffected, whereas K concentrations dropped from adequate levels within 3 days to half in roots and to only one fifth in shoots (Figure 23E-F; 24E-F). Within the next 3 days they dropped to a constant level of approx. 5 mg g^{-1} in roots, which remained stable, or first to approx. 9 and then to 5 mg g^{-1} in leaves, indicating K deficiency in both organs.

As a consequence of K starvation and reduced plant biomass (Figure 22C, D), K contents decreased by four- to six-fold in roots and by four-fold in shoots after 6 and 3 days of growth in the absence of K, respectively (Figure 23G; 24G). At the same time frame, Rb influx increased by approx. ten-fold within 3 days and doubled again over the next 3 days of K starvation before it established at a lower level thereafter (Figure 23H). Meanwhile, root-to-shoot translocation rates of Rb remained unaffected in 6 days and decreased to even lower values than at the beginning of the K starvation period within next 6 days (Figure 24H), implicating an exhausted translocation capacity for K. In K-starved plants grown under supply of Si, Si concentrations boosted from approx. 0.2 to more than 3 mg g^{-1} in roots and shoots within 12 days (Figure 23I; 24I). Like in the absence of Si, root K concentrations and contents dropped after 6 days, but then decreased to even lower levels during the following 6 days (Figure 23F-G, J-K). Irrespective of Si supply, the initial phase of K depletion in roots was associated with a significant increase in Rb influx (Figure 23H, L).

However, only in the presence of Si there was a further three- to four-fold increase in Rb influx at day 9 and 12, which was in sharp contrast to roots grown in the absence of Si where influx declined (Figure 23H, L). In Si-exposed shoots, K concentrations dropped after 3 days to a similarly low level as in the absence of Si, however, at d 9 and 12 they did not drop further but remained approx. two-fold higher than in absence of Si (Figure 24F, J). Within the first 3 days, K contents remained stable, but increased near 1.5-fold in the next 6 days and then doubled again within the last 3 days which was ten-fold higher than in shoots grown in the absence of Si, suggesting that Si increased the pool size of available K in shoots (Figure 24G, K). Along the same line, increased K contents coincided with an enhanced root-to-shoot translocation of Rb, in particular the latter phase, which associated with higher root Rb influx at day 12 (Figure 23L; 24L). Considering the tracer function of Rb for K, Si increased the capacity for root-to-shoot translocation of K immediately after onset of K starvation and again at a more advanced stage.

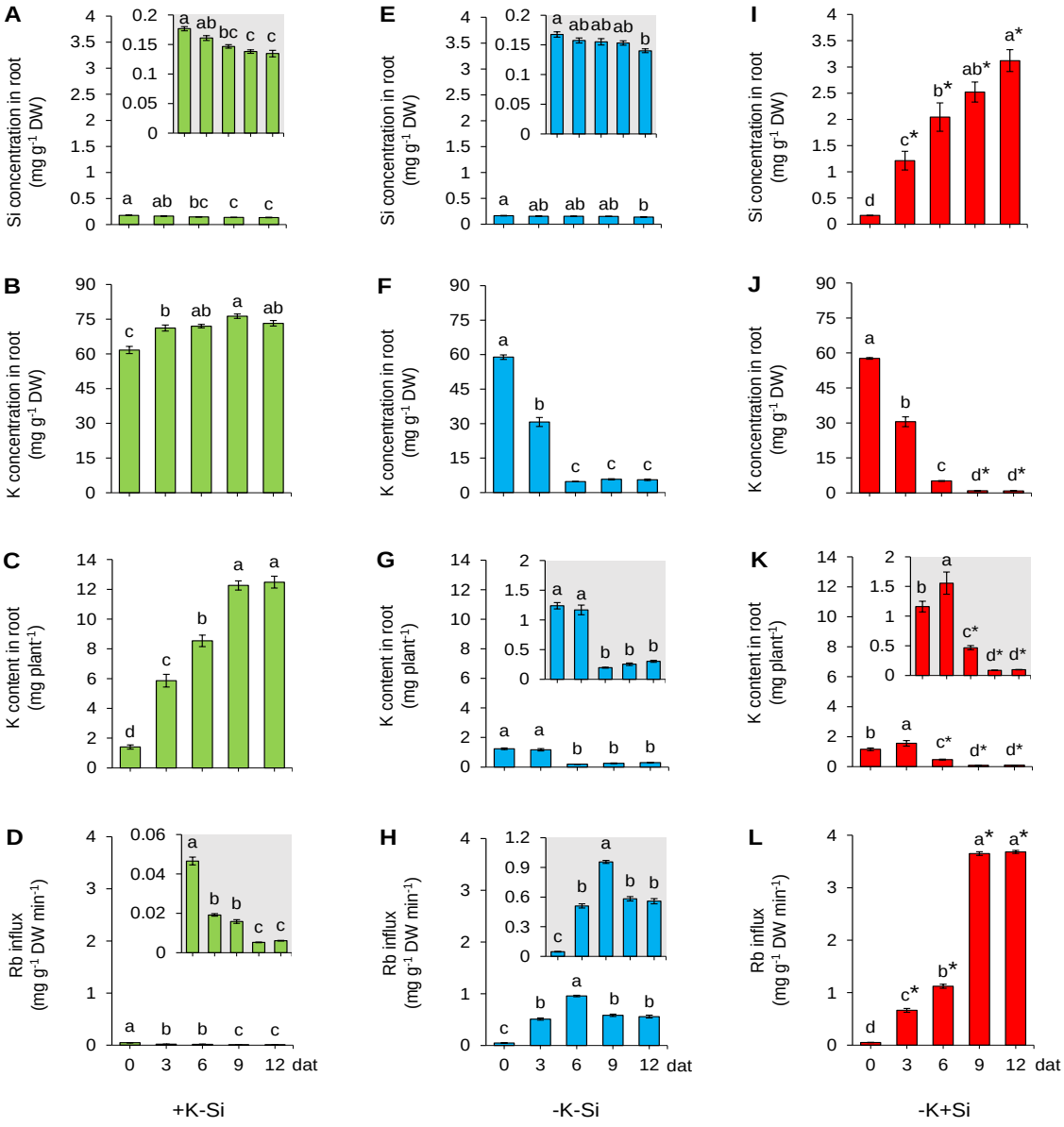

Figure 23. Influence of Si supply on Si and K accumulation and Rb influx in roots of barley plants grown with adequate or without K supply. (A-L) Concentrations of silicon (Si; A, E, I), potassium (K; B, F, J), contents of K (C, G, K), and uptake rates of rubidium (Rb influx; D, H, L) in roots. After 7 days of germination, plants were grown under continuous supply of adequate (2 mM) K (A-D) or in K-free nutrient solution (E-L) for 12 days either in the absence of Si (A-H) or presence of 1.78 mM Si (I-L). Rb influx was assessed by exposing roots to 1 mM Rb for 10 min. Roots were examined every 3 days between 0 and 12 days after transfer to K and Si treatments. Bars indicate means ± SE. Different letters denote significant differences among time points and stars denote significant differences between -K-Si and -K+Si according to one-way ANOVA and post-hoc Tukey's test ($p < 0.05$; $n = 6$).

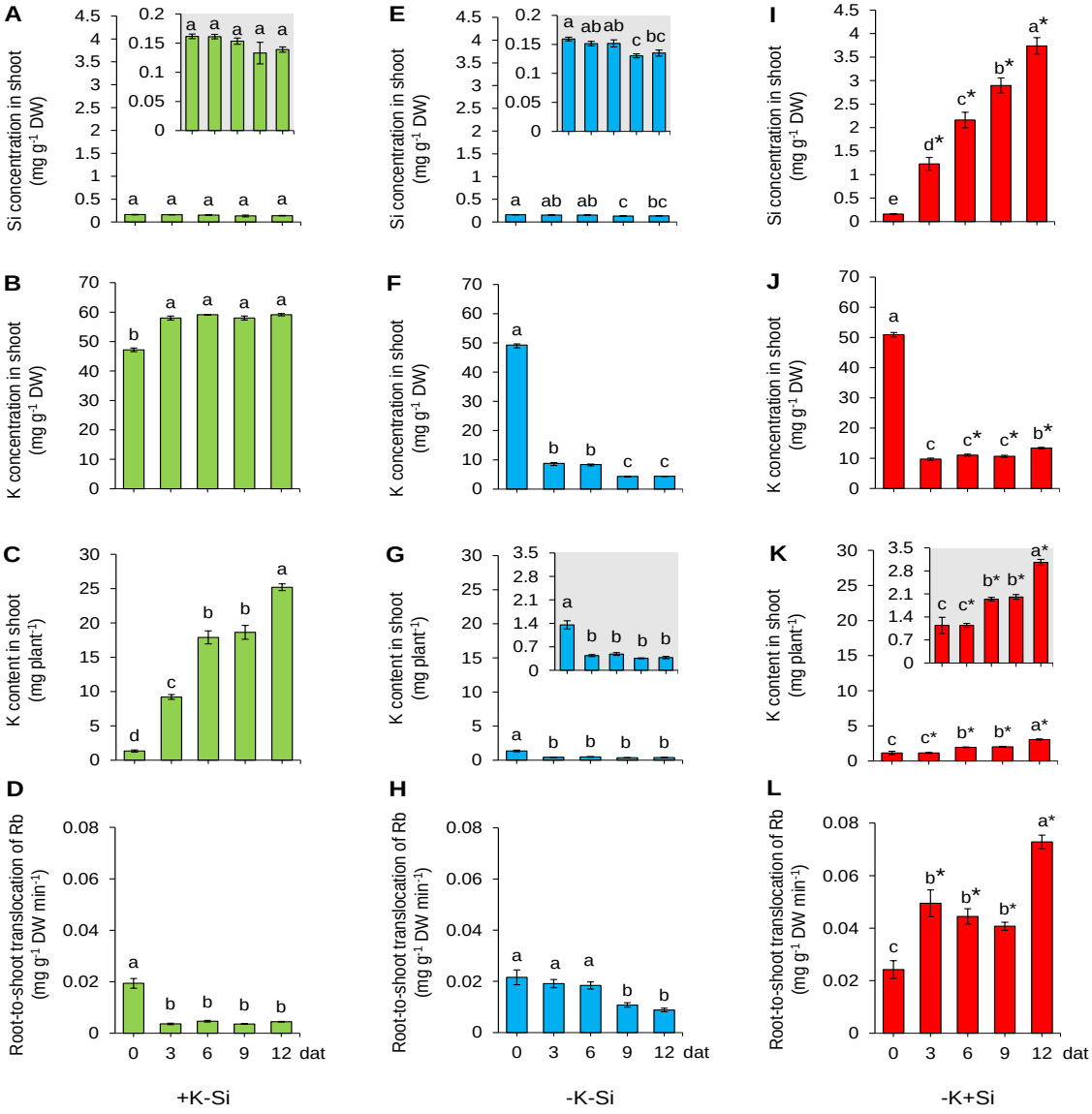

Figure 24. Influence of Si supply on Si and K accumulation in shoots and root-to-shoot translocation rates of Rb in barley plants grown with adequate or without K supply. (A-L) Concentrations of silicon (Si; A, E, I), potassium (K; B, F, J), contents of K (C, G, K) in shoots, and root-to-shoot translocation of Rb (D, H, L). After 7 days of germination, plants were grown under continuous supply of adequate (2 mM) K (A-D) or in K-free nutrient solution (E-L) for 12 days either in the absence of Si (A-H) or presence of 1.78 mM Si (I-L). Root-to-shoot translocation of Rb was assessed by exposing roots to 1 mM Rb for 10 min. Shoots were examined every 3 days between 0 and 12 days after transfer to K and Si treatments. Bars indicate means ± SE. Different letters denote significant differences among time points and stars denote significant differences between -K-Si and -K+Si according to one-way ANOVA and post-hoc Tukey's test ($p < 0.05$; $n = 6$).

Subsequently, the transcriptional response of K and Si transporter genes in shoots and roots was assessed in response to the different treatments. As expected, the continuous growth of plants under adequate K supply and in absence of Si did not significantly alter the transcript levels of K transporters in roots. 3-6 days after transfer, there was a slight upregulation of the low-affinity K channel *AKT1* and a slight repression of the high-affinity transporter *HAK1* and *HAK4* as well as of the vacuolar K exporter *KCO1* (Figure 25A-F). When K was withheld from the nutrient solution, transcript levels of several root K transporters and channels increased. *HAK1*, *HAK4*, *AKT2* and with some delay also *AKT1* were upregulated under K deficiency for a period of 3-9 days before declining (Figure 25G-L), indicating their induction or de-repression by K deficiency as shown for *HAK1* (Fulgenzi *et al.*, 2008). This response largely coincided with changes in Rb influx in roots (Figure 23H). In contrast, when K-starved roots were grown in the presence of Si, the earliest and strongest upregulation was observed for *KCO1*, whose mRNA levels increased by three-fold within the first 3 days before gradually decreasing thereafter (Figure 25M-R). With some delay, the mRNA levels of *AKT2* also showed a transient increase. Interestingly, transcript levels of *HAK1*, *HAK4* and *AKT1* peaked much later at day 9 or 12; this also held true for the xylem loader *SKOR*. Thus, Si supplementation provoked a differential transcriptional response of K transporters to K starvation, characterized by an initial activation of *KCO1* and a subsequent stepwise upregulation of *AKT2*, *HAK4*, *HAK1*, *SKOR* and finally *AKT1*. In general, transcript levels of Si transporters in roots were hardly affected by K nutrition and Si supply. The most remarkable response was observed for *Lsi1* and *Lsi2*, which were downregulated in K-deficient roots under the prolonged presence of Si at day 12 (Figure 26A-I).

In shoots of plants grown continuously under adequate K and in the absence of Si, only *AKT2* was significantly upregulated from day 6 onwards, which may reflect its involvement in K uptake in mesophyll leaves and K cycling via the phloem (Feng *et al.*, 2020); at the same time, *HAK4* and *KCO1* were slightly downregulated (Figure 27A-F). Changes in gene expression were rather weak in the shoots of plants grown under K starvation and in the absence of Si. Only the mRNA levels of *HAK1* and *AKT2* significantly increased at day 6 (Figure 27G-L), which coincided with a higher rate of root-to-shoot translocation of Rb at this time point (Figure 24H). As a consequence of Si supply to K-starved plants, transcript levels of *HAK4* increased at day 6, followed by an increase of *AKT2* and *AKT1* (Figure 27M-R). Compared to Si-depleted plants, this transcriptional response indicates that the presence of Si alters both, the type of K transporters and the timing of their regulation during progressing K starvation in leaves. Also in shoots, transcript levels of all Si transporters remained at a rather constant expression level without considerable changes in response to the K and Si treatments (Figure 28A-I).

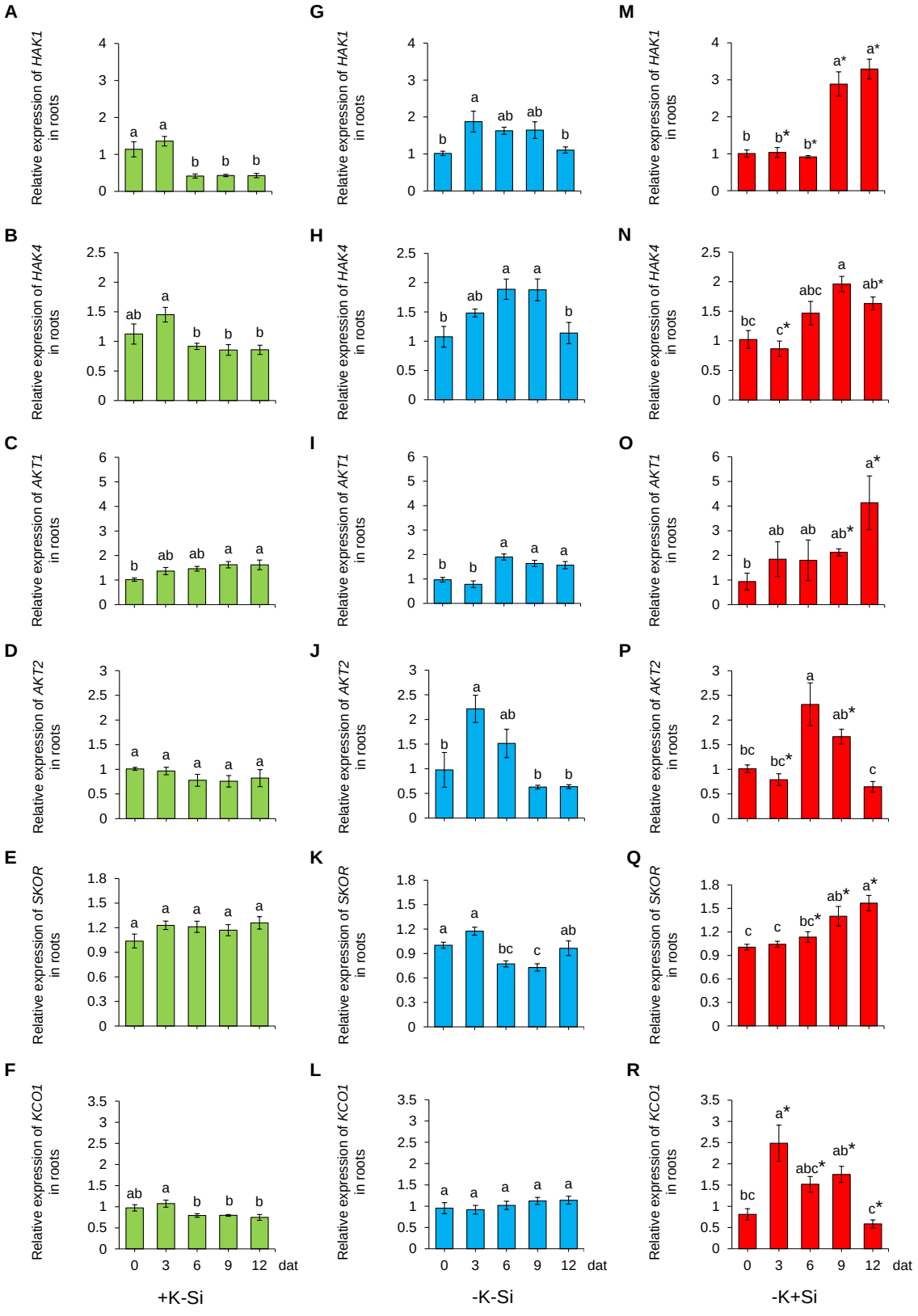

Figure 25. Influence of Si supply on relative expression of K transporter genes in roots of barley plants grown with adequate or without K supply. (A-R) Relative mRNA levels of the high-affinity K transporter *HAK1* (A, G, M) and *HAK4* (B, H, N), inward-rectifying K channel *AKT1* (C, I, O), K-selective channel *AKT2* (D, J, P), stelar outward-rectifying K channel *SKOR* (E, K, Q), and tonoplast outward-rectifying K channel *KCO1* (F, L, R). After 7 days of germination, plants were grown under continuous supply of adequate (2 mM) K (A-F) or in K-free nutrient solution (G-R) for 12 days either in the absence of Si (A-L) or presence of 1.78 mM Si (M-R). Gene expression was assessed by quantitative real-time PCR analysis and normalized to *UBI* and *CYP*. Bars indicate means ± SE. Different letters denote significant differences among time points and stars denote significant differences between -K-Si and -K+Si according to one-way ANOVA and post-hoc Tukey's test ($p < 0.05$; $n = 6$).

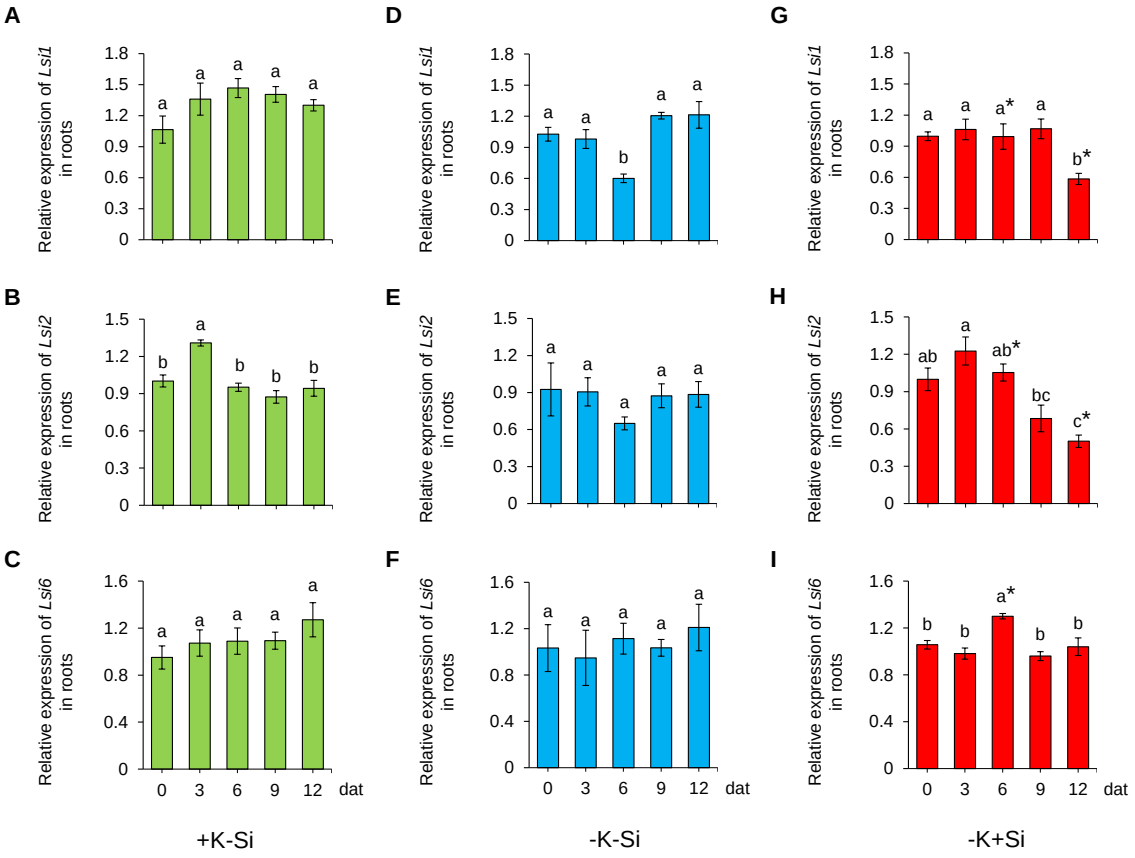

Figure 26. Influence of Si supply on relative expression of Si transporter genes in roots of barley plants grown with adequate or without K supply. (A-I) Relative mRNA levels of the influx Si transporter *Lsi1* (A, D, G), efflux Si transporter *Lsi2* (B, E, H), and inter-vascular Si transporter *Lsi6* (C, F, I). After 7 days of germination, plants were grown under continuous supply of adequate (2 mM) K (A-C) or in K-free nutrient solution (D-I) for 12 days either in the absence of Si (A-F) or presence of 1.78 mM Si (G-I). Gene expression was assessed by quantitative real-time PCR analysis and normalized to *UBI* and *CYP*. Bars indicate means ± SE. Different letters denote significant differences among time points and stars denote significant differences between -K-Si and -K+Si according to one-way ANOVA and post-hoc Tukey's test ($p < 0.05$; $n = 6$).

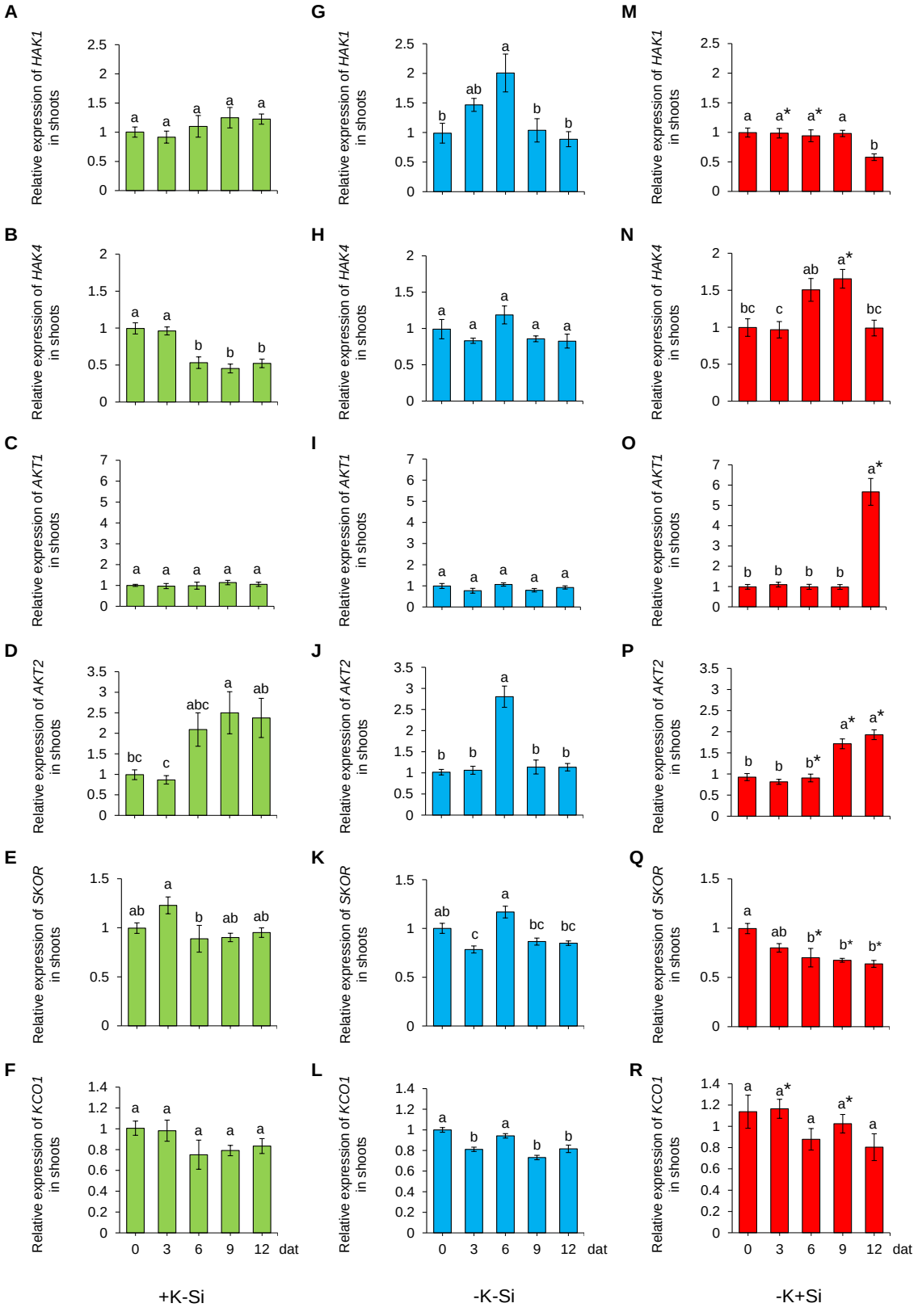

Figure 27. Influence of Si supply on relative expression of K transporter genes in shoots of barley plants grown with adequate or without K supply. (A-R) Relative mRNA levels of the high-affinity K transporter *HAK1* (A, G, M) and *HAK4* (B, H, N) inward-rectifying K channel *AKT1*(C, I, O), K-selective channel *AKT2* (D, J, P), stelar outward-rectifying K channel *SKOR* (E, K, Q), and tonoplast outward-rectifying K channel *KCO1* (F, L, R). After 7 days of germination, plants were grown under continuous supply of adequate (2 mM) K (A-F) or in K-free nutrient solution (G-R) for 12 days either in the absence of Si (A-L) or presence of 1.78 mM Si (M-R). Gene expression was assessed by quantitative real-time PCR analysis and normalized to *UBI* and *CYP*. Bars indicate means ± SE. Different letters denote significant differences among time points and stars denote significant differences between -K-Si and -K+Si according to one-way ANOVA and post-hoc Tukey's test ($p < 0.05$; $n = 6$).

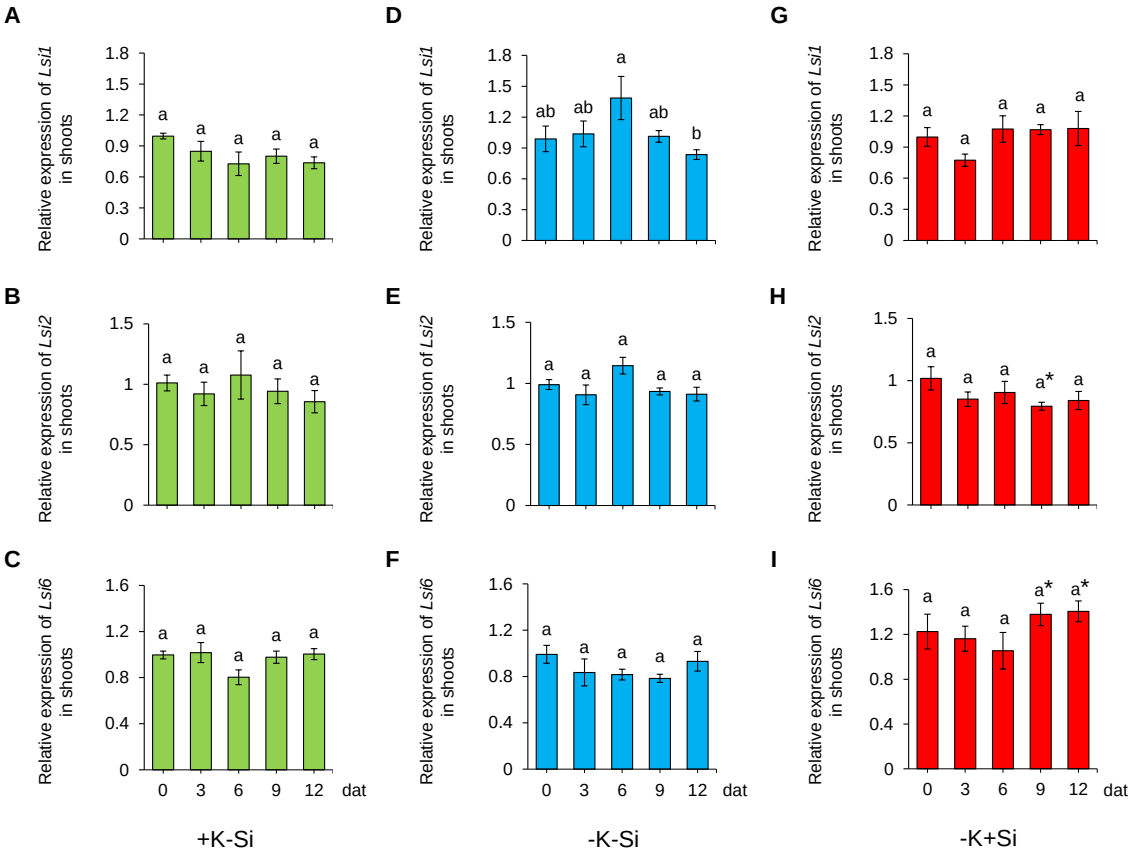

Figure 28. Influence of Si supply on relative expression of Si transporter genes in shoots of barley plants grown with adequate or without K supply. (A-I) Relative mRNA levels of the influx Si transporter *Lsi1* (A, D, G), efflux Si transporter *Lsi2* (B, E, H), and inter-vascular Si transporter *Lsi6* (C, F, I). After 7 days of germination, plants were grown under continuous supply of adequate (2 mM) K (A-C) or in K-free nutrient solution (D-I) for 12 days either in the absence of Si (A-F) or presence of 1.78 mM Si (G-I). Gene expression was assessed by quantitative real-time PCR analysis and normalized to *UBI* and *CYP*. Bars indicate means ± SE. Different letters denote significant differences among time points and stars denote significant differences between -K-Si and -K+Si according to one-way ANOVA and post-hoc Tukey's test ($p < 0.05$; $n = 6$).

4.7 Effect of manipulated gibberellin biosynthesis on silicon-mediated mitigation of potassium deficiency

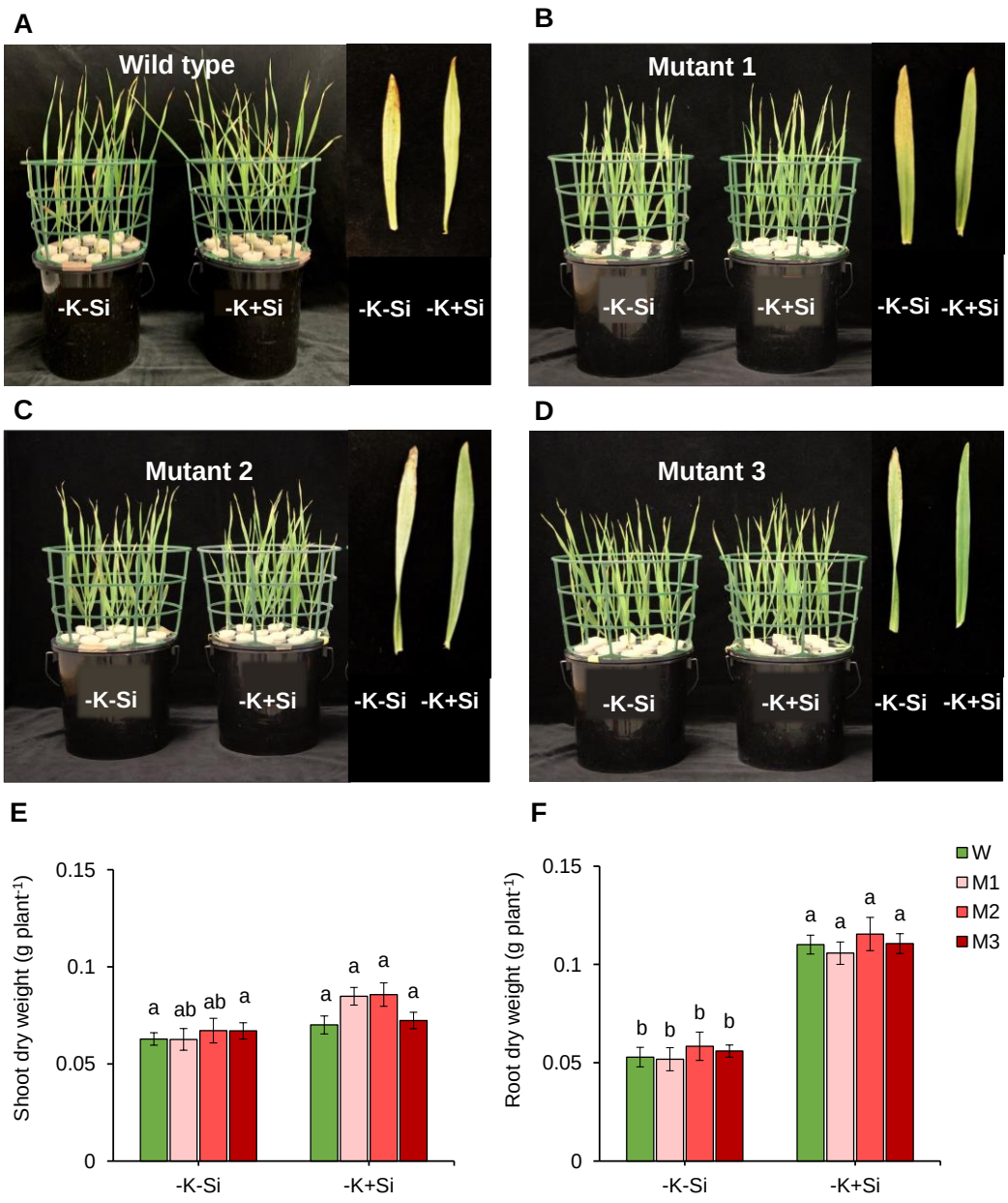

Figure 29. Influence of Si supply on visual appearance as well as shoot and root dry weights of wild-type and *GA20-oxidase2* mutated lines 1, 2, and 3 (W, M1, M2, M3) grown without K supply. (A-D) Visual appearance of shoots and of individual source leaves, (E) shoot dry weights, and (F) root dry weights of plants. After 7 days of germination, plants were grown continuously in K-free nutrient solution for 14 days either in the absence or presence of 1.78 mM Si. Bars indicate means ± SE. Different letters denote significant differences among treatments according to one-way ANOVA and post-hoc Tukey's test ($p < 0.05$; $n = 5$).

Based on transcriptome changes after long-term K deficiency, one group of genes that showed a highly significant transcriptional response to K and Si was related to gibberellins-dependent processes (Table 2A). These results raised the hypothesis of whether Si interferes with gibberellins biosynthesis and signaling pathways to restore cell elongation and growth-related processes. To verify a dependency of the beneficial Si effect on K-deficient plants, a hydroponic experiment was conducted with three barley *GA$_{20}$-oxidase2* mutated lines and a

wild-type line as reference, Si was applied in the absence of K, and the growth response was monitored after 14 days. Unexpectedly, in contrast to the former experiments, Si supplementation did not result in higher shoot biomass, but only increased root dry weights by approx. two-fold (Figure 29E, F). This different growth response to Si might be due to the fact that a different barley genotype, cv. Golden Promise, had to be used in this experiment to allow comparison with the existing *GA$_{20}$-oxidase2*-genome-edited plants. In fact, Si partially alleviated K starvation-induced chlorosis and necrosis in old leaves of the wild-type and all *GA$_{20}$-oxidase2* mutated lines (Figure 29A-D), suggesting that the beneficial effect of Si on K starvation symptoms is independent of gibberellins biosynthesis or at least of GA$_{20}$-oxidase2-dependent gibberellins biosynthesis.

To address the question of whether Si increased the uptake capacity, translocation or internal distribution of K in a GA$_{20}$-oxidase2-dependent manner, elemental analysis of roots and shoots was performed by ICP-OES. Continuous growth of K-starved wild-type plants and *GA$_{20}$-oxidase2* mutated lines in the presence of Si allowed the plants to increase their Si concentrations from 0.1 to approx. 3.5 mg g^{-1} in old leaves, young leaves and roots (Figure 30A-C), proving sufficient Si enrichment to provoke a similar effect as in the previous experiment (Figure 6A, B). As a consequence of Si accumulation, K concentrations in old leaves decreased in wild-type and the *GA$_{20}$-oxidase2* mutated lines 2 and 3 (Figure 30D). However, K concentrations in young leaves and roots showed no significant differences between the wild-type and mutated lines in the absence or presence of Si, indicating that Si improves root growth under K starvation independently of *GA$_{20}$-oxidase2*-dependent gibberellins biosynthesis (Figure 30E, F).

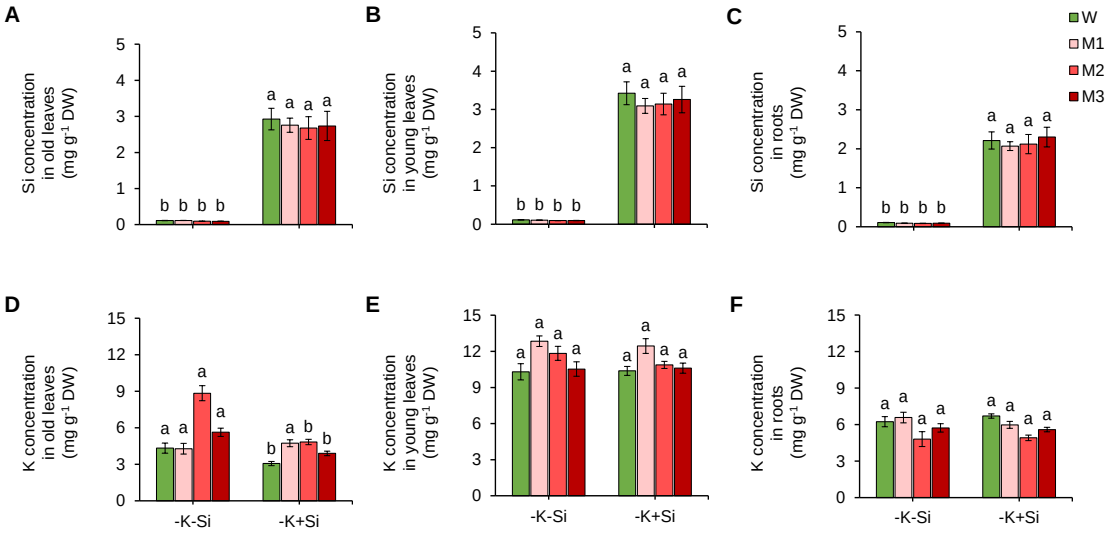

Figure 30. Influence of Si supply on Si and K concentrations of wild-type, *GA20-oxidase2* mutated lines 1, 2, and 3 (W, M1, M2, M3) growth without K supply. (A-F) Concentrations of silicon (Si; A-C) and potassium (K; D-F) in old leaves (A, D), young leaves (B, E), and roots (C, F). After 7 days of germination, plants were grown continuously in K-free nutrient solution for 14 days either in the absence or presence of 1.78 mM Si. Bars indicate means ± SE. Different letters denote significant differences among treatments according to one-way ANOVA and post-hoc Tukey's test ($p < 0.05$; $n = 5$).

To assess whether Si supply modulates gibberellins hormone homeostasis in a GA_{20}-oxidase2-dependent manner, different forms of gibberellins from the gibberellins biosynthesis pathway were analyzed in shoots and roots. $Gibberellin_{53}$ levels in shoots and roots of the wild-type plants, and of *GA_{20}-oxidase2* mutated lines 1 and 2 remained quite stable across two treatments, whereas they were significantly lower in old and young leaves of *GA_{20}-oxidase2* mutated line 3 upon Si application (Figure 31A-C). In the old leaves of wild-type plants and all *GA_{20}-oxidase2* mutated lines, concentrations of GA_{44} decreased with Si supply, while this trend was only observed in the roots of *GA_{20}-oxidase2* mutated lines. In contrast, the young leaf concentrations of GA_{44} slightly increased in *GA_{20}-oxidase2* mutated line 3 after Si application (Figure 31D-F). The levels of GA_{19} in shoots and roots of wild-type plants and all *GA_{20}-oxidase2* mutated lines remained quite stable in both treatments (Figure 31G-I). $Gibberellin_9$ levels in young leaves of wild-type plants and *GA_{20}-oxidase2* mutated line 1 did not change in either treatment, whereas they were lower in *GA_{20}-oxidase2* mutated lines 2 and 3 after Si supply (Figure 31J-L). Concentrations of GA_1 increased in old leaves of *GA_{20}-oxidase2* mutated line 3 and roots of *GA_{20}-oxidase2* mutated line 1, while they decreased in roots of *GA_{20}-oxidase2* mutated line 2 upon Si application (Figure 31M-O). The levels of GA_3 in all tissues of all *GA_{20}-oxidase2* mutated lines were higher than in wild-type plants under K starvation, but hardly affected by Si supply (Figure 31P-R). Concentrations of GA_8 in old leaves of *GA_{20}-oxidase2* mutated lines were higher than in wild-type plants under low K, while GA_8 levels in old and young leaves of K-starved wild-type plants and *GA_{20}-oxidase2* mutated lines were much lower after Si application. Only the root levels of GA_8 increased in wild-type plants by Si (Figure 31S-U). Taken together, Si application improved root growth under K starvation, but not necessarily by changing the levels of bioactive GA_1 and GA_3 in *GA_{20}-oxidase2* mutated lines, whereas Si nutrition prevented the accumulation of deactivated GA_8 independent of GA_{20}-oxidase2-dependent gibberellins biosynthesis.

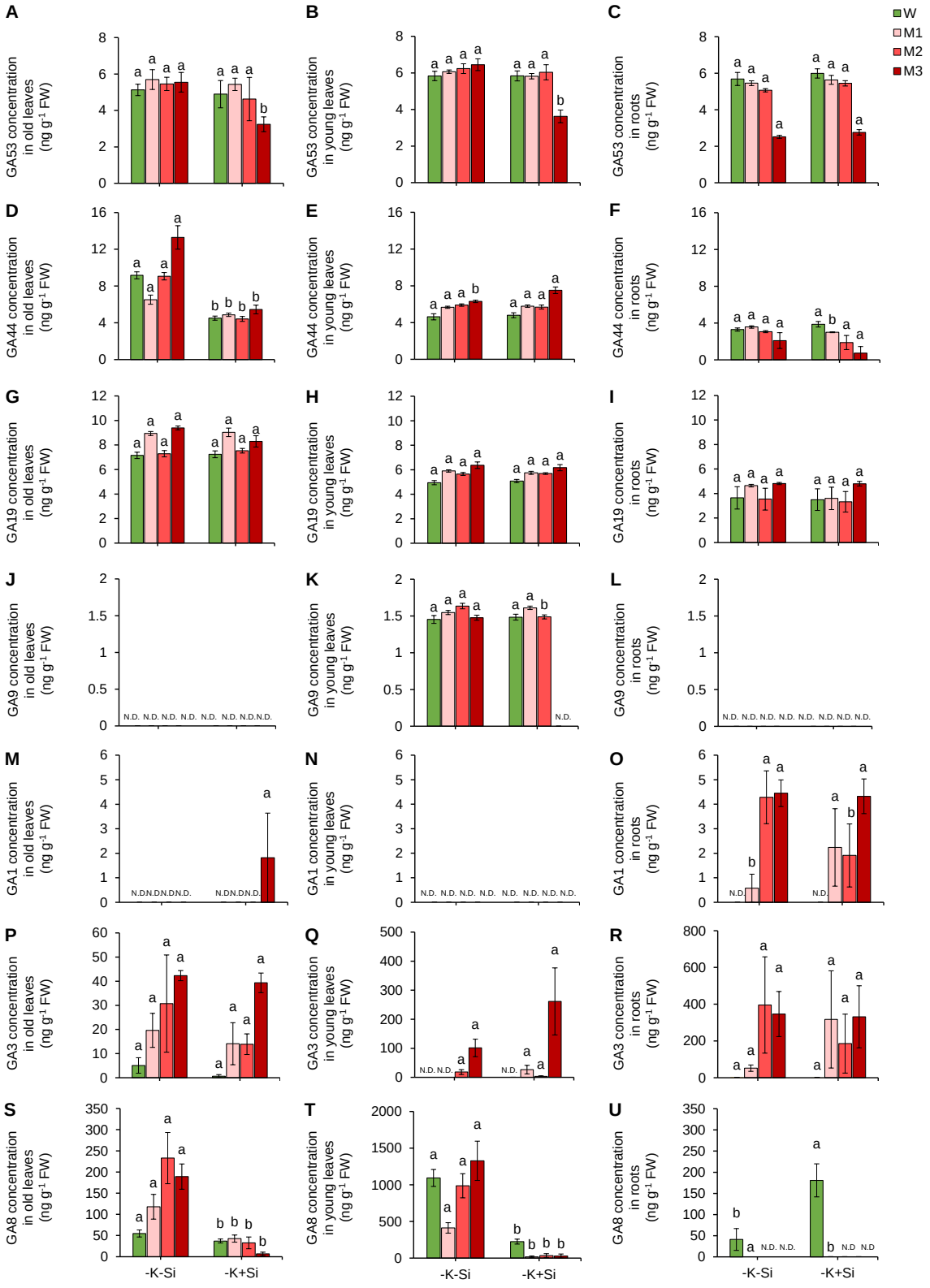

Figure 31. Influence of Si supply on concentrations of gibberellins of wild-type, *GA20-oxidase2* mutated lines 1, 2, and 3 (W, M1, M2, M3) growth without K supply. (A-U) Concentrations of gibberellin-53 (GA53; A-C), gibberellin-44 (GA44; D-F), gibberellin-19 (GA19; G-I), gibberellin-9 (GA9; J-L), gibberellin-1 (GA1; M-O), gibberellin-3 (GA3; P-R), and gibberellin-8 (GA8; S-U) in old leaves (A, D, G, J, M, P, S), young leaves (B, E, H, K, N, Q, T), and roots (C, F, I, L, O, R, U). After 7 days of germination, plants were grown continuously in K-free nutrient solution for 14 days either in the absence or presence of 1.78 mM Si. Bars indicate means ± SE. Different letters denote significant differences among treatments according to one-way ANOVA and post-hoc Tukey's test ($p < 0.05$; $n = 5$).

4.8 Impact of silicon application on plant growth under drought stress

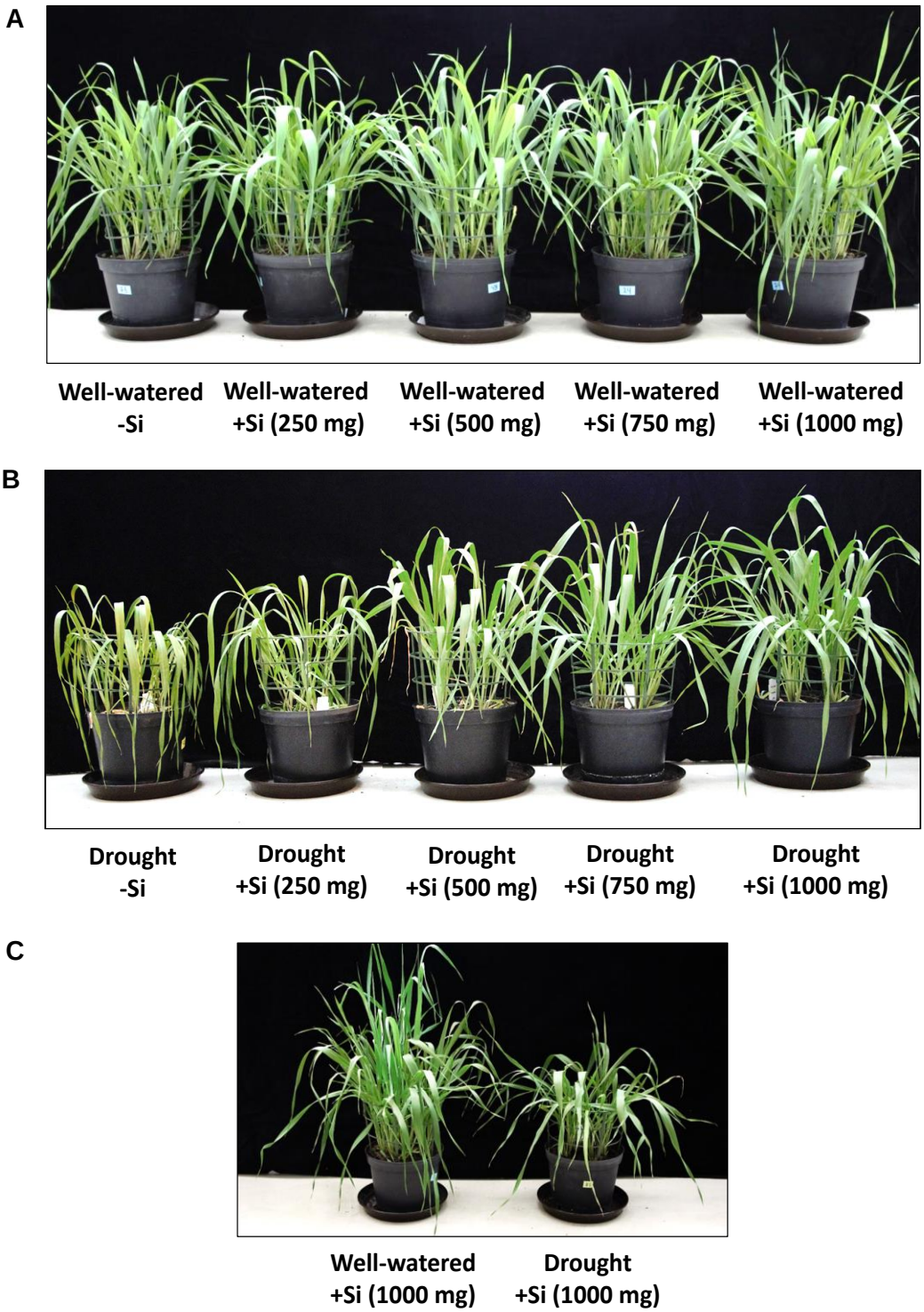

Figure 32. Influence of different doses of Si supply on visual appearance of barley plants grown under sufficient water supply or drought stress. (A-C) Visual appearance of shoots after continuous water supply (A) or 2 weeks without water supply (B). (C) Direct comparison of the visual appearance of Si-supplied well-watered or drought-stressed plants. After 7 days of germination, plants were transplanted into pots containing a peat/sand-based substrate and supplied each week 0, 250, 500, 750, or 1000 mg Si per 5 L pots during a period of 3 weeks. Thereafter, plants in each Si treatment were either well-watered or subjected to drought stress condition for 2 more weeks.

To investigate whether and how Si can alleviate drought stress, barley plants were grown in soil with sufficient water and every 7 days supplied with different doses of Si, ranging from 0 to 1000 mg per 5 L pot over a period of 21 days. Afterwards, plants were subjected to either drought stress or well-watered condition for 14 more days before final harvest (Figure 32). In leaves of well-watered plants, chlorophyll concentrations and relative water contents were high, 1.5 mg g^{-1} FW and 98%, respectively, which is in the typical range of non-stressed barley flag leaves (Figure 33A, B; Hosseini *et al.*, 2016). Leaf traits of these plants were not affected by any dose of Si application. However, under drought stress, chlorophyll concentrations and relative water contents declined by up to 37 and 34%, respectively, as plants showed some chlorosis and wilting symptoms in their leaves (Figure 32), whereas when treated with 500 to 1000 mg Si, chlorophyll concentrations and relative water contents were close to those of well-watered plants (Figure 33A, B). Under adequate water supply, shoot dry weights were close to 0.9 g $plant^{-1}$, while shoot biomass gradually increased by up to 18% with 250 and 500 mg Si treatments (Figure 33C). Higher Si doses did not further promote shoot biomass formation. By contrast, in drought-stressed plants, shoot dry weights increased only from 500 to 1000 mg Si treatment, but then by more than 154% (Figure 33C). Thus, Si supply improves growth in both stressed and non-stressed plants in a dose-dependent manner, and this improvement is linked with restored chlorophyll levels and higher relative water contents in fully expanded leaves.

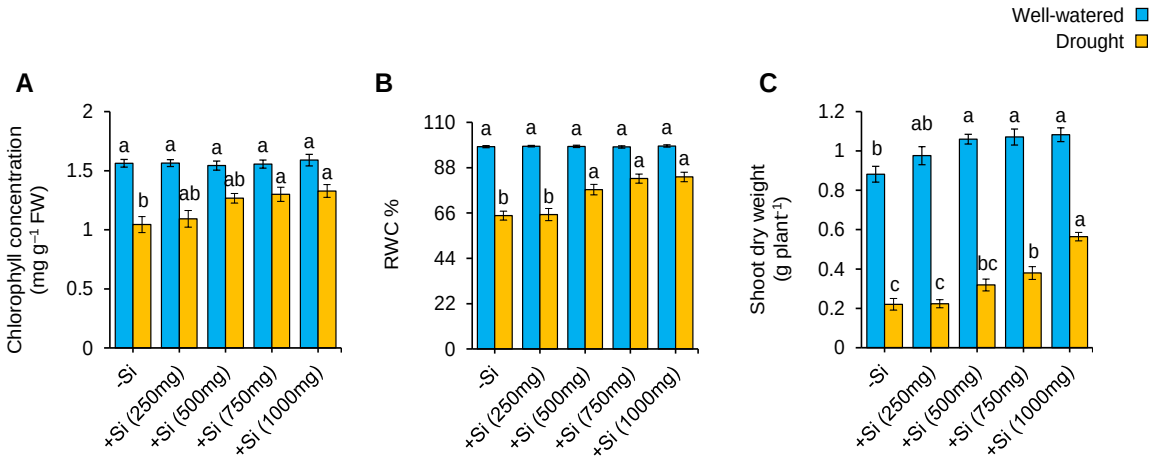

Figure 33. Influence of different doses of Si supply on chlorophyll concentrations, relative water contents and shoot dry weights of barley plants grown under sufficient water supply or drought stress. (A-C) Chlorophyll concentrations (A), and relative water contents (RWC; B) in leaves, and shoot dry weights (C). After 7 days of germination, plants were transplanted into pots containing a peat/sand-based substrate and supplied each week 0, 250, 500, 750, or 1000 mg Si per 5 L pots during a period of 3 weeks. Thereafter, plants in each Si treatment were either well-watered or subjected to drought stress condition for 2 more weeks. Leaf analysis is based on the last fully expanded leaf. Bars indicate means ± SE. Different letters denote significant differences among Si treatments according to one-way ANOVA and post-hoc Tukey's test ($p < 0.05$; $n = 8$).

4.9 Impact of silicon application on the nutritional status of plants under drought stress

To investigate how Si nutrition affects the plant nutrient status under drought stress, concentrations of all nutrients were determined in fully expanded leaves by ICP-OES. Under sufficient water supply without Si supplementation, leaf levels of Si were around 4 mg g^{-1} DW, which decreased by 50% under drought stress (Figure 34A). As expected, leaf concentrations of Si increased up to 14 mg g^{-1} DW in control plants at the highest Si dose, but still remained approx. 25% lower in drought-stressed plants. Although all determined nutrient concentrations were above critical deficiency levels (Marschner, 2012), concentrations of K and N in fully expanded leaves were higher in drought-stressed than in well-watered plants, whereas those of P were mostly lower (Figure 34B-D). Under zero Si application, concentrations of K were significantly higher under drought stress than under watering, but this difference decreased with increasing Si supply, indicating that more K accumulated when plants suffered from drought and concomitant biomass reduction. Likewise, N concentrations in well-watered plants increased with Si supply to an optimum in the 500 mg treatment, which may indicate a promotive effect of Si on N uptake. Unexpectedly under drought stress, leaf concentrations of N established at a higher level, around 5%, irrespective of Si supply (Figure 34D). By contrast, P concentrations slightly decreased under drought stress and remained hardly affected by Si treatments (Figure 34C). Leaf concentrations of other macro- and microelements were adequate regardless of water supply (Figure 35A-I; Marschner, 2012). Interestingly, three elements underwent a drastic decrease upon Si supply to well-watered plants. Calcium, B and Al levels dropped even at the lowest Si dose, possibly related to Si-mediated antagonism during uptake, either via competition for NIP-type transporters, as in case of B, or through Si-mediated Al and Ca retention in the root apoplast (Wang *et al.*, 2004; Mitani-Ueno *et al.*, 2011). Carbon concentrations altered neither under well-watered or drought condition, nor in the absence or presence of Si (Figure 35J). Altogether, Si application did not considerably change the nutritional status in plants under drought stress.

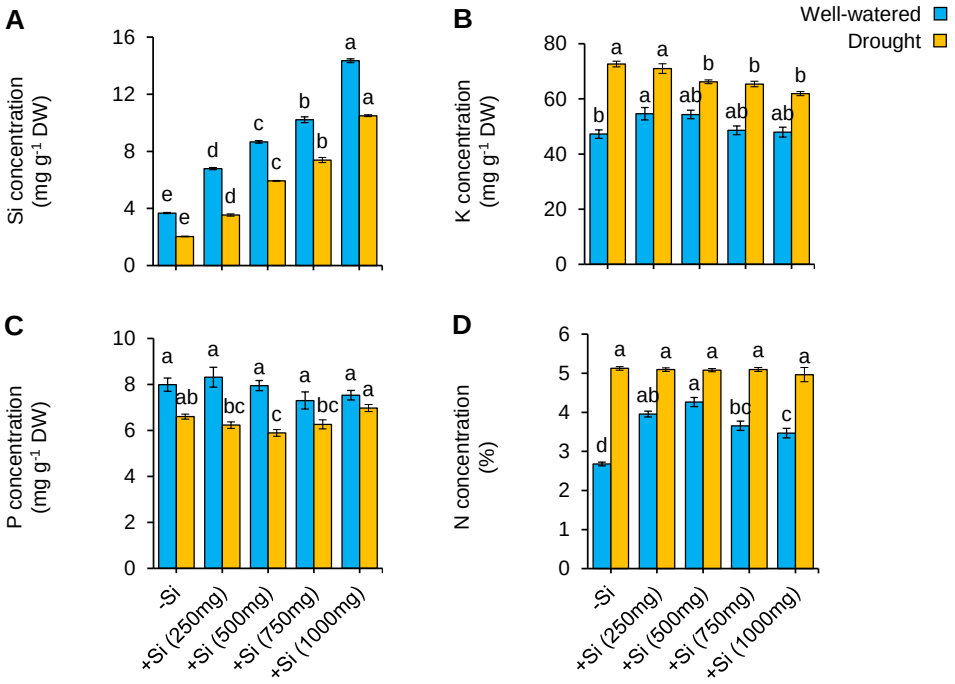

Figure 34. Influence of different doses of Si supply on Si, K, P and N concentrations in leaves of barley plants grown under sufficient water supply or drought stress. (A-D) Concentrations of silicon (Si; A), potassium (K; B), phosphorus (P; C), and nitrogen (N; D) in leaves. After 7 days of germination, plants were transplanted into pots containing a peat/sand-based substrate and supplied each week 0, 250, 500, 750, or 1000 mg Si per 5 L pots during a period of 3 weeks. Thereafter, plants in each Si treatment were either well-watered or subjected to drought stress condition for 2 more weeks. Leaf analysis is based on the last fully expanded leaf. Bars indicate means ± SE. Different letters denote significant differences among Si treatments according to one-way ANOVA and post-hoc Tukey's test ($p < 0.05$; $n = 8$).

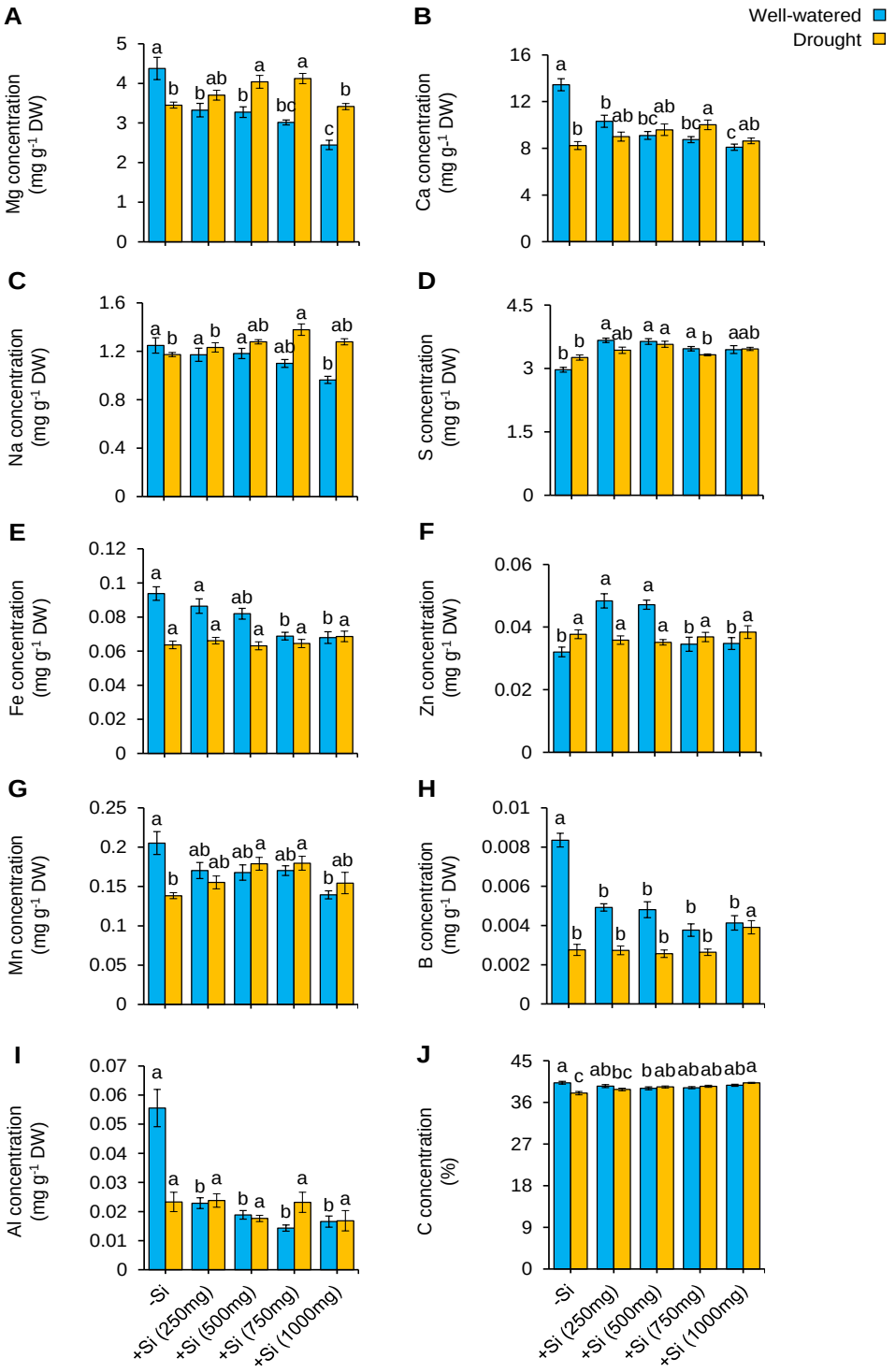

Figure 35. Influence of different doses of Si supply on Mg, Ca, Na, S, Fe, Zn, Mn, B, Al and C concentrations in leaves of barley plants grown under sufficient water supply or drought stress. (A-J) Concentrations of magnesium (Mg; A), calcium (Ca; B), sodium (Na; C), sulfur (S; D), iron (Fe; E), zinc (Zn; F), manganese (Mn; G), boron (B; H), aluminum (Al; I), and carbon (C; J) in leaves. After 7 days of germination, plants were transplanted into pots containing a peat/sand-based substrate and supplied each week 0, 250, 500, 750, or 1000 mg Si per 5 L pots during a period of 3 weeks. Thereafter, plants in each Si treatment were either well-watered or subjected to drought stress condition for 2 more weeks. Leaf analysis is based on the last fully expanded leaf. Bars indicate means ± SE. Different letters denote significant differences among Si treatments according to one-way ANOVA and post-hoc Tukey's test ($p < 0.05$; $n = 8$).

4.10 Impact of silicon application on phytohormone homeostasis of plants under drought stress

To assess whether Si supply modulates phytohormone homeostasis under drought stress, several phytohormone species were profiled in fully expanded leaves. Under sufficient water supply, leaf concentrations of ABA and its degradation products PA and DPA were low around 120, 1400 and 700 ng g^{-1} DW, respectively, which is in the typical range of non-stressed barley flag leaves (Figure 36A-C; Seiler *et al.*, 2011). However, as plants received the lowest dose of Si, ABA levels declined by 3.5-fold and PA and DPA levels decreased by 1.5-fold lower, but did not change with higher doses of Si, suggesting that even control plants may have experienced some stress that could be alleviated by Si application. In contrast, under drought stress leaf concentrations of ABA, PA, DPA and its conjugate ABAGlc were drastically higher reaching approx. 4000, 12000 and 700 ng g^{-1} DW, respectively (Figure 36A-D). While application of up to 750 mg Si to the growth substrate was ineffective in lowering concentrations of different ABA forms, the 1000 mg treatment effectively suppressed accumulation of all ABA species down to the same level as in well-watered control plants (Figure 36A-D). This shows a rather high Si requirement for plants to be less susceptible to drought stress. In leaves of well-watered plants, concentrations of SA were approx. 200 ng g^{-1} DW but gradually increased by two-fold with increasing Si supply (Figure 36E). By contrast, leaf SA levels were slightly lower under drought stress and hardly affected by any of the Si treatments. On the contrary, leaf JA levels in control plants decreased by seven-fold as soon as plants were supplied with Si, whereas they increased dramatically under drought stress only in the 1000 mg treatment, implying an antagonistic interaction with ABA levels in fully expanded leaves of drought-stressed plants (Figure 36A, F).

Concentrations of IAA in leaves of well-watered plants were near 35 ng g^{-1} DW, which is in the typical range of non-stressed barley plants (Gruszka *et al.*, 2016), and hardly affected by Si, whereas under drought stress leaf IAA levels gradually declined from a similar level down to approx. 50% lower, suggesting that Si application prevented auxin accumulation in leaves of plants under drought stress (Figure 37A). Among the different cytokinins forms in leaves of control plants, concentrations of zeatin and IPR were approx. 12 and 4 ng g^{-1} DW, respectively, and were not affected by any dose of Si application (Figure 37B, C). However, under drought stress leaf zeatin levels showed a substantial increase by 50% only in the 1000 mg Si treatment. Concentrations of IPR were not altered by either drought stress or by Si treatments in leaves of drought-stressed plants. In control plants, leaf cZ and cZR concentrations were around 3-4 ng g^{-1} DW, while cZ levels decreased by four-fold, but cZR levels declined much less with application of Si (Figure 37D, E). Unexpectedly, leaf concentrations of cZ and cZR in leaves were three- to six-fold higher under drought stress, but decreased dramatically when plants received 750 to 1000 mg Si, suggesting that higher doses of Si suppress the accumulation of less active cytokinin forms in favour of the more active one under drought stress (Figure 37B-E). Among the different forms of gibberellins, only three of the precursors could be detected. In leaves of control plants, concentrations of GA_{53} were approx. 4 ng g^{-1} FW and hardly affected by any of the Si treatments (Figures 37F). In contrast, under drought

stress, leaf levels of GA_{53} increased by 28%, which remained quite constant upon Si application. Leaf GA_{44} levels in control plants were near 2 ng g^{-1} FW and increased by up to 2.5-fold when supplied with Si (Figures 37G). Under drought-stress, GA_{44} concentrations in leaves were initially at a 2.3-fold higher level and increased even more in the 750 and 1000 mg treatments, suggesting that Si supply can effectively increase the accumulation of GA_{44} in leaves of both stressed and non-stressed plants. Leaf concentrations of GA_{19}, the closest precursor to the physiologically active form GA_1, were approx. 6 ng g^{-1} FW in control plants and increased by 67% under drought condition (Figures 37H). However, none of the Si treatments altered GA_{19} levels in leaves of well-watered or drought-stressed plants, only 1000 mg treatment slightly decreased GA_{19} concentrations under drought stress. Altogether, these results show that Si, in particular the 1000 mg treatment, has a major impact on ABA and cytokinins levels in leaves of drought-stressed plants by bringing them back close to the levels of control plants.

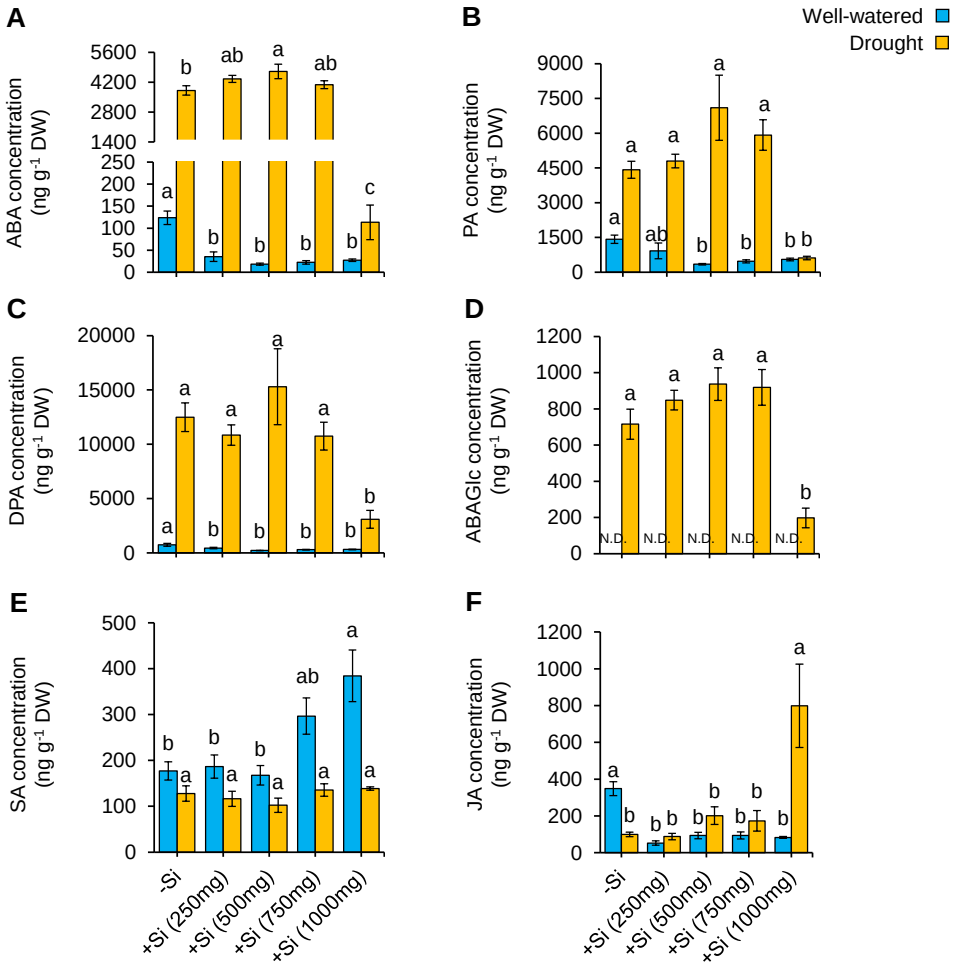

Figure 36. Influence of different doses of Si supply on ABA, PA, DPA, ABAGlc, SA and JA in leaves of barley plants grown under sufficient water supply or drought stress. (A-F) Concentrations of abscisic acid (ABA; A), phaseic acid (PA; B), dihydrophaseic acid (DPA; C), abscisic acid glucose ester (ABAGlc; D), salicylic acid (SA; E), and jasmonic acid (JA; F) in leaves. After 7 days of germination, plants were transplanted into pots containing a peat/sand-based substrate and supplied each week 0, 250, 500, 750, or 1000 mg Si per 5 L pots during a period of 3 weeks. Thereafter, plants in each Si treatment were either well-watered or subjected to drought stress condition for 2 more weeks. Leaf analysis is based on the last fully expanded leaf. Bars indicate means ± SE. Different letters denote significant differences among Si treatments according to one-way ANOVA and post-hoc Tukey's test ($p < 0.05$; $n = 8$).

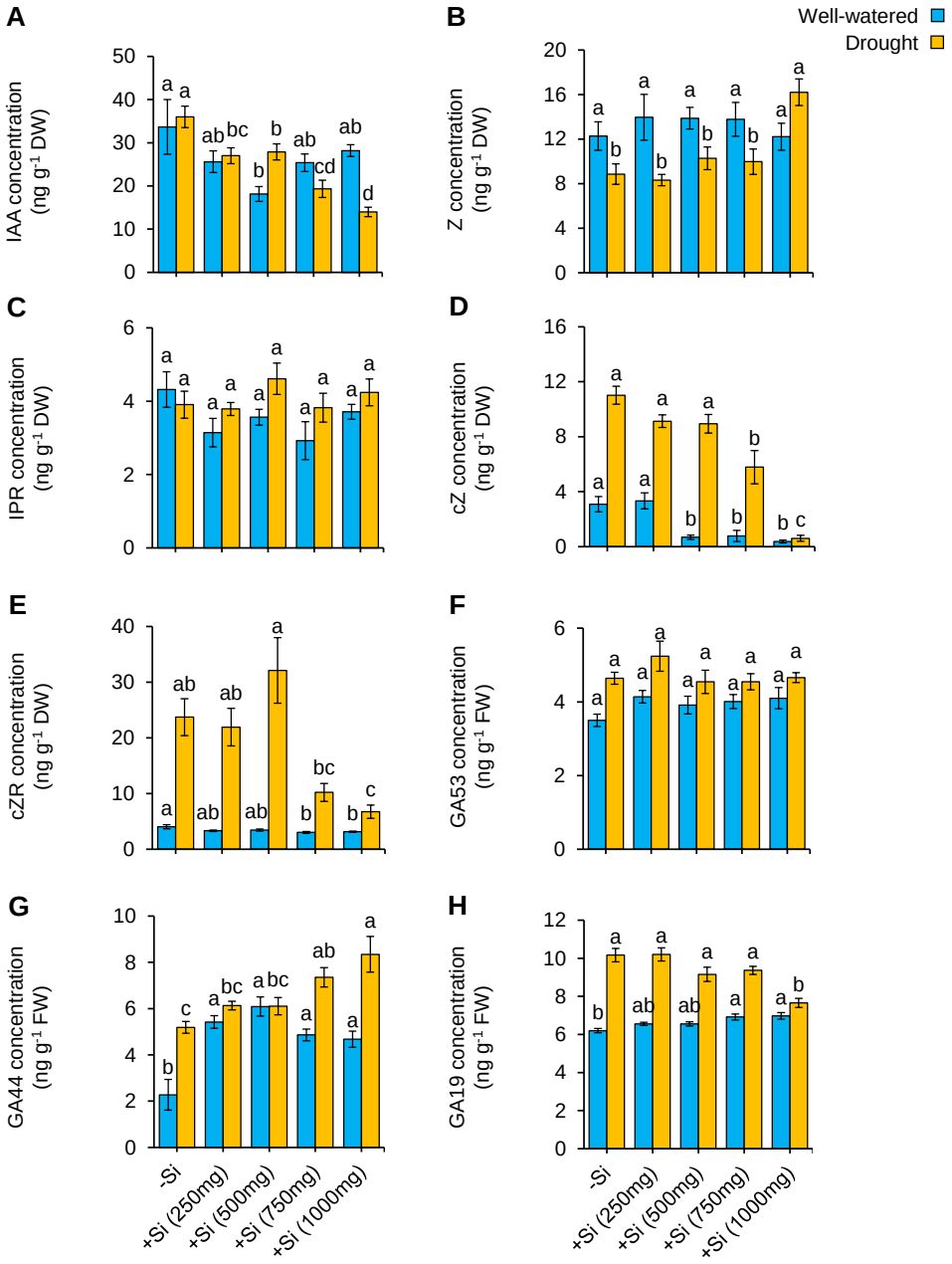

Figure 37. Influence of different doses of Si supply on IAA, Z, IPR, cZ, cZR, GA53, GA44 and GA19 concentrations in leaves of barley plants grown under sufficient water supply or drought stress. (A-H) Concentrations of indole-3-acetic acid (IAA; A), zeatin (Z; B), isopentenyl adenine riboside (IPR; C), cis-zeatin (cZ; D), cis-zeatin riboside (cZR; E), gibberellin-53 (GA53; F), gibberellin-44 (GA44; G), and gibberellin-19 (GA19; H) in leaves. After 7 days of germination, plants were transplanted into pots containing a peat/sand-based substrate and supplied each week 0, 250, 500, 750, or 1000 mg Si per 5 L pots during a period of 3 weeks. Thereafter, plants in each Si treatment were either well-watered or subjected to drought stress condition for 2 more weeks. Leaf analysis is based on the last fully expanded leaf. Bars indicate means ± SE. Different letters denote significant differences among Si treatments according to one-way ANOVA and post-hoc Tukey's test ($p < 0.05$; $n = 8$).

5 Discussion

The beneficial effect of Si on plant growth and alleviation of biotic and abiotic stresses has been well documented (Bélanger *et al.*, 2003; Rémus-Borel *et al.*, 2009; Flam-Shepherd *et al.*, 2018). In particular the Si-mediated mitigation of nutrient deficiencies and drought stress have received special attention due to the importance of these constraints in agriculture and the potential of Si nutrition to advance sustainable crop production (Miao *et al.*, 2010; Shi *et al.*, 2016). To effectively benefit from Si and maximize its advantages, it is important to better understand the processes by which Si directly affects stress tolerance in plants. So far, all previous studies have been restricted to the description of coincidences or correlative evidence and have not provided a mechanistic understanding of the processes induced by Si. Therefore, the objectives of the present thesis were to investigate more deeply the physiological and molecular mechanism(s) by which Si nutrition mitigates K deficiency and enhances drought tolerance.

5.1 Silicon prevents long-term potassium deficiency responses by increasing internal potassium utilization and reconstituting hormonal and metabolite homeostasis

In order to investigate the mode of action of Si when alleviating long-term K deficiency, hydroponically-grown barley plants were subjected to adequate or low K supply in the absence or presence of Si and several physiological and molecular traits were measured. It is well known that K, as one of the essential macronutrients, has an important impact on plant growth, and K deficiency is typically associated with lower shoot and/or root biomass (Kanai *et al.*, 2007; Ma *et al.*, 2012; Wang and Wu, 2013; Zeng *et al.*, 2018). In this study, continuous low K supply in the absence of Si suppressed the formation of tillers and new leaves as well as root growth, which expressed in two- to three-fold lower shoot and root dry weights (Figure 5A-C). By contrast, shoot and root biomass of K-deficient plants increased by 66 and 100%, respectively, in the presence of Si. However, Si supply caused only a small, non-significant increase in shoot dry weights in K-sufficient plants. Since Si treatment was applied from the beginning of K deficiency, this result clearly showed that Si nutrition prevented K deficiency-induced growth inhibition, which is in consistent with previous findings in barley, sorghum and soybean (Miao *et al.*, 2010; Chen *et al.*, 2016a; 2016b).

Plant growth retardation under K deficiency has been partially attributed to impaired photosynthesis (Kanai *et al.*, 2011; Jákli *et al.*, 2017). This is mainly due to the essential role of K in photosynthesis, CO_2 fixation, stomatal regulation and activation of photosynthesis enzymes such as ribulose-1,5-bisphosphat carboxylase (Pfluger and Cassier, 1977; Prajapati and Modi, 2012; Marschner, 2012). In this study, low K supply in the absence of Si resulted in significant suppression of chlorophyll concentrations in fully expanded leaves, whereas such a decline of chlorophyll concentrations was prevented by Si treatment (Figure 5D). This result suggests that Si nutrition prevents K deficiency-induced growth inhibition by maintaining chlorophyll concentrations, which improves photosynthesis under K deficiency. The positive role of Si on plant growth and yield, through enhanced photosynthesis has already been studied. It was reported that Si supply mediated low K tolerance in sorghum by improving

chlorophyll content, chlorophyll a/b ratio, photosynthetic rate, stomatal conductance and transpiration rate, which was accompanied by enhanced total plant biomass under K deficiency (Chen *et al.*, 2016a; 2016b). Even in non-stressed rice plants, Si nutrition increased grain yield through enhanced CO_2 fixation capacity and mesophyll conductance (Detmann *et al.*, 2012; Lavinsky *et al.*, 2016).

Although plant growth depends on photosynthesis, continued growth requires the acquisition of nutrients and conversion into biomass. In this study, low K supply decreased K concentrations below 1% in both leaves and roots, which is indicative of K deficiency in barley (Figure 6C, D; Bergmann, 1992). Application of Si significantly increased leaf levels of K, which were still far below adequate K levels, while K concentrations in roots were not affected by Si. These disparate responses are unexpected, considering that Si accumulation and biomass gain of both organs profited equally from supplemented Si, and Si improved just marginally but not substantially the nutritional status of K in leaves (Figure 5A-C). Taking a closer look at the RNA sequencing and qPCR results revealed a considerable number of high-affinity K transporter and channel genes responsible for *de novo* uptake of K, like *HAK1* and *AKT1*, to be strongly upregulated in leaves and roots under low K supply (Figure 21; Table 2), which is a typical response of plants to K deficiency (Wang *et al.*, 1998; Ashley *et al.*, 2006; Gierth and Mäser, 2007; Kim *et al.*, 2009). In contrast, *AKT2*, encoding a K-selective channel important for K recycling and sugar loading into the phloem, and *KCO1*, encoding tonoplast transporter that effectively releases vacuolar K under K deficiency, were downregulated in leaves (Table 2A; Figure 21) (Walker *et al.*, 1996; Voelker *et al.*, 2006; Gobert *et al.*, 2007; Barragán *et al.*, 2012). Application of Si suppressed the expression of genes for high-affinity K transporters and channels in both leaves and roots, which also led to the disappearance of their representative GO terms (Table 1). It was also previously reported in K-deficient sorghum that Si supply improved root and shoot biomass without raising tissue K levels, which was accompanied by downregulation of *HAK5* and *AKT1* in roots (Chen *et al.*, 2016b). However, the present transcriptome results showed upregulation of *KCO1* and *AKT2* in leaves by Si (Table 2A; Figure 21), indicating that Si may revert or prevent K deficiency-induced responses via increasing internal K availability and utilization in plants instead of *de novo* uptake in roots, which might be the mode of action of Si under long-term K deficiency.

Among the other nutrients, Si application led to considerable Si accumulation in leaf and root tissues, while Si concentrations were lower in K-deficient than in K-sufficient plants (Figure 6A, B), which was consistent with downregulation of *Lsi1* and *Lsi2* genes in leaves of plants under K-limiting condition (Figure 20; Table 2A). This result suggests that K deficiency supresses Si uptake and distribution, which is in contrast to previous finding in barley, that K deficiency increased Si concentrations in leaves and roots through induced Si transporter genes (Hosseini *et al.*, 2017). Moreover, low K concentrations in shoots and roots of K-deficient plants were accompanied by an increase in the concentrations of Mg, Ca and Na (Figure 7A-F). This reflects a typical response of plants to K deficiency, which compensates for lower K uptake by enhanced acquisition of other cations (Marschner, 2012). While these elevated levels of Mg and Ca remained unaffected by Si supply, Na concentrations increased in both tissues after Si application, but remained far below a growth-inhibitory level

(Marschner, 2012). In a previous study, the compensating effects of Na and positive effect of Si on plant growth were compared in K-deficient soybean, when half of the K-deficient plants were supplied with Na_2SiO_3 and the other half with NaCl. Improved plant biomass turned out to be mainly related to the Na_2SiO_3 treatment, while NaCl hardly affected shoot and root dry weights of K-deficient soybean (Miao *et al.*, 2010). Therefore in the present study, it is likely that enhanced growth of K-deficient plants supplied with Si is not the result of compensatory effects of Na in exchange of K. Altogether, these results suggest that Si application alleviates long-term K deficiency and prevents growth suppression in barley neither by improving the K nutritional status nor by alleviating K deficiency-induced imbalances in ion uptake.

Under K deficiency, reductions in plant growth are typically associated with increased levels of stress-related hormones. This holds true for ABA that regulates both stress responses and plant growth. It was reported that increased ABA levels in grains and flag leaves of wheat (Haeder and Beringer, 1981), in roots, xylem, and phloem sap of castor bean (Peuke *et al.*, 2002), in leaves of *Arabidopsis* (Kim *et al.*, 2009), and in roots and xylem of cotton (Wang *et al.*, 2012) were accompanied by reduced plant biomass under K deficiency. Abscisic acid homeostasis in plant tissues relies on a balance between *de novo* synthesis, export, conjugation, and degradation (Cutler and Krochko, 1999; Boursiac *et al.*, 2013). In the majority of plant tissues, ABA is inactivated through a catabolic pathway converting ABA to PA, and then further PA is reduced to DPA (Cutler and Krochko, 1999). In this study, low K supply increased the concentrations of ABA, PA and DPA in both tissues, as well as its conjugate ABAGlc in leaves, which resulted in lower shoot and root biomass (Figure 5A-C; 9). Interestingly in leaves, Si application decreased the accumulation of PA, DPA and ABAGlc, while it did not change the concentrations of ABA. By contrast, Si even increased the levels of ABA, PA and DPA in K-deficient roots. This result suggests that Si nutrition decreases the stress level via lower ABA turnover in leaves that prevents growth inhibition during the stress period. Alternatively, increasing Si application in barley was reported to alleviate K deficiency and osmotic stress via enhancing conversion of ABA to PA and DPA through Si-induced expression of ABA degradation genes in leaves (Hosseini *et al.*, 2017).

Besides ABA, the levels of two other stress-related hormones SA, JA and its bioactive conjugate JA-Ile, also increased in both tissues in response to low K supply (Figure 10). Salicylic acid is a phytohormone that functions as a signaling molecule with important roles in increasing antioxidative protection (Xu and Tian, 2008). Several lines of evidence demonstrated an alleviating role of SA during salinity, as exogenous SA application decreased the Na/K ratio in leaves of barley or prevented K leakage through outward-rectifying K channels in *Arabidopsis* roots (Shakirova *et al.*, 2003; Fayez and Bazaid, 2014; Jayakannan *et al.*, 2015). On the other hand, SA accumulation can cause reduction in the photosynthetic rate and ribulose-1,5-bisphosphat-carboxylase/-oxygenase (RuBisCO) activity in barley plants (Pancheva *et al.*, 1996), decrease chlorophyll contents in cowpea, wheat, and *Arabidopsis* (Rao *et al.*, 1997; Chandra and Bhatt, 1998; Moharekar *et al.*, 2003), or suppress growth in *Arabidopsis* plants (Mateo *et al.*, 2006). Jasmonic acid is another stress-related hormone that is well known for its role in plant defence responses against insect herbivores and fungi, which are the most relevant pathogens of K-starved plants (Perrenoud, 1977; Kessler and Baldwin,

2002; Kunkel and Brooks, 2002). Increased transcript levels of JA biosynthesis genes in *Arabidopsis* under K deficiency suggests a role of JA in plant adaptation to low K stress, which might be mediated through the upregulation of JA-inducible defence responses (Armengaud *et al.*, 2004). Also, transgenic rice plants overexpressing one of the key genes related to JA biosynthesis exhibited higher tolerance to low K stress via increased acquisition and root-to-shoot translocation of K, supporting a crucial role of JA in plant responses to K deficiency (Li *et al.*, 2017). Here, Si application decreased leaf concentrations of SA, JA and JA-Ile under K deficiency (Figure 10), which is in line with transcriptome results showing Si-dependent upregulation of *JAR1*, encoding an enzyme that conjugates jasmonate to amino acids (Table 2A). Declining JA concentrations upon Si treatment also agrees with a previous study, in which Si alleviated salt stress in rice via decreased JA levels (Kim *et al.*, 2014). However, in maize plants under Mg deficiency, Si increased concentrations of JA and JA-Ile in both shoots and roots (Hosseini *et al.*, 2019), showing that the impact of Si on JA levels remains controversial, probably because hormone measurements were conducted under different stress intensities and accompanying growth conditions. Taken together, these results suggest that Si-supplied plants experienced a lower K deficiency-induced stress level via suppressed leaf accumulation of SA and JA.

Contrary to the typical response of plants to low K condition that is accompanied by production and accumulation of ethylene (Jung *et al.*, 2009), the present transcriptome results showed that two genes, *ACO3,* which oxidises 1-aminocyclopropane-1-carboxylic acid (ACC) and converts it to ethylene (Tang *et al.*, 1994; Barry and Giovannoni, 2007), and *RAP2-7*, which plays an important role in ethylene signaling (Licausi *et al.*, 2013) were downregulated in leaves of K deficient-plants (Table 2A). In *Arabidopsis*, ethylene is an early signaling molecule that triggers ROS production and ultimately induces the expression of high-affinity K transporter genes, root hair elongation and modulates stomatal conductance under K deficiency (Shin and Schachtman, 2004). Here, Si application increased the transcript levels of *ACO3* and *RAP2-7* in leaves, and of *ACO1* and *ACS1,* responsible for ACC synthesis, in roots under K-limiting condition (Table 2). This is in contrast to previous findings, in which Si suppressed ethylene signaling in sorghum under salinity (Yin *et al.*, 2016). Again, this discrepancy may be due to the relatively long period of K deficiency and Si exposure, as applied here, allowing plants to reach a new steady-state, in which some of the early physiological and molecular responses are attenuated.

Growth-promoting plant hormones, in particular cytokinins, have mostly an antagonistic interaction with ABA. It has been shown that higher ABA concentrations in *Arabidopsis* or maize were associated with a reduction in cytokinins levels that stimulated adaptive responses in plants to low K condition (Nam *et al.*, 2012; Zhao *et al.*, 2016). In agreement with these results, here low K supply decreased the root levels of tZR and IPR in favour of a higher accumulation of the less active cytokinin form cZR (Figure 11). However, Si nutrition prevented this conversion and slightly increased the level of IPR in roots of K-deficient plants. This is in line with a previous finding, where Si application increased IP concentrations and decreased ABA levels in leaves of barley plants under low K and osmotic stress (Hosseini *et al.*, 2017). A similar interaction was also found in roots of maize plants under Mg deficiency,

when Si supply increased the levels of IP and IPR (Hosseini *et al.*, 2019). This result indicates that Si alleviates growth retardants under K deficiency by improving polar auxin transport from the shoot (Song *et al.*, 2015) and increasing the level of more active cytokinin forms in roots.

Cytokinins are the key regulators of cell division, but plant growth and development result from a combination of cell division and expansion. Potassium is a prerequisite for turgor-driven cell extension in plants due to its role in stabilising the membrane potential, cytosolic pH and increasing the osmotic potential in the vacuoles (Lang, 1983; Walker *et al.*, 1996). Therefore, K deficiency in plants significantly reduces cell turgor, size and expansion of leaves and roots (Mengel and Arneke, 1982; Pfeiffenschneider and Beringer, 1989; Dolan and Davies, 2004; Jordan-Meille and Pellerin, 2004; Kanai *et al.*, 2007; Jordan-Meille and Pellerin, 2008). It has been shown in *Amaranthus caudatus* that stimulation of stem elongation by gibberellins also depends on K concentration, as K supply prevented the inhibitory effect of chlorocholine chloride on GA_3 synthesis, emphasizing a synergistic interaction between K and gibberellins in plant growth (Kende and Lang, 1964; De La Guardia and Benlloch, 1980; Guruprasad and Guruprasad, 1988; Chen *et al.*, 2001). In the present study, leaf and root concentrations of GA_{53} and GA_{19} remained quite stable under low K condition, while the levels of GA_{44} and GA_9, which are precursors of the physiologically active species GA_1 and GA_4, decreased in leaves (Figure 13). In turn, GA_8 the downstream product of GA_1, strongly increased under K deficiency, suggesting that low K concentrations in plants induce deactivation and degradation of gibberellins in leaves. This is in agreement with the transcriptome results (Table 2A), as *GA_{20}-oxidase2* that plays a key role in gibberellins biosynthesis and *PIF4*, encoding a light-regulated transcription factor that positively controls cell elongation (De Lucas *et al.*, 2008), were downregulated, while *GA_2-oxidase3* involved in gibberellins catabolism (Hedden and Sponsel, 2015) was upregulated in leaves under K deficiency, supporting the notion that low K supply supresses gibberellins biosynthesis in plants.

In contrast, Si application increased the leaf concentrations of GA_9 in K deficient-plants and GA_3 under both K sufficiency and K deficiency, while the leaf levels of GA_8 dramatically decreased by Si under low K condition (Figure 13). This suggests that Si nutrition increases the production of bioactive GA_3 independently of K concentrations and prevents degradation of gibberellins in leaves under K deficiency. Also in leaves of K-deficient plants *GA_{20}-oxidase2* and *PIF4* genes were upregulated and *GA_2-oxidase3* was downregulated by Si (Table 2A), which is in line with previous studies reporting that higher doses of Si application increased bioactive gibberellins contents in a variety of salt-stressed plant species (Hwang *et al.*, 2007; Hamayun *et al.*, 2010; Lee *et al.*, 2010). Quite the contrary, in the present transcriptome results, *GA_2-oxidase*, involves in gibberellins catabolism, *RGA1*, encoding a DELLA-type repressor of the gibberellins signaling pathway (Silverstone *et al.*, 1998; Dill *et al.*, 2001; Rizza and Jones, 2019), and *CBF1*, a cold-responsive transcription factor suppressing gibberellins biosynthesis (Achard *et al.*, 2008) were downregulated in leaves of K deficient plants, while *WRKY12*, a transcription factor positively regulating gibberellins-related genes (Li *et al.*, 2016) was upregulated. All of these genes showed an opposite regulation under Si supply (Table 2A). Although this is in contrast to the negative effect of K deficiency and positive impact of

Si nutrition on gibberellins biosynthesis, evidence for a role of gibberellins in Si-dependent alleviation of K deficiency and plant growth should not be ruled out. Therefore, this aspect was addressed in a separate experiment with three barley *GA$_{20}$-oxidase2* mutated lines that were subjected to K starvation in the presence or absence of Si.

Unlike in the former long-term K deficiency experiment, Si supplementation did not result in higher shoot biomass but only in higher root dry weight (Figure 29E, F). This different growth response to Si might be due to the fact that a different barley genotype, cv. Golden Promise, had to be used in this experiment to enable comparison with the existing *GA$_{20}$-oxidase2*-genome-edited plants. Nonetheless, Si partially alleviated K starvation-induced chlorosis and necrosis in old leaves of the wild-type and all three *GA$_{20}$-oxidase2* mutated lines (Figure 29), suggesting that the beneficial effect of Si on K deficiency symptoms is independent of gibberellins biosynthesis. Potassium concentrations in old leaves decreased by Si in the wild-type and the *GA$_{20}$-oxidase2* mutated lines 2 and 3, while K concentrations in young leaves and roots of all plants showed no significant difference, indicating that Si improves root growth independently of *GA$_{20}$-oxidase2*-dependent gibberellins biosynthesis under K starvation (Figure 30). Moreover, Si application decreased GA_{44} concentrations in old leaves of wild-type plants and all *GA$_{20}$-oxidase2* mutated lines, while the levels of GA_{53}, GA_{19} and GA_9 were hardly affected by Si (Figure 31). In contrast, Si supply increased GA_1 levels only in old leaves of *GA$_{20}$-oxidase2* mutated line 3 and in roots of line 1, while GA_8 concentrations decreased in old and young leaves of wild-type plants as well as all *GA$_{20}$-oxidase2* mutated lines by Si. These findings reveals that Si mainly influences the downstream products of the gibberellins biosynthesis pathway, which is partially consistent with the hormone and transcriptome results from the long-term K deficiency experiment, where GA_8 concentrations decreased (Figure 13K), and *GA$_2$-oxidase3* expression was downregulated in leaves of K-deficient plants by Si (Table 2A). However, there is no evidence that levels of GA_1 decreased in any of the *GA$_{20}$-oxidase2* mutated lines. Therefore, this experiment cannot prove whether these lines are *GA$_{20}$-oxidase2*-defective and thus gibberellins-depleted lines or not. Taken together, Si nutrition alleviated K deficiency and promoted plant growth via increased gibberellins production and weaker accumulation of deactivated GA_8 but most likely not necessarily through the *GA$_{20}$-oxidase2*-dependent gibberellins biosynthesis pathway.

Besides cell turgor and extension, another critical roles of K in plants is assimilate partitioning and sugar transport from source to sink by maintaining the membrane potential in phloem cells and contributing to the osmotic potential in the sieve tubes (Peel and Rogers, 1982; Marschner, 2012; Chérel *et al.*, 2014). Therefore, K deficiency leads to impaired phloem transport, decreased sugar levels in the roots and thus reduced root growth (Cakmak, 1994). Indeed, in the present study, low K supply increased not only the leaf accumulation of sucrose, glucose and fructose, but also of phosphorylated sugars and energy carriers, while the concentration of starch and its precursors remained unaffected (Figure 14-17). In contrast, Si application prevented sugar accumulation in leaves but increased Suc, Glc and Fru levels in roots of K-deficient plants, which corroborates a recent finding in barley, in which Si nutrition increased Suc levels in roots (Hosseini *et al.*, 2017). Improved phloem transport of sugars by Si in K-deficient plants may be a consequence of increased internal availability and re-

translocation of K, as the present transcriptome results showed upregulation of *KCO1* and *AKT2* after Si treatment (Figure 21; Table 2A). This is in agreement with a previous study showing that carbon metabolites were less affected by K deficiency in a high K-retaining barley genotype compared to another low K-retaining one (Hosseini *et al.,* 2016). Therefore, the present results showed that Si efficiently contributed to phloem transport of sugars from shoots-to-roots that was manifested in higher root biomass under K deficiency (Figure 5A, C). Additionally, K deficiency affected N metabolites and led to the accumulation of di-aminated, cationic amino acids, which helps maintaining the cation-anion balance (Figure 14; 15; 18; Armengaud *et al.*, 2009). However, Si application prevented the excessive leaf accumulation of di-aminated and stress-responsive amino acids and increased the levels of glutamate and aspartate, suggesting that Si confers low K tolerance and improves root and shoot growth by reconstituting metabolite homeostasis under K deficiency. Altogether, it can be concluded that Si nutrition induced adaptive responses to long-term low K stress through enhanced photosynthesis, increased internal K utilization, reconstituted hormonal homeostasis by increasing cytokinins and GA_1 levels, but at same time suppressing ABA, SA and JA accumulation and improved phloem transport of sugars, which all resulted in higher shoot and root biomass production. It is noteworthy that Si-mediated alleviation from K deficiency stress was primarily triggered by an improved physiological status of the shoot, while root traits only partially recovered, which was most likely as a downstream event of restored shoot metabolism, implying an altered systemic shoot-to-root signaling in the presence of Si. However, it still remains unclear whether these Si-mediated changes in plant metabolism were a cause or a consequence of Si supply.

5.2 Silicon temporarily delays short-term potassium starvation responses by increasing internal potassium availability and *de novo* potassium uptake in roots

In the former long-term low K experiment (Figure 5), and in previous other studies (Miao *et al.*, 2010; Chen *et al.*, 2016b; Hosseini *et al.*, 2019), only single sampling points were analyzed mostly after long-term K and Si treatments. Such an experimental design cannot provide a mechanistic understanding of the processes and physiological components conferring the beneficial action of Si, but rather describes a newly achieved physiological steady-state. To assess the short-term effects of Si on K uptake and translocation in roots and shoots, hydroponically-grown barley plants were subjected to K starvation in the absence or presence of Si and sampled over a time course (Figure 22). In addition, Rb was used as a tracer to monitor K fluxes. In the absence of Si, K-adequate plants showed continuous growth and high K enrichment in roots and shoots (Figure 22; 23B; 24B). This trend became manifest in higher plant biomass (Figure 22C, D), and enhanced K contents in both tissues (Figure 23C; 24C), which was accompanied by low root influx and root-to-shoot translocation of Rb (Figure 23D; 24D). Taking a closer look at the transcript level of genes involved in K transport in roots showed that after 6 days the high-affinity transporters *HAK1* and *HAK4* as well as the vacuolar K exporter *KCO1* were expressed at rather low levels while only the low-affinity K channel *AKT1* was slightly upregulated (Figure 25A-F). Along the observed time line, *HAK4* was downregulated and *AKT2* was upregulated in shoots (Figure 27A-F). Thus, adequate K

nutrition maintained high K concentrations in control plants, probably via enhanced activity of the low-affinity K channel AKT1 in roots and of the K channel AKT2 in shoots, which consequently decreased the need for *de novo* uptake by the high-affinity transporters HAK1 and HAK4 and for vacuolar K release via the KCO1 channel.

After 12 days of K starvation, K concentrations in roots and shoots as well as biomass decline and partitioning (Figure 22; 23F; 24F), were almost the same as after 24 days of growth under low K supply (Figure 5, 6). Monitoring the dynamic changes showed that internal K concentrations dropped to severe starvation levels close to 5 mg g^{-1} after 6 and 9 days in roots and shoots, respectively (Figure 23F; 24F), which was accompanied by reduced plant biomass, strong chlorosis and necrosis in leaves (Figure 22), and declined K contents in both tissues after 3-6 days of growth in the absence of K (Figure 23G; 24G). Considering the intense cycling of K in the vascular system (Ragel *et al.*, 2019), root and shoot K was most likely leaked to the medium via the roots. Such a net loss of K from roots and shoots was concomitant with an increased influx of Rb in roots within 3 days (Figure 23H). This increase in K uptake capacity was reflected in a tight upregulation of several K transporters and channels including *HAK1*, *HAK4*, *AKT1* and *AKT2* in roots (Figure 25G-L) and *HAK1* and *AKT2* in shoots (Figure 27G-L). These results indicate that K starvation decreased K concentrations in plants leading to rapid responses in root and shoot that resulted in increased expression levels of low- and high-affinity K transporters and channels genes for *de novo* uptake mainly at day 6. However, since no K was supplied, the transcript levels of these transporters were later suppressed at day 9 and 12.

In roots of K-starved plants supplied with Si, K concentrations dropped after 6 days to a similarly low level as in the absence of Si, and then declined even further during the following 6 days (Figure 23F, J), indicating a more efficient depletion of root K pools in the presence of Si. This trend coincided with the transcriptional upregulation of plasma membrane-localized K importers in K-deficient barley roots, incl. *HAK4, AKT1*, *AKT2* (Boscari *et al.*, 2009; Feng *et al.*, 2020), and in particular *HAK1* (Figure 25M-R; Santa-María et al., 1997), that became delayed and peaked with higher levels at day 9-12, matching exactly with the strongly increased Rb influx in roots (Figure 23L). Such a response 3-6 days later than in the absence of Si suggests that Si most likely disconnects the transcriptional regulation of root K importers from systemic K deficiency signaling or alters their posttranslational activation to sustain the observed increase in K uptake capacity. Since the cellular K status is proposed to be initially sensed at the plasma membrane, but on the long run by changes in cytosolic K concentrations (Wang and Wu, 2013; Chérel et al., 2014), transcript levels and activities of *de novo* K uptake transporters at the plasma membrane are tightly connected to vacuolar loaders and unloaders of K at the tonoplast to maintain cytosolic K homeostasis. In the first 3 days, the vacuolar K unloader *KCO1* (Tang *et al.*, 2020) showed an opposite transcriptional regulation upon Si treatment in roots and was strongly upregulated with the beginning of K starvation (Figure 25R). Earlier activation of *KCO1* and intense re-mobilization of previously root-stored K by Si might play an important role in a temporally differentiated regulatory and delayed response in *de novo* uptake of K in roots.

Along the same line, further increasing shoot K contents, closely matching with the amount of K lost by the roots after 6 days, revealed that the root-mobilized K had been efficiently translocated to the shoot in the presence of Si (Figure 23K; 24K), caused higher biomass and weaker chlorosis and necrosis in leaves (Figure 22A-C). Likewise, the highest root-to-shoot translocation rates of Rb observed after 12 days of K starvation coincided with the highest transcript levels of the xylem loader *SKOR* (Figure 24L; 25Q), while the earlier increase in Rb translocation from day 3 on was apparently not limited by *SKOR* expression levels. In turn, the expression levels of *HAK1*, *HAK4* and *KCO1*, that are most likely involved in vacuolar K release in shoots were suppressed, while *AKT2* levels increased at day 12 (Figure 27M-R), suggesting that Si nutrition induces not only K root-to-shoot translocation, but also K re-translocation via the phloem, ultimatley leading to higher shoot and root biomass in K-starved plants. These results are in agreement with previous studies reporting that Si supplementation to K-deficient plants improves root-to-shoot translocation of K (Liang, 1999; Miao *et al.*, 2010; Chen *et al.*, 2016b), which was partly associated with an improved plant water status and higher transpiration rates of Si-supplied plants (Chen *et al.*, 2016b).

It is noteworthy that the activation of multiple transporters for K uptake from the soil and K re-mobilization from the vacuolar storage, including HAK-, AKT- and KCO/TPK-type transporters, under low K stress is tightly controlled and stimulated by Ca- and ROS-mediated signaling pathways (Wang and Wu, 2013; Ragel *et al.*, 2019; Tang *et al.*, 2020). Considering the frequently reported property of Si to suppress ROS formation in stressed plant cells (Cooke and Leishman, 2016; Coskun *et al.*, 2019) and the fact that CDPK- and CBL-type Ca^{2+} sensors together with their interacting CIPKs activate NADPH oxidases in a Ca^{2+}-dependent manner (Drerup *et al.*, 2013), Si may alter ROS production and K transporter activation or their transcriptional regulation (Figure 25; 27) already at the level of Ca signaling. This is an efficient way to connect vacuolar and plasma membrane transport processes (Cubero-Font and De Angeli, 2021). Altogether, Si nutrition temporarily delayed short-term K starvation responses by modulating membrane permeability and membrane transport processes of K locally in the roots, most probably as a prerequisite to prevent K leakage and to increase internal K availability as well as K translocation to the shoot.

5.3 Silicon mediates drought tolerance by improving water content and reconstituting hormonal homeostasis

To elucidate the mechanistic role of Si in alleviating drought stress, barley plants were grown in soil and after supplying them with adequate water and different doses of Si, plants were subjected to drought stress before several physiological traits were measured (Figure 32). It is well known that an impairment of water uptake by roots under drought stress results in ROS production and alters Ca signaling leading to enhanced ABA biosynthesis which triggers stomatal closure to prevent transpirational water loss in plants (Cheong *et al.*, 2007). Closure of stomata decreases CO_2 influx and spares more electrons for the formation of active oxygen species that ultimately decrease chlorophyll content and photosynthetic rate (Loreto *et al.*, 1995; Meyer and Genty, 1998; Bota *et al.*, 2004; Farooq *et al.*, 2009; Aroca *et al.*, 2012; Seiler *et al.*, 2014). In the present study, chlorophyll concentrations and relative water contents

were high in leaves of well-watered plants and not affected by any dose of Si application (Figure 33A, B). However, drought stress decreased chlorophyll concentrations and relative water contents in leaves as soon as plants showed weak chlorosis and wilting symptoms (Figure 32). Here, application of 500 to 1000 mg Si to the growth substrate increased their levels near to those of control plants. These results clearly indicate that the accumulation of Si in leaves can alleviate drought stress by restoring photosynthesis and improving water content in plants. The positive role of Si in photosynthesis and plant water conservation has already been studied before (Zhu and Gong, 2014). It was reported that Si supply mediates drought tolerance in wheat, maize, pepper and rice plants under osmotic stress, water-limiting or drought conditions through maintenance of the contents of photosynthetic pigments such as chlorophyll a and b, or carotenoids (Kaya *et al.*, 2006; Lobato *et al.*, 2009; Pei *et al.*, 2010; Chen *et al.*, 2011). Silicon also improved the relative water content in leaves of sunflower and maize plants under drought stress (Kaya *et al.*, 2006; Gunes *et al.*, 2008). Transpiration rate and stomatal conductance are two important criteria that influence the water content of plants (Farooq *et al.*, 2009). Several researchers have postulated that the formation of a silica-cuticle double layer on leaf epidermal cells may be responsible for the observed reduction in leaf transpiration of plants treated with Si (Yoshida, 1965; Wong *et al.*, 1972; Matoh *et al.*, 1991). Although decreased plant transpiration is an important mechanism for Si-mediated drought tolerance, application of Si does not always decrease transpiration rates. Several studies suggest that Si-mediated drought tolerance may be associated with improved root water uptake (Sonobe *et al.*, 2010; Yin *et al.*, 2014). Such an observation was reported in tomato, when Si supply increased transpiration rate, photosynthesis, and leaf water content via increased root hydraulic conductivity and water uptake under drought stress (Shi *et al.*, 2016). In sorghum seedlings, Si also conferred osmotic stress tolerance and increased root hydraulic conductance through enhanced expression of some aquaporin genes (Liu *et al.*, 2014). These results suggest that the beneficial effects of Si under drought stress can be partially attributed to its positive impact on the water status and photosynthesis of the plants.

Moreover, some studies have shown that Si can improve plant growth under drought stress. When drought stress occurs, plants reduce their photosynthesis and assimilate allocation, slow down their growth and start wilting. If water scarcity persists, yield formation will be limited by suppressed tillering and a shorter grain filling period (Gan, 2003; Sreenivasulu *et al.*, 2007). In this study, barley plants grew well under sufficient water supply (Figure 32), but drought stress suppressed their shoot biomass formation. Application of 250 and 500 mg Si increased shoot dry weights up to 18% under control condition, while under drought stress 750 and 1000 mg treatments boosted shoot dry weights by more than 150% (Figure 33C). This result reveals that growth improvement by Si is in a dose-dependent manner under both stressed and non-stressed conditions, whereas higher Si application is required for stressed than well-watered plants. This finding is partially in accordance with previous reports, as Si application positively affected shoot and root biomass of drought-stressed sorghum (Hattori *et al.*, 2005; Ahmed *et al.*, 2011; Yin *et al.*, 2014), and shoot dry weights of drought-stressed

wheat and maize (Kaya *et al.*, 2006; Gong and Chen, 2012), indicating that Si nutrition can induce tolerance in plants by improving their growth under drought condition.

It has been suggested that Si-mediated improvement of plant growth under drought is related not only to increased water content and photosynthesis (Ahmed *et al.*, 2011), but also to enhanced nutrient uptake. One of the early consequences of low water availability under drought is a decrease in total nutrient uptake and lower nutrient translocation to the shoots mainly due to the reduced transpirational flow and hence a decreased mass flow of soil water containing soluble nutrients to the root surface. Particularly, under long-term drought stress, a disconnection of the water film between the roots and the soil matrix will decrease the accessibility and uptake of N, P and K (Barber *et al.*, 1988; Kant *et al.*, 2002; Marschner, 2012; Shabbir *et al.*, 2016). Addition of Si to maize plants improved drought tolerance via enhanced Ca levels in shoots and roots and K concentrations in shoots under water-limiting condition (Kaya *et al.*, 2006). In drought-stressed wheat plants, Si application increased K concentrations in shoots and grains, which ultimately helped plants to maintain their water content and produce more biomass (Ahmad *et al.*, 2016). One possible mechanism by which Si increases K accumulation in drought-stressed plants may be through enhanced K uptake via increased H^+-ATPase activity in the root membranes (Liang, 1999). Also, application of Si increased the uptake and root-to-shoot translocation of NH_4^+ and S in tomato under osmotic stress (Ali *et al.*, 2018). Quite the contrary, Si treatment in rice plants significantly reduced the levels of K, Na, Ca, Mg and Fe, which increased during drought stress, indicating that Si application mediates drought tolerance by adjusting the nutritional status of several essential elements (Chen *et al.*, 2011).

In the present study, leaf levels of Si were around 4 mg g^{-1} DW under sufficient water supply that decreased by 50% under drought stress (Figure 34A). A decline in Si concentration was also observed in drought-stressed rice and explained through decreased expression levels of *Lsi1* and *Lsi2* genes by ABA (Yamaji and Ma, 2007; 2011). Here, addition of Si between 250 to 1000 mg increased Si concentrations by two- to five-fold in leaves of both control and drought-stressed plants relative to non-Si-treated leaves. Under sufficient water supply, concentrations of K in leaves were adequate (Marschner, 2012), and hardly affected by Si, whereas drought stress increased leaf K levels by 54% (Figure 34B), which may be a consequence of biomass reduction and its effect on K concentrations. In contrast, application of 500 to 1000 mg Si slightly decreased K accumulation, which was the same doses of Si that improved relative water content in leaves, and shoot biomass of drought-stressed plants (Figure 33B; 34B). Although here the impact of Si on leaf K levels was very small, this observation suggests that the higher Si accumulation in leaves can adjust the K nutritional status, which leading to a higher relative water content under drought stress.

Under sufficient water supply, concentrations of N in leaves were around 3% and adequate (Marschner, 2012), whereas with the 250 mg treatment N levels increased to around 4%, that remained quite constant in response to higher doses of Si supply (Figure 34D). In contrast, drought stress increased leaf N concentrations by two-fold regardless of Si supply. These results show that Si nutrition stimulated N accumulation or uptake in well-watered plants. Leaf levels of other macro- and microelements either remained stable or slightly decreased

after Si supply (Figure 34C; 35A-I), but without falling below a critical threshold (Marschner, 2012). In principle, lower concentrations of nutrients in Si-treated plants might be due to the build-up of apoplastic barriers, either in the form of Casparian band (CB) formation or a suberin layer sealing inside the cell walls (Fleck *et al.*, 2011; 2015). Apoplastic Si deposition in the form of silica (SiO_2) (Gong *et al.*, 2006), or co-precipitation of Si and mineral elements might have also blocked apoplastic transport routes, and thus reduced root-to-shoot translocation of nutrients (Kidd *et al.*, 2001; Wang *et al.*, 2004; Shi *et al.*, 2005; Ma *et al.*, 2016; Wu *et al.*, 2016). However, such an impact of Si was mostly reported in stressed-plants (Neumann and Zur Nieden, 2001; Rogalla and Römheld, 2002; Gong *et al.*, 2006; Che *et al.*, 2016). In contrast, drought stress significantly decreased leaf levels of Mg, Ca, Fe, Mn, B and Al, probably due to the reduced transpiration and mass flow of nutrient within the transpiration stream, which is of particular importance for elements like Ca, Mg and B (Figure 35A-I; Marschner, 2012). Taken together, all these results indicate that Si application induces drought tolerance and increases biomass by restoring photosynthesis and elevating water content in fully expanded leaves, but not necessarily by improving the nutritional status of plants.

Among the different plant responses to drought stress, many are typically regulated by the major drought stress-related phytohormone ABA (Seki *et al.*, 2007). Drought stress-induced ABA biosynthesis triggers stomatal closure to prevent transpirational water loss in plants which ultimately leads to a decrease in photosynthesis rate, nutrient uptake and plant growth (Turner *et al.*, 2001; Cheong *et al.*, 2007). The endogenous level of this hormone is determined by its biosynthesis, catabolism, and transport rate through the plant, as well as by species, organ and in particular duration and severity of drought stress (Voisin *et al.*, 2006; Llanes *et al.*, 2016). Here, under sufficient water supply, leaf concentrations of ABA, PA and DPA were low and in the typical range of non-stressed barley flag leaves (Figure 36A-C; Seiler *et al.*, 2011). However, application of Si decreased ABA, PA and DPA levels in leaves by several-fold, suggesting that even control plants may have experienced some stress that could be alleviated by Si application. By contrast, drought stress drastically increased concentrations of ABA, PA, DPA and ABAGlc in leaves, and application of up to 750 mg Si to the growth substrate was ineffective in reducing the concentrations of different ABA forms (Figure 36A-D). Only the 1000 mg Si treatment effectively suppressed the levels of all ABA species down to the same level as in the well-watered control plants. These results reveal that an elevated accumulation of Si is required to make plants less susceptible to drought stress, even though it still remains unclear whether and at what step Si nutrition interferes with ABA biosynthesis, degradation or ABA-related signaling. Recently, it was reported that Si nutrition decreases ABA levels via suppressing ABA biosynthesis genes in barley shoots under combined osmotic stress and K deficiency or osmotic stress and S deficiency (Hosseini *et al.*, 2017; Maillard *et al.*, 2018). However, again no evidence was found regarding how Si interferes with ABA.

Apart from ABA, SA and JA are known to play important roles in plant responses to drought stress (Singh and Usha, 2003; Seo *et al.*, 2011; de Ollas *et al.*, 2015; 2013). It was reported that concentrations of SA increased in leaves of *Phillyrea angustifolia L*. in response to water-limiting conditions (Munne-Bosch and Penuelas, 2003), and JA levels increased in leaves and

roots of rice under drought or salt stress (Moons *et al.*, 1997; Kiribuchi *et al.*, 2005). Recently, few studies attempted to explain the complex network and interaction between ABA, JA and SA, and their signaling pathways under drought condition (Yasuda *et al.*, 2008; Muñoz-Espinoza *et al.*, 2015). For instance, it was observed that drought stress induced an early and transient accumulation of JA and SA in roots and leaves of tomato before ABA biosynthesis became induced (Muñoz-Espinoza *et al.*, 2015). Other studies in citrus and wheat suggested a cross-talk between JA and ABA. They showed that JA accumulation under drought stress is needed to increase ABA levels, but not vice versa, and both hormones are required for priming-induced drought tolerance (de Ollas *et al.*, 2013; Wang *et al.*, 2020). However, an antagonistic interaction between SA, ABA and JA was also reported in rapeseed, in which exogenous SA treatment suppressed the accumulation of ABA and JA under drought stress (Lee *et al.*, 2019).

In this study, concentrations of SA in leaves of well-watered plants were low, while application of 750 and 1000 mg Si increased SA levels by 50 and 100%, respectively, which is in the similar range of Si treatments that suppressed the accumulation of different ABA forms in leaves of control plants (Figure 36A-E). By contrast, drought stress slightly decreased SA concentrations in leaves, which were hardly affected by any dose of Si supply. This result points to an antagonistic interaction between SA and ABA depending on Si supply under sufficient water condition, whereas such a behavior was not observed in drought-stressed plants, in which Si was unable to affect SA levels. In leaves of well-watered plants, concentrations of JA were low, and they decreased even further as soon as Si was applied (Figure 36F). Under drought stress, leaf concentrations of JA were also low and hardly altered by up to 750 mg Si, while application of 1000 mg dramatically increased JA levels. Interestingly, in control plants, JA and ABA showed similar responses to Si treatments, whereas under drought stress these two hormones had an antagonistic behavior in response to 1000 mg Si supply (Figure 36A-D). In a previous finding, Si application alleviated the adverse effect of PEG-induced osmotic stress in soybean via decreased SA and JA concentrations in leaves (Hamayun *et al.*, 2010). This apparent discrepancy emphasizes the need to investigate such hormone cross-talk in a time- and concentration-dependent manner of the stress-inducing or -relieving factors.

Besides ABA, SA and JA, further phytohormones are involved in stress-related signaling under drought conditions. To date, little is known about the meaning of changes of endogenous IAA levels in drought-stressed cereal crops and the experimental evidence collected so far remains controversial. For example, decreased IAA concentrations was observed in leaves of rice plants as a consequence of suppressed expression of auxin biosynthesis-related genes after 2-3 days of drought stress (Du *et al.*, 2013). In maize, IAA levels decreased in shoots but increased in roots in response to short-term drought condition (Xin *et al.*, 1997). Transgenic tobacco ectopically expressing auxin biosynthesis genes showed higher drought tolerance in comparison to wild-type plants (Pustovoitova *et al.*, 2000). In the present study, concentrations of IAA in leaves of well-watered plants were high and hardly affected by Si (Figure 37A). Drought stress also did not change leaf IAA levels, whereas increasing Si supply slightly decreased auxin concentrations down to a 2.5-fold lower level. This suggests that auxin accumulation in leaves decreased when shoot growth was promoted by Si, irrespective

of drought stress (Figure 33C; 37). An increase in root growth or root-to-shoot ratio is part of a plant's adaptation to water shortage (Verslues *et al.*, 2006). Although in this study root dry weights and root auxin levels could not be measured, this decline in shoot IAA concentration may reflect a consequence of Si-promoted auxin translocation from shoots to roots, improving water uptake and root biomass formation. This conclusion is supported by a study in barley, where Si alleviated combined osmotic and S deficiency stress, which was accompanied by enhanced auxin accumulation and biomass in roots and lower IAA levels in shoots (Maillard *et al.*, 2018).

There is also increasing evidence that cytokinins play an important role in the regulation of plant responses to osmotic or drought stress through intensive interactions and cross-talk with ABA (HavlovA *et al.*, 2008; Nishiyama *et al.*, 2011; Wang *et al.*, 2011). For example, many ABA-mediated physiological processes induced by water deficit, including stomata closure and acceleration of leaf senescence, are counteracted by cytokinins (Stoll *et al.*, 2000; Pospisilova, 2005). Hence, prolonged drought stress was reported to be associated with downregulation of active cytokinin contents (Kudoyarova *et al.*, 2007; Albacete *et al.*, 2008; Ghanem *et al.*, 2008). In this study, concentrations of zeatin in leaves of well-watered plants were high and hardly altered by Si treatments (Figure 37B). Under drought stress leaf zeatin levels were slightly lower and remained stable up to the 750 mg Si dose, but increased by 60% when plants supplied with the highest Si level. Interestingly, application of this highest Si dose also suppressed all ABA forms under drought condition down to the same level as in well-watered plants (Figure 36A-D), suggesting that declining ABA levels coincided with increasing zeatin concentrations when drought tolerance was induced by Si. Although it has remained unclear here how Si nutrition interferes with ABA and cytokinins biosynthesis or degradation under drought stress, in a recent study in barley, Si nutrition delayed osmotic stress-induced leaf senescence via restored cytokinins and decreased ABA levels through suppression of ABA biosynthesis genes in shoots (Hosseini *et al.*, 2017). Here, leaf concentrations of cZ and cZR decreased with Si supplementations in the opposite direction to zeatin (Figure 37D, E). Thus, drought-stressed plants tended to slow down the conversion of zeatin to cZ and cZR, which may also represent a biochemical process by which Si induces drought tolerance.

Gibberellins constitute another class of phytohormones that is involved in adaptive responses to drought stress. There is a range of studies demonstrating that reduced sensitivity to gibberellins may induce a greater tolerance to water stress. For instance, wheat mutants *Rht8*, *Rht-1b* and *Rht-D1b*, with reduced gibberellins sensitivity, were more tolerant to drought stress compared to their respective wild-type plants (Landjeva *et al.*, 2008; Alghabari *et al.*, 2014; 2016). Likewise, GA_3 levels in maize and wheat were described to decrease during drought conditions (Wang *et al.*, 2008; Coelho Filho *et al.*, 2013). Recent investigations revealed a cross-talk between ABA and gibberellins under water-limiting conditions, in which ABA biosynthesis and the control of stomatal conductance were regulated by the soluble receptor for gibberellins, GIBBERELLIN-INSENSITIVE DWARF 1 (GID1). The *gid1* rice mutant, which is impaired in gibberellins signaling, showed lower levels of ABA and higher stomatal conductance in comparison to wild-type plants under drought stress (Du *et al.*, 2015). In the present study, leaf concentrations of GA_{53} responded most consistently to Si applications

under well-watered and drought conditions (Figure 37F). Gibberellin$_{44}$ levels increased in leaves by Si under both treatments (Figure 37G), while GA_{19} levels declined with increasing Si application in control plants (Figure 37H). In the early 13-hydroxylation pathway of gibberellins biosynthesis, GA_{53}, GA_{44} and GA_{19} are converted in this order through GA_{20} into the bioactive forms GA_1 and GA_3 (Hedden and Sponsel, 2015). Accumulation of GA_{44} in response to Si supplementation under drought stress suggests that Si nutrition directly or indirectly suppresses the production of bioactive gibberellins forms in barley. Although GA_1 and GA_3 could not been detected in this study, these results are in line with previous findings that showed decreasing GA_3 levels were associated with increasing drought tolerance in wheat and maize plants (Wang *et al.*, 2008; Coelho Filho *et al.*, 2013). Also, higher doses of Si reduced GA_1 levels and alleviated drought stress in leaves of soybean (Hamayun *et al.*, 2010). These reports and the present results argue in favour of Si leading to lower levels of bioactive gibberellins forms that appear to be beneficial for plants in acquiring drought tolerance. Taken together, the present analysis indicates that Si strongly interferes with phytohormone homeostasis by shifting the abundance from growth-suppressing hormones towards the growth-promoting ones as a dominant part of Si-mediated mitigation of drought stress.

6 Conclusion

Despite previous reports showing that Si application can increase tolerance to K deficiency or drought stress, the underlying mechanisms have remained unclear. The present study provides physiological and molecular evidence, that Si nutrition in the first few days after K starvation temporary delayed the stress responses by an earlier and enhanced internal K re-mobilization and a subsequent stronger *de novo* uptake through low- and high-affinity K transporters and channels in roots, which was accompanied by an increased K root-to-shoot translocation. In contrast, under long-term low K stress, Si suppressed most high- and low-affinity K transporters genes, but enhanced preferential K provision of the shoot, allowing there to maintain K-dependent metabolic processes, suppression of stress and overall higher plant biomass. Likewise, Si nutrition mediated drought tolerance and increased shoot biomass by suppressing ABA accumulation and reconstituting homeostasis of growth-promoting hormones without affecting ion imbalances in leaves. The observed prevention of growth retardation may point to a general mode of action of Si under low K and drought stress, which may rely on an improved internal availability of limiting resources for the sake of improved photosynthesis and biomass gain primarily in the shoot.

7 References

Achard, P., Gong, F., Cheminant, S., Alioua, M., Hedden, P. and Genschik, P. (2008) The cold-inducible CBF1 factor–dependent signaling pathway modulates the accumulation of the growth-repressing DELLA proteins via its effect on gibberellin metabolism. *The Plant Cell*, **20**, 2117–2129.

Adriano, D.C. (2001) Arsenic. In *Trace elements in terrestrial environments*. Springer, pp. 219–261.

Ahkami, A.H., Lischewski, S., Haensch, K.-T., et al. (2009) Molecular physiology of adventitious root formation in *Petunia hybrida* cuttings: involvement of wound response and primary metabolism. *New Phytologist*, **181**, 613–625.

Ahmad, I. and Maathuis, F.J. (2014) Cellular and tissue distribution of potassium: physiological relevance, mechanisms and regulation. *Journal of Plant Physiology*, **171**, 708–714.

Ahmad, I., Mian, A. and Maathuis, F.J. (2016) Overexpression of the rice AKT1 potassium channel affects potassium nutrition and rice drought tolerance. *Journal of Experimental Botany*, **67**, 2689–2698.

Ahmad, M., El-Saeid, M.H., Akram, M.A., Ahmad, H.R., Haroon, H. and Hussain, A. (2016) Silicon fertilization–A tool to boost up drought tolerance in wheat (*Triticum aestivum L.*) crop for better yield. *Journal of Plant Nutrition*, **39**, 1283–1291.

Ahmad, R., Zaheer, S.H. and Ismail, S. (1992) Role of silicon in salt tolerance of wheat (*Triticum aestivum L.*). *Plant Science*, **85**, 43–50.

Ahmed, M., Hassen, F.U., Qadeer, U. and Aslam, M.A. (2011) Silicon application and drought tolerance mechanism of sorghum. *African Journal of Agricultural Research*, **6**, 594–607.

Albacete, A., Ghanem, M.E., Martínez-Andújar, C., Acosta, M., Sánchez-Bravo, J., Martínez, V., Lutts, S., Dodd, I.C. and Pérez-Alfocea, F. (2008) Hormonal changes in relation to biomass partitioning and shoot growth impairment in salinized tomato (*Solanum lycopersicum L.*) plants. *Journal of Experimental Botany*, **59**, 4119–4131.

Alcázar, R., Altabella, T., Marco, F., Bortolotti, C., Reymond, M., Koncz, C., Carrasco, P. and Tiburcio, A.F. (2010) Polyamines: molecules with regulatory functions in plant abiotic stress tolerance. *Planta*, **231**, 1237–1249.

Alghabari, F., Ihsan, M.Z., Khaliq, A., Hussain, S., Daur, I., Fahad, S. and Nasim, W. (2016) Gibberellin-sensitive Rht alleles confer tolerance to heat and drought stresses in wheat at booting stage. *Journal of Cereal Science*, **70**, 72–78.

Alghabari, F., Lukac, M., Jones, H.E. and Gooding, M.J. (2014) Effect of Rht Alleles on the Tolerance of Wheat Grain Set to High Temperature and Drought Stress During Booting and Anthesis. *Journal of Agronomy and Crop Science*, **200**, 36–45.

Ali, N., Schwarzenberg, A., Yvin, J.-C. and Hosseini, S.A. (2018) Regulatory role of silicon in mediating differential stress tolerance responses in two contrasting tomato genotypes under osmotic stress. *Frontiers in Plant Science*, **9**, 1475.

Amtmann, A. and Sanders, D. (1998) Mechanisms of Na^+ uptake by plant cells. In *Advances in Botanical Research*. Elsevier, pp. 75–112.

Amtmann, A., Troufflard, S. and Armengaud, P. (2008) The effect of potassium nutrition on pest and disease resistance in plants. *Physiologia Plantarum*, **133**, 682–691.

Anders, S. and Huber, W. (2010) Differential expression analysis for sequence count data. *Nature Precedings*, 1–1.

Armengaud, P., Breitling, R. and Amtmann, A. (2004) The potassium-dependent transcriptome of *Arabidopsis* reveals a prominent role of jasmonic acid in nutrient signaling. *Plant Physiology*, **136**, 2556–2576.

Armengaud, P., Sulpice, R., Miller, A.J., Stitt, M., Amtmann, A. and Gibon, Y. (2009) Multilevel analysis of primary metabolism provides new insights into the role of potassium nutrition for glycolysis and nitrogen assimilation in *Arabidopsis* roots. *Plant Physiology*, **150**, 772–785.

Arnon, D.I. and Stout, P.R. (1939) The essentiality of certain elements in minute quantity for plants with special reference to copper. *Plant Physiology*, **14**, 371.

Aroca, R., Porcel, R. and Ruiz-Lozano, J.M. (2012) Regulation of root water uptake under abiotic stress conditions. *Journal of Experimental Botany*, **63**, 43–57.

Ashley, M.K., Grant, M. and Grabov, A. (2006) Plant responses to potassium deficiencies: a role for potassium transport proteins. *Journal of Experimental Botany*, **57**, 425–436.

Ashraf, M., Afzal, M., Ahmed, R., Mujeeb, F., Sarwar, A. and Ali, L. (2010) Alleviation of detrimental effects of NaCl by silicon nutrition in salt-sensitive and salt-tolerant genotypes of sugarcane (*Saccharum officinarum L.*). *Plant and Soil*, **326**, 381–391.

Barber, S.A., Mackay, A.D., Kuchenbuch, R.O. and Barraclough, P.B. (1988) Effects of soil temperature and water on maize root growth. *Plant and Soil*, **111**, 267–269.

Barragán, V., Leidi, E.O., Andrés, Z., Rubio, L., De Luca, A., Fernández, J.A., Cubero, B. and Pardo, J.M. (2012) Ion exchangers NHX1 and NHX2 mediate active potassium uptake into vacuoles to regulate cell turgor and stomatal function in *Arabidopsis*. *The Plant Cell*, **24**, 1127–1142.

Barry, C.S. and Giovannoni, J.J. (2007) Ethylene and fruit ripening. *Journal of Plant Growth Regulation*, **26**, 143–159.

Bélanger, R.R., Benhamou, N. and Menzies, J.G. (2003) Cytological evidence of an active role of silicon in wheat resistance to powdery mildew (*Blumeria graminis f. sp. tritici*). *Phytopathology*, **93**, 402–412.

Bergmann, W. (1992) Nutritional Disorders of Plants. *New York*: Gustav Fischer Verlag,741.

Bharwana, S.A., Ali, S., Farooq, M.A., Iqbal, N., Abbas, F. and Ahmad, M.S.A. (2013) Alleviation of lead toxicity by silicon is related to elevated photosynthesis, antioxidant enzymes suppressed lead uptake and oxidative stress in cotton. *Journal of Bioremediation and Biodegradation*, **4**.

Blumwald, E. (2000) Sodium transport and salt tolerance in plants. *Current Opinion in Cell Biology*, **12**, 431–434.

Boscari, A., Clement, M., Volkov, V., Golldack, D., Hybiak, J., Miller, A.J., Amtmann, A. and Fricke, W. (2009) Potassium channels in barley: cloning, functional characterization and expression analyses in relation to leaf growth and development. *Plant, Cell & Environment*, **32**, 1761–1777.

Bota, J., Medrano, H. and Flexas, J. (2004) Is photosynthesis limited by decreased Rubisco activity and RuBP content under progressive water stress? *New phytologist*, **162**, 671–681.

Boursiac, Y., Léran, S., Corratgé-Faillie, C., Gojon, A., Krouk, G. and Lacombe, B. (2013) ABA transport and transporters. *Trends in Plant Science*, **18**, 325–333.

Bustin, S.A., Benes, V., Garson, J.A., et al. (2009) The MIQE Guidelines: Minimum Information for Publication of Quantitative Real-Time PCR Experiments, *Oxford University Press*.

Cakmak, I. (1994) Activity of ascorbate-dependent H_2O_2-scavenging enzymes and leaf chlorosis are enhanced in magnesium- and potassium-deficient leaves, but not in phosphorus-deficient leaves. *Journal of Experimental Botany*, **45**, 1259–1266.

Cakmak, I. (2005) The role of potassium in alleviating detrimental effects of abiotic stresses in plants. *Journal of Plant Nutrition and Soil Science*, **168**, 521–530.

Cao, B., Wang, L., Gao, S., Xia, J. and Xu, K. (2017) Silicon-mediated changes in radial hydraulic conductivity and cell wall stability are involved in silicon-induced drought resistance in tomato. *Protoplasma*, **254**, 2295–2304.

Chandra, A. and Bhatt, R.K. (1998) Biochemical and physiological response to salicylic acid in relation to the systemic acquired resistance. *Photosynthetica*, **35**, 255–258.

Che, J., Yamaji, N., Shao, J.F., Ma, J.F. and Shen, R.F. (2016) Silicon decreases both uptake and root-to-shoot translocation of manganese in rice. *Journal of Experimental Botany*, **67**, 1535–1544.

Chen, D., Cao, B., Qi, L., Yin, L., Wang, S. and Deng, X. (2016a) Silicon-moderated K-deficiency-induced leaf chlorosis by decreasing putrescine accumulation in sorghum. *Annals of Botany*, **118**, 305–315.

Chen, D., Cao, B., Wang, S., Liu, P., Deng, X., Yin, L. and Zhang, S. (2016b) Silicon moderated the K deficiency by improving the plant-water status in sorghum. *Scientific Reports*, **6**, 1–14.

Chen, L., Nishizawa, T., Higashitani, A., Suge, H., Wakui, Y., Takeda, K. and Takahashi, H. (2001) A variety of wheat tolerant to deep-seeding conditions: elongation of the first internode depends on the response to gibberellin and potassium. *Plant, Cell & Environment*, **24**, 469–476.

Chen, W., Yao, X., Cai, K. and Chen, J. (2011) Silicon alleviates drought stress of rice plants by improving plant water status, photosynthesis and mineral nutrient absorption. *Biological Trace Element Research*, **142**, 67–76.

Cheong, Y.H., Pandey, G.K., Grant, J.J., Batistic, O., Li, L., Kim, B.-G., Lee, S.-C., Kudla, J. and Luan, S. (2007) Two calcineurin B-like calcium sensors, interacting with protein kinase CIPK23, regulate leaf transpiration and root potassium uptake in *Arabidopsis*. *The Plant Journal*, **52**, 223–239.

Chérel, I., Lefoulon, C., Boeglin, M. and Sentenac, H. (2014) Molecular mechanisms involved in plant adaptation to low K^+ availability. *Journal of Experimental Botany*, **65**, 833–848.

Chiba, Y., Mitani, N., Yamaji, N. and Ma, J.F. (2009) HvLsi1 is a silicon influx transporter in barley. *The Plant Journal*, **57**, 810–818.

Coelho Filho, M.A., Colebrook, E.H., Lloyd, D.P., Webster, C.P., Mooney, S.J., Phillips, A.L., Hedden, P. and Whalley, W.R. (2013) The involvement of gibberellin signalling in the effect of soil

resistance to root penetration on leaf elongation and tiller number in wheat. *Plant and Soil*, **371**, 81–94.

Colmsee, C., Beier, S., Himmelbach, A., Schmutzer, T., Stein, N., Scholz, U. and Mascher, M. (2015) BARLEX–the barley draft genome explorer. *Molecular Plant*, **8**, 964–966.

Cooke, J. and Leishman, M.R. (2016) Consistent alleviation of abiotic stress with silicon addition: a meta-analysis. *Functional Ecology*, **30**, 1340–1357.

Cornelis, J.-T., Delvaux, B., Georg, R.B., Lucas, Y., Ranger, J. and Opfergelt, S. (2011) Tracing the origin of dissolved silicon transferred from various soil-plant systems towards rivers: a review. *Biogeosciences*, **8**, 89–112.

Coskun, D., Britto, D.T., Huynh, W.Q. and Kronzucker, H.J. (2016) The role of silicon in higher plants under salinity and drought stress. *Frontiers in Plant Science*, **7**, 1072.

Coskun, D., Deshmukh, R., Sonah, H., Menzies, J.G., Reynolds, O., Ma, J.F., Kronzucker, H.J. and Bélanger, R.R. (2019) The controversies of silicon's role in plant biology. *New Phytologist*, **221**, 67–85.

Cruz de Carvalho, M.H. (2008) Drought stress and reactive oxygen species: production, scavenging and signaling. *Plant Signaling & Behavior*, **3**, 156–165.

Cubero-Font, P. and De Angeli, A. (2021) Connecting vacuolar and plasma membrane transport networks. *New Phytologist*, **229**, 755–762.

Cutler, A. and Krochko, J. (1999) Formation and breakdown of ABA. *Trends in Plant Science.* **4**, 472–478.

Datnoff, L.E., Snyder, G.H. and Korndörfer, G.H. (2001) *Silicon in Agriculture*, Elsevier.

DE LA GUARDIA, M.D. and BENLLOCH, M. (1980) Effects of potassium and gibberellic acid on stem growth of whole sunflower plants. *Physiologia Plantarum*, **49**, 443–448.

De Lucas, M., Daviere, J.-M., Rodríguez-Falcón, M., et al. (2008) A molecular framework for light and gibberellin control of cell elongation. *Nature*, **451**, 480–484.

Deeken, R., Geiger, D., Fromm, J., Koroleva, O., Ache, P., Langenfeld-Heyser, R., Sauer, N., May, S.T. and Hedrich, R. (2002) Loss of the AKT2/3 potassium channel affects sugar loading into the phloem of *Arabidopsis*. *Planta*, **216**, 334–344.

Detmann, K.C., Araújo, W.L., Martins, S.C., et al. (2012) Silicon nutrition increases grain yield, which, in turn, exerts a feed-forward stimulation of photosynthetic rates via enhanced mesophyll conductance and alters primary metabolism in rice. *New Phytologist*, **196**, 752–762.

Dietzel, M. (2002) Interaction of polysilicic and monosilicic acid with mineral surfaces. In *Water-Rock Interaction*. Springer, pp. 207–235.

Dill, A., Jung, H.-S. and Sun, T. (2001) The DELLA motif is essential for gibberellin-induced degradation of RGA. *Proceedings of the National Academy of Sciences*, **98**, 14162–14167.

Dolan, L. and Davies, J. (2004) Cell expansion in roots. *Current Opinion in Plant Biology*, **7**, 33–39.

Drerup, M.M., Schlücking, K., Hashimoto, K., Manishankar, P., Steinhorst, L., Kuchitsu, K. and Kudla, J. (2013) The calcineurin B-like calcium sensors CBL1 and CBL9 together with their interacting

protein kinase CIPK26 regulate the *Arabidopsis* NADPH oxidase RBOHF. *Molecular Plant*, **6**, 559–569.

Du, H., Chang, Y., Huang, F. and Xiong, L. (2015) GID1 modulates stomatal response and submergence tolerance involving abscisic acid and gibberellic acid signaling in rice. *Journal of Integrative Plant Biology*, **57**, 954–968.

Du, H., Liu, H. and Xiong, L. (2013) Endogenous auxin and jasmonic acid levels are differentially modulated by abiotic stresses in rice. *Frontiers in Plant Science*, **4**, 397.

Eggert, K. and Wirén, N. von (2017) Response of the plant hormone network to boron deficiency. *New Phytologist*, **216**, 868–881.

Epstein, E. (1999) Silicon. *Annual Review of Plant Biology*, **50**, 641–664.

Farmer, V.C., Delbos, E. and Miller, J.D. (2005) The role of phytolith formation and dissolution in controlling concentrations of silica in soil solutions and streams. *Geoderma*, **127**, 71–79.

Farooq, M., Wahid, A., Kobayashi, N., Fujita, D. and Basra, S.M.A. (2009) Plant drought stress: effects, mechanisms and management. In *Sustainable Agriculture*. Springer, pp. 153–188.

Fayez, K.A. and Bazaid, S.A. (2014) Improving drought and salinity tolerance in barley by application of salicylic acid and potassium nitrate. *Journal of the Saudi Society of Agricultural Sciences*, **13**, 45–55.

Feng Shao, J., Che, J., Yamaji, N., Fang Shen, R. and Feng Ma, J. (2017) Silicon reduces cadmium accumulation by suppressing expression of transporter genes involved in cadmium uptake and translocation in rice. *Journal of Experimental Botany*, **68**, 5641–5651.

Feng, X., Liu, W., Qiu, C.-W., Zeng, F., Wang, Y., Zhang, G., Chen, Z.-H. and Wu, F. (2020) HvAKT2 and HvHAK1 confer drought tolerance in barley through enhanced leaf mesophyll H^+ homoeostasis. *Plant Biotechnology Journal*, **18**, 1683–1696.

Flam-Shepherd, R., Huynh, W.Q., Coskun, D., Hamam, A.M., Britto, D.T. and Kronzucker, H.J. (2018) Membrane fluxes, bypass flows, and sodium stress in rice: the influence of silicon. *Journal of Experimental Botany*, **69**, 1679–1692.

Fleck, A.T., Nye, T., Repenning, C., Stahl, F., Zahn, M. and Schenk, M.K. (2011) Silicon enhances suberization and lignification in roots of rice (*Oryza sativa*). *Journal of Experimental Botany*, **62**, 2001–2011.

Fleck, A.T., Schulze, S., Hinrichs, M., Specht, A., Waßmann, F., Schreiber, L. and Schenk, M.K. (2015) Silicon promotes exodermal casparian band formation in Si-accumulating and Si-excluding species by forming phenol complexes. *PLoS One*, **10**, e0138555.

Flowers, T.J., Troke, P.F. and Yeo, A.R. (1977) The mechanism of salt tolerance in halophytes. *Annual Review of Plant Physiology*, **28**, 89–121.

Foster, K.J. and Miklavcic, S.J. (2014) On the competitive uptake and transport of ions through differentiated root tissues. *Journal of Theoretical Biology*, **340**, 1–10.

Fulgenzi, F.R., Peralta, M.L., Mangano, S., Danna, C.H., Vallejo, A.J., Puigdomenech, P. and Santa-María, G.E. (2008) The ionic environment controls the contribution of the barley HvHAK1 transporter to potassium acquisition. *Plant Physiology*, **147**, 252–262.

Gambale, F. and Uozumi, N. (2006) Properties of shaker-type potassium channels in higher plants. *The Journal of Membrane Biology*, **210**, 1–19.

Gan, S. (2003) Mitotic and postmitotic senescence in plants. *Science of Aging Knowledge Environment*, **2003**, 7.

Gaymard, F., Pilot, G., Lacombe, B., Bouchez, D., Bruneau, D., Boucherez, J., Michaux-Ferriere, N., Thibaud, J.-B. and Sentenac, H. (1998) Identification and disruption of a plant shaker-like outward channel involved in K^+ release into the xylem sap. *Cell*, **94**, 647–655.

Ghaffari, M.R., Shahinnia, F., Usadel, B., Junker, B., Schreiber, F., Sreenivasulu, N. and Hajirezaei, M.R. (2016) The metabolic signature of biomass formation in barley. *Plant and Cell Physiology*, **57**, 1943–1960.

Ghanem, M.E., Albacete, A., Martínez-Andújar, C., Acosta, M., Romero-Aranda, R., Dodd, I.C., Lutts, S. and Pérez-Alfocea, F. (2008) Hormonal changes during salinity-induced leaf senescence in tomato (*Solanum lycopersicum L.*). *Journal of Experimental Botany*, **59**, 3039–3050.

Gierth, M. and Mäser, P. (2007) Potassium transporters in plants–involvement in K^+ acquisition, redistribution and homeostasis. *FEBS Letters*, **581**, 2348–2356.

Gobert, A., Isayenkov, S., Voelker, C., Czempinski, K. and Maathuis, F.J. (2007) The two-pore channel TPK1 gene encodes the vacuolar K^+ conductance and plays a role in K^+ homeostasis. *Proceedings of the National Academy of Sciences*, **104**, 10726–10731.

Gong, H. and Chen, K. (2012) The regulatory role of silicon on water relations, photosynthetic gas exchange, and carboxylation activities of wheat leaves in field drought conditions. *Acta Physiologiae Plantarum*, **34**, 1589–1594.

Gong, H.J., Randall, D.P. and Flowers, T.J. (2006) Silicon deposition in the root reduces sodium uptake in rice (*Oryza sativa L.*) seedlings by reducing bypass flow. *Plant, Cell & Environment*, **29**, 1970–1979.

Greenway, H. and Munns, R. (1980) Mechanisms of salt tolerance in nonhalophytes. *Annual Review of Plant Physiology*, **31**, 149–190.

Gruszka, D., Janeczko, A., Dziurka, M., Pociecha, E., Oklestkova, J. and Szarejko, I. (2016) Barley brassinosteroid mutants provide an insight into phytohormonal homeostasis in plant reaction to drought stress. *Frontiers in Plant Science*, **7**, 1824.

Gunes, A., Inal, A., Bagci, E.G., Coban, S. and Sahin, O. (2007) Silicon increases boron tolerance and reduces oxidative damage of wheat grown in soil with excess boron. *Biologia Plantarum*, **51**, 571–574.

Gunes, A., Pilbeam, D.J., Inal, A. and Coban, S. (2008) Influence of silicon on sunflower cultivars under drought stress, I: Growth, antioxidant mechanisms, and lipid peroxidation. *Communications in Soil Science and Plant Analysis*, **39**, 1885–1903.

Guntzer, F., Keller, C. and Meunier, J.-D. (2012) Benefits of plant silicon for crops: a review. *Agronomy for Sustainable Development*, **32**, 201–213.

Guntzer, F., Keller, C. and Meunier, J.D. (2010) Determination of the silicon concentration in plant material using Tiron extraction. *New Phytologist*, **188**, 902–906.

Guo, W., Zhang, J., Teng, M. and Wang, L.H. (2009) Arsenic uptake is suppressed in a rice mutant defective in silicon uptake. *Journal of Plant Nutrition and Soil Science*, **172**, 867–874.

Guruprasad, A. and Guruprasad, K.N. (1988) Interaction of potassium ions and gibberellin in the control of hypocotyl growth in *Amaranthus caudatus*. *Physiologia Plantarum*, **74**, 154–158.

Ha, S., Vankova, R., Yamaguchi-Shinozaki, K., Shinozaki, K. and Tran, L.-S.P. (2012) Cytokinins: metabolism and function in plant adaptation to environmental stresses. *Trends in Plant Science*, **17**, 172–179.

Haddad, C., Arkoun, M., Jamois, F., Schwarzenberg, A., Yvin, J.-C., Etienne, P. and Laîné, P. (2018) Silicon promotes growth of *Brassica napus L.* and delays leaf senescence induced by nitrogen starvation. *Frontiers in Plant Science*, **9**, 516.

Haeder, H.E. and Beringer, H. (1981) Influence of potassium nutrition and water stress on the content of abscisic acid in grains and flag leaves of wheat during grain development. *Journal of the Science of Food and Agriculture*, **32**, 552–556.

Haghighi, M., Da Silva, J.T., Mozafarian, M. and Afifipour, Z. (2013) Can Si and nano-Si alleviate the effect of drought stress induced by PEG in seed germination and seedling growth of tomato. *Minerva Biotecnologica*, **25**, 17–22.

Hajirezaei, M.-R., Takahata, Y., Trethewey, R.N., Willmitzer, L. and Sonnewald, U. (2000) Impact of elevated cytosolic and apoplastic invertase activity on carbon metabolism during potato tuber development. *Journal of Experimental Botany*, **51**, 439–445.

Hamayun, M., Sohn, E.-Y., Khan, S.A., Shinwari, Z.K., Khan, A.L. and Lee, I.-J. (2010) Silicon alleviates the adverse effects of salinity and drought stress on growth and endogenous plant growth hormones of soybean (*Glycine max L.*). *Pakistan Journal of Botany*, **42**, 1713–1722.

Hansen, H.B., Wetche, T.P., Raulund-Rasmussen, K. and Borggaard, O.K. (1994) Stability constants for silicate adsorbed to ferrihydrite. *Clay Minerals*, **29**, 341–350.

Hashemi, A., Abdolzadeh, A. and Sadeghipour, H.R. (2010) Beneficial effects of silicon nutrition in alleviating salinity stress in hydroponically grown canola, *Brassica napus L.*, plants. *Soil Science & Plant Nutrition*, **56**, 244–253.

Hattori, T., Inanaga, S., Araki, H., An, P., Morita, S., Luxová, M. and Lux, A. (2005) Application of silicon enhanced drought tolerance in Sorghum bicolor. *Physiologia Plantarum*, **123**, 459–466.

HavlovA, M., Dobrev, P.I., Motyka, Vac., ŠTORCHOVÁ, H., LIBUS, J., DobrA, J., MALBECK, J., GaudinovA, A. and VankovA, R. (2008) The role of cytokinins in responses to water deficit in tobacco plants over-expressing trans-zeatin O-glucosyltransferase gene under 35S or SAG12 promoters. *Plant, Cell & Environment*, **31**, 341–353.

Hedden, P. and Sponsel, V. (2015) A century of gibberellin research. *Journal of Plant Growth Regulation*, **34**, 740–760.

Heyl, A., Werner, T. and Schmülling, T. (2006) Cytokinin metabolism and signal transduction. *Plant Hormone Signaling*, 93–123.

Hirsch, R.E., Lewis, B.D., Spalding, E.P. and Sussman, M.R. (1998) A role for the AKT1 potassium channel in plant nutrition. *Science*, **280**, 918–921.

Hosseini, S.A., Hajirezaei, M.R., Seiler, C., Sreenivasulu, N. and Wirén, N. von (2016) A potential role of flag leaf potassium in conferring tolerance to drought-induced leaf senescence in barley. *Frontiers in Plant Science*, **7**, 206.

Hosseini, S.A., Maillard, A., Hajirezaei, M.R., Ali, N., Schwarzenberg, A., Jamois, F. and Yvin, J.-C. (2017) Induction of Barley Silicon Transporter HvLsi1 and HvLsi2, increased silicon concentration in the shoot and regulated Starch and ABA Homeostasis under Osmotic stress and Concomitant Potassium Deficiency. *Frontiers in Plant Science*, **8**, 1359.

Hosseini, S.A., Naseri Rad, S., Ali, N. and Yvin, J.-C. (2019) The Ameliorative Effect of Silicon on Maize Plants Grown in Mg-Deficient Conditions. *International Journal of Molecular Sciences*, **20**, 969.

Hsiao, T.C. and Lauchli, A. (1986) Role of potassium in plant-water relations. *Advances in Plant Nutrition (USA)*.

Hwang, S.-J., Hamayun, M., Kim, H.-Y., Na, C.-I., Kim, K.-U., Shin, D.-H., Kim, S.-Y. and Lee, I.-J. (2007) Effect of nitrogen and silicon nutrition on bioactive gibberellin and growth of rice under field conditions. *Journal of Crop Science and Biotechnology*, **10**, 281–286.

Inal, A., Pilbeam, D.J. and Gunes, A. (2009) Silicon increases tolerance to boron toxicity and reduces oxidative damage in barley. *Journal of Plant Nutrition*, **32**, 112–128.

Jákli, B., Tavakol, E., Tränkner, M., Senbayram, M. and Dittert, K. (2017) Quantitative limitations to photosynthesis in K deficient sunflower and their implications on water-use efficiency. *Journal of Plant Physiology*, **209**, 20–30.

Jayakannan, M., Bose, J., Babourina, O., Shabala, S., Massart, A., Poschenrieder, C. and Rengel, Z. (2015) The NPR1-dependent salicylic acid signalling pathway is pivotal for enhanced salt and oxidative stress tolerance in *Arabidopsis*. *Journal of Experimental Botany*, **66**, 1865–1875.

Jordan-Meille, L. and Pellerin, S. (2004) Leaf area establishment of a maize (*Zea mays L.*) field crop under potassium deficiency. *Plant and Soil*, **265**, 75–92.

Jordan-Meille, L. and Pellerin, S. (2008) Shoot and root growth of hydroponic maize (*Zea mays L.*) as influenced by K deficiency. *Plant and Soil*, **304**, 157–168.

Jung, J.-Y., Shin, R. and Schachtman, D.P. (2009) Ethylene mediates response and tolerance to potassium deprivation in *Arabidopsis*. *The Plant Cell*, **21**, 607–621.

Kanai, S., Moghaieb, R.E., El-Shemy, H.A., Panigrahi, R., Mohapatra, P.K., Ito, J., Nguyen, N.T., Saneoka, H. and Fujita, K. (2011) Potassium deficiency affects water status and photosynthetic rate of the vegetative sink in green house tomato prior to its effects on source activity. *Plant Science*, **180**, 368–374.

Kanai, S., Ohkura, K., Adu-Gyamfi, J.J., Mohapatra, P.K., Nguyen, N.T., Saneoka, H. and Fujita, K. (2007) Depression of sink activity precedes the inhibition of biomass production in tomato plants subjected to potassium deficiency stress. *Journal of Experimental Botany*, **58**, 2917–2928.

Kant, S., Kafkafi, U., Pasricha, N. and Bansal, S. (2002) Potassium and abiotic stresses in plants. *Potassium for sustainable crop production. Potash Institute of India, Gurgaon*, **233**, 251.

Kaya, C., Tuna, L. and Higgs, D. (2006) Effect of silicon on plant growth and mineral nutrition of maize grown under water-stress conditions. *Journal of Plant Nutrition*, **29**, 1469–1480.

Kende, H. and Lang, A. (1964) Gibberellins and light inhibition of stem growth in peas. *Plant Physiology*, **39**, 435.

Kessler, A. and Baldwin, I.T. (2002) Plant responses to insect herbivory: the emerging molecular analysis. *Annual Review of Plant Biology*, **53**, 299–328.

Kidd, P.S., Llugany, M., Poschenrieder, C.H., Gunse, B. and Barcelo, J. (2001) The role of root exudates in aluminium resistance and silicon-induced amelioration of aluminium toxicity in three varieties of maize (*Zea mays L.*). *Journal of Experimental Botany*, **52**, 1339–1352.

Kim, M.J., Ciani, S. and Schachtman, D.P. (2010) A peroxidase contributes to ROS production during *Arabidopsis* root response to potassium deficiency. *Molecular Plant*, **3**, 420–427.

Kim, M.J., Shin, R. and Schachtman, D.P. (2009) A nuclear factor regulates abscisic acid responses in *Arabidopsis*. *Plant Physiology*, **151**, 1433–1445.

Kim, Y.H., Khan, A.L., Waqas, M., Shim, J.K., Kim, D.H., Lee, K.Y. and Lee, I.J. (2014) Silicon application to rice root zone influenced the phytohormonal and antioxidant responses under salinity stress. *Journal of Plant Growth Regulation*, **33**, 137–149.

Kiribuchi, K., Jikumaru, Y., Kaku, H., et al. (2005) Involvement of the basic helix-loop-helix transcription factor RERJ1 in wounding and drought stress responses in rice plants. *Bioscience, Biotechnology, and Biochemistry*, **69**, 1042–1044.

Knight, C.T. and Kinrade, S.D. (2001) A primer on the aqueous chemistry of silicon. In *Studies in Plant Science*. Elsevier, pp. 57–84.

Kochian, L.V. and Lucas, W.J. (1983) Potassium transport in corn roots: II. The significance of the root periphery. *Plant Physiology*, **73**, 208–215.

Kostic, L., Nikolic, N., Bosnic, D., Samardzic, J. and Nikolic, M. (2017) Silicon increases phosphorus (P) uptake by wheat under low P acid soil conditions. *Plant and Soil*, **419**, 447–455.

Krishnamurthy, P., Ranathunge, K., Nayak, S., Schreiber, L. and Mathew, M.K. (2011) Root apoplastic barriers block Na^+ transport to shoots in rice (*Oryza sativa L.*). *Journal of Experimental Botany*, **62**, 4215–4228.

Kudoyarova, G.R., Vysotskaya, L.B., Cherkozyanova, A. and Dodd, I.C. (2007) Effect of partial rootzone drying on the concentration of zeatin-type cytokinins in tomato (*Solanum lycopersicum L.*) xylem sap and leaves. *Journal of Experimental Botany*, **58**, 161–168.

Kunkel, B.N. and Brooks, D.M. (2002) Cross talk between signaling pathways in pathogen defense. *Current Opinion in Plant Biology*, **5**, 325–331.

Kusano, T., Berberich, T., Tateda, C. and Takahashi, Y. (2008) Polyamines: essential factors for growth and survival. *Planta*, **228**, 367–381.

Lacombe, B., Pilot, G., Michard, E., Gaymard, F., Sentenac, H. and Thibaud, J.-B. (2000) A shaker-like K^+ channel with weak rectification is expressed in both source and sink phloem tissues of *Arabidopsis*. *The Plant Cell*, **12**, 837–851.

Landjeva, S., Korzun, V., Stoimenova, E., Truberg, B., Ganeva, G. and Börner, A. (2008) The contribution of the gibberellin-insensitive semi-dwarfing (Rht) genes to genetic variation in

wheat seedling growth in response to osmotic stress. *The Journal of Agricultural Science*, **146**, 275–286.

Lang, A. (1983) Turgor-regulated translocation. *Plant, Cell & Environment*, **6**, 683–689.

Lavinsky, A.O., Detmann, K.C., Reis, J.V., et al. (2016) Silicon improves rice grain yield and photosynthesis specifically when supplied during the reproductive growth stage. *Journal of Plant Physiology*, **206**, 125–132.

Lee, B.-R., Islam, M.T., Park, S.-H., Jung, H., Bae, D.-W. and Kim, T.-H. (2019) Characterization of salicylic acid-mediated modulation of the drought stress responses: Reactive oxygen species, proline, and redox state in *Brassica napus*. *Environmental and Experimental Botany*, **157**, 1–10.

Lee, S.K., Sohn, E.Y., Hamayun, M., Yoon, J.Y. and Lee, I.J. (2010) Effect of silicon on growth and salinity stress of soybean plant grown under hydroponic system. *Agroforestry Systems*, **80**, 333–340.

LEIGH, R.A. and STOREY, R. (1993) Intercellular compartmentation of ions in barley leaves in relation to potassium nutrition and salinity. *Journal of Experimental Botany*, **44**, 755–762.

Leigh, R.A. and Wyn Jones, R.G. (1984) A hypothesis relating critical potassium concentrations for growth to the distribution and functions of this ion in the plant cell. *New Phytologist*, **97**, 1–13.

Li, G., Wu, Y., Liu, G., et al. (2017) Large-scale proteomics combined with transgenic experiments demonstrates an important role of jasmonic acid in potassium deficiency response in wheat and rice. *Molecular & Cellular Proteomics*, **16**, 1889–1905.

Li, J., Wu, W.-H. and Wang, Y. (2017) Potassium channel AKT1 is involved in the auxin-mediated root growth inhibition in *Arabidopsis* response to low K^+ stress. *Journal of Integrative Plant Biology*, **59**, 895–909.

Li, P., Song, A., Li, Z., Fan, F. and Liang, Y. (2012) Silicon ameliorates manganese toxicity by regulating manganese transport and antioxidant reactions in rice (*Oryza sativa L.*). *Plant and Soil*, **354**, 407–419.

Li, W., Wang, H. and Yu, D. (2016) *Arabidopsis* WRKY transcription factors WRKY12 and WRKY13 oppositely regulate flowering under short-day conditions. *Molecular Plant*, **9**, 1492–1503.

Liang, Y. (1999) Effects of silicon on enzyme activity and sodium, potassium and calcium concentration in barley under salt stress. *Plant and Soil*, **209**, 217–224.

Liang, Y., Zhang, W., Chen, Q. and Ding, R. (2005) Effects of silicon on H^+-ATPase and H^+-PPase activity, fatty acid composition and fluidity of tonoplast vesicles from roots of salt-stressed barley (*Hordeum vulgare L.*). *Environmental and Experimental Botany*, **53**, 29–37.

Liang, Y., Zhang, W., Chen, Q., Liu, Y. and Ding, R. (2006) Effect of exogenous silicon (Si) on H^+-ATPase activity, phospholipids and fluidity of plasma membrane in leaves of salt-stressed barley (*Hordeum vulgare L.*). *Environmental and Experimental Botany*, **57**, 212–219.

Licausi, F., Ohme-Takagi, M. and Perata, P. (2013) APETALA 2/Ethylene Responsive Factor (AP 2/ERF) transcription factors: Mediators of stress responses and developmental programs. *New Phytologist*, **199**, 639–649.

Liebersbach, H., Steingrobe, B. and Claassen, N. (2004) Roots regulate ion transport in the rhizosphere to counteract reduced mobility in dry soil. *Plant and Soil*, **260**, 79–88.

Liu, P., Yin, L., Deng, X., Wang, S., Tanaka, K. and Zhang, S. (2014) Aquaporin-mediated increase in root hydraulic conductance is involved in silicon-induced improved root water uptake under osmotic stress in *Sorghum bicolor L*. *Journal of Experimental Botany*, **65**, 4747–4756.

Liu, P., Yin, L., Wang, S., Zhang, M., Deng, X., Zhang, S. and Tanaka, K. (2015) Enhanced root hydraulic conductance by aquaporin regulation accounts for silicon alleviated salt-induced osmotic stress in *Sorghum bicolor L. Environmental and Experimental Botany*, **111**, 42–51.

Llanes, A., Andrade, A., Alemano, S. and Luna, V. (2016) Alterations of endogenous hormonal levels in plants under drought and salinity. *American Journal of Plant Sciences*, **7**, 1357.

Lobato, A.K.S., Coimbra, G.K., Neto, M.A.M., et al. (2009) Protective action of silicon on water relations and photosynthetic pigments in pepper plants induced to water deficit. *Research Journal of Biological Sciences*, **4**, 617–623.

Loreto, F., Tricoli, D. and Marco, G.D. (1995) On the relationship between electron transport rate and photosynthesis in leaves of the C4 plant *Sorghum bicolor* exposed to water stress, temperature changes and carbon metabolism inhibition. *Functional Plant Biology*, **22**, 885–892.

Love, M.I., Huber, W. and Anders, S. (2014) Moderated estimation of fold change and dispersion for RNA-seq data with DESeq2. *Genome Biology*, **15**, 1–21.

Ma, D., Sun, D., Wang, C., Qin, H., Ding, H., Li, Y. and Guo, T. (2016) Silicon application alleviates drought stress in wheat through transcriptional regulation of multiple antioxidant defense pathways. *Journal of Plant Growth Regulation*, **35**, 1–10.

Ma, J.F. (2004) Role of silicon in enhancing the resistance of plants to biotic and abiotic stresses. *Soil Science and Plant Nutrition*, **50**, 11–18.

Ma, J.F., Miyake, Y. and Takahashi, E. (2001) Silicon as a beneficial element for crop plants. *Studies in Plant Science*, **8**, 17–39.

Ma, J.F. and Takahashi, E. (2002) *Soil, fertilizer, and plant silicon research in Japan*, Elsevier.

Ma, J.F. and Yamaji, N. (2015) A cooperative system of silicon transport in plants. *Trends in Plant Science*, **20**, 435–442.

Ma, J.F., Yamaji, N., Mitani, N., Xu, X.-Y., Su, Y.-H., McGrath, S.P. and Zhao, F.-J. (2008) Transporters of arsenite in rice and their role in arsenic accumulation in rice grain. *Proceedings of the National Academy of Sciences*, **105**, 9931–9935.

Ma, T.-L., Wu, W.-H. and Wang, Y. (2012) Transcriptome analysis of rice root responses to potassium deficiency. *BMC Plant Biology*, **12**, 1–13.

Maillard, A., Ali, N., Schwarzenberg, A., Jamois, F., Yvin, J.-C. and Hosseini, S.A. (2018) Silicon transcriptionally regulates sulfur and ABA metabolism and delays leaf senescence in barley under combined sulfur deficiency and osmotic stress. *Environmental and Experimental Botany*, **155**, 394–410.

Marschner, H. (2012) *Marschner's mineral nutrition of higher plants. Vol. 89*, Academic press.

Marten, I., Hoth, S., Deeken, R., Ache, P., Ketchum, K.A., Hoshi, T. and Hedrich, R. (1999) AKT3, a phloem-localized K^+ channel, is blocked by protons. *Proceedings of the National Academy of Sciences*, **96**, 7581–7586.

Mascher, M., Gundlach, H., Himmelbach, A., et al. (2017) A chromosome conformation capture ordered sequence of the barley genome. *Nature*, **544**, 427–433.

Mateo, A., Funck, D., Mühlenbock, P., Kular, B., Mullineaux, P.M. and Karpinski, S. (2006) Controlled levels of salicylic acid are required for optimal photosynthesis and redox homeostasis. *Journal of Experimental Botany*, **57**, 1795–1807.

Matoh, T., Murata, S. and Takahashi, E. (1991) Effect of silicate application on photosynthesis of rice [*Oryza sativa*] plants. *Japanese Journal of Soil Science and Plant Nutrition (Japan)*.

Mendiburu, F. de and Mendiburu, M.F. de (2019) Package 'agricolae.' *R Package, Version*, 1–2.

Mengel, K. and Arneke, W.-W. (1982) Effect of potassium on the water potential, the pressure potential, the osmotic potential and cell elongation in leaves of *Phaseolus vulgaris. Physiologia Plantarum*, **54**, 402–408.

Meyer, S. and Genty, B. (1998) Mapping Intercellular CO_2 Mole Fraction (C_i) in *Rosa rubiginosa* Leaves Fed with Abscisic Acid by Using Chlorophyll Fluorescence Imaging: Significance of C_i Estimated from Leaf Gas Exchange. *Plant Physiology*, **116**, 947–957.

Miao, B.-H., Han, X.-G. and Zhang, W.-H. (2010) The ameliorative effect of silicon on soybean seedlings grown in potassium-deficient medium. *Annals of Botany*, **105**, 967–973.

Ming, D.F., Pei, Z.F., Naeem, M.S., Gong, H.J. and Zhou, W.J. (2012) Silicon alleviates PEG-induced water-deficit stress in upland rice seedlings by enhancing osmotic adjustment. *Journal of Agronomy and Crop Science*, **198**, 14–26.

Mitani, N., Chiba, Y., Yamaji, N. and Ma, J.F. (2009) Identification and characterization of maize and barley Lsi2-like silicon efflux transporters reveals a distinct silicon uptake system from that in rice. *The Plant Cell*, **21**, 2133–2142.

Mitani-Ueno, N., Yamaji, N., Zhao, F.-J. and Ma, J.F. (2011) The aromatic/arginine selectivity filter of NIP aquaporins plays a critical role in substrate selectivity for silicon, boron, and arsenic. *Journal of Experimental Botany*, **62**, 4391–4398.

Moharekar, S.T., Lokhande, S.D., Hara, T., Tanaka, R., Tanaka, A. and Chavan, P.D. (2003) Effect of salicylic acid on chlorophyll and carotenoid contents of wheat and moong seedlings. *Photosynthetica*, **41**, 315–317.

Moons, A., Prinsen, E., Bauw, G. and Van Montagu, M. (1997) Antagonistic effects of abscisic acid and jasmonates on salt stress-inducible transcripts in rice roots. *The Plant Cell*, **9**, 2243–2259.

Munne-Bosch, S. and Penuelas, J. (2003) Photo-and antioxidative protection, and a role for salicylic acid during drought and recovery in field-grown Phillyrea angustifolia plants. *Planta*, **217**, 758–766.

Munns, R. and Tester, M. (2008) Mechanisms of salinity tolerance. *Annual Review of Plant Biology*, **59**, 651–681.

Muñoz-Espinoza, V.A., López-Climent, M.F., Casaretto, J.A. and Gómez-Cadenas, A. (2015) Water stress responses of tomato mutants impaired in hormone biosynthesis reveal abscisic acid, jasmonic acid and salicylic acid interactions. *Frontiers in Plant Science*, **6**, 997.

Nam, Y.-J., Tran, L.-S.P., Kojima, M., Sakakibara, H., Nishiyama, R. and Shin, R. (2012) Regulatory roles of cytokinins and cytokinin signaling in response to potassium deficiency in *Arabidopsis*. *PLoS One*, **7**, e47797.

Neumann, D. and Zur Nieden, U. (2001) Silicon and heavy metal tolerance of higher plants. *Phytochemistry*, **56**, 685–692.

Nieves-Cordones, M., Alemán, F., Martínez, V. and Rubio, F. (2014) K^+ uptake in plant roots. The systems involved, their regulation and parallels in other organisms. *Journal of Plant Physiology*, **171**, 688–695.

Nishiyama, R., Watanabe, Y., Fujita, Y., et al. (2011) Analysis of cytokinin mutants and regulation of cytokinin metabolic genes reveals important regulatory roles of cytokinins in drought, salt and abscisic acid responses, and abscisic acid biosynthesis. *The Plant Cell*, **23**, 2169–2183.

Niu, X., Bressan, R.A., Hasegawa, P.M. and Pardo, J.M. (1995) Ion homeostasis in NaCl stress environments. *Plant Physiology*, **109**, 735.

Ollas, C. de, Arbona, V. and GóMez-Cadenas, A. (2015) Jasmonoyl isoleucine accumulation is needed for abscisic acid build-up in roots of *Arabidopsis* under water stress conditions. *Plant, Cell & Environment*, **38**, 2157–2170.

Ollas, C. de, Hernando, B., Arbona, V. and Gómez-Cadenas, A. (2013) Jasmonic acid transient accumulation is needed for abscisic acid increase in citrus roots under drought stress conditions. *Physiologia Plantarum*, **147**, 296–306.

Pancheva, T.V., Popova, L.P. and Uzunova, A.N. (1996) Effects of salicylic acid on growth and photosynthesis in barley plants. *Journal of Plant Physiology*, **149**, 57–63.

Patro, R., Duggal, G., Love, M.I., Irizarry, R.A. and Kingsford, C. (2017) Salmon provides fast and bias-aware quantification of transcript expression. *Nature Methods*, **14**, 417–419.

Pavlovic, J., Samardzic, J., Kostic, L., Laursen, K.H., Natic, M., Timotijevic, G., Schjoerring, J.K. and Nikolic, M. (2016) Silicon enhances leaf remobilization of iron in cucumber under limited iron conditions. *Annals of Botany*, **118**, 271–280.

Pavlovic, J., Samardzic, J., Maksimović, V., et al. (2013) Silicon alleviates iron deficiency in cucumber by promoting mobilization of iron in the root apoplast. *New Phytologist*, **198**, 1096–1107.

Peel, A.J. and Rogers, S. (1982) Stimulation of sugar loading into sieve elements of willow by potassium and sodium salts. *Planta*, **154**, 94–96.

Pei, Z.F., Ming, D.F., Liu, D., Wan, G.L., Geng, X.X., Gong, H.J. and Zhou, W.J. (2010) Silicon improves the tolerance to water-deficit stress induced by polyethylene glycol in wheat (*Triticum aestivum L.*) seedlings. *Journal of Plant Growth Regulation*, **29**, 106–115.

Perrenoud, S. (1977) *Potassium and plant health*, International Potash Institute Bern.

Pettigrew, W.T. (2008) Potassium influences on yield and quality production for maize, wheat, soybean and cotton. *Physiologia Plantarum*, **133**, 670–681.

Peuke, A.D., Jeschke, W.D. and Hartung, W. (2002) Flows of elements, ions and abscisic acid in *Ricinus communis* and site of nitrate reduction under potassium limitation. *Journal of Experimental Botany*, **53**, 241–250.

Pfeiffenschneider, Y. and Beringer, H. (1989) Measurement of turgor potential in carrots of different K nutrition by using the cell pressure probe. *Methods of K-Research in Plants*, 203–217.

Pfluger, R. and Cassier, A. (1977) Influence of monovalent cations on photosynthetic CO_2 fixation. In *Fertilizer Use and Production of Carbohydrates and Lipids; Proc Colloq Int Potash Inst*.

Porra, R.J., Thompson, W.A. and Kriedemann, P.E. (1989) Determination of accurate extinction coefficients and simultaneous equations for assaying chlorophylls a and b extracted with four different solvents: verification of the concentration of chlorophyll standards by atomic absorption spectroscopy. *Biochimica et Biophysica Acta (BBA)-Bioenergetics*, **975**, 384–394.

Pospisilova, J. (2005) Role of plant regulators in stomatal limitation of photosynthesis during water stress. *Handbook of Photosynthesis*, 811–825.

Prajapati, K. and Modi, H.A. (2012) The importance of potassium in plant growth–a review. *Indian Journal of Plant Sciences*, **1**, 177–186.

Pustovoitova, T.N., Bavrina, T.V. and Zhdanova, N.E. (2000) Drought tolerance of transgenic tobacco plants carrying the *iaaM* and *iaaH* genes of auxin biosynthesis. *Russian Journal of Plant Physiology*, **47**, 380–385.

Ragel, P., Raddatz, N., Leidi, E.O., Quintero, F.J. and Pardo, J.M. (2019) Regulation of K^+ nutrition in plants. *Frontiers in Plant Science*, **10**, 281.

Rao, M.V., Paliyath, G., Ormrod, D.P., Murr, D.P. and Watkins, C.B. (1997) Influence of salicylic acid on H_2O_2 production, oxidative stress, and H_2O_2-metabolizing enzymes (salicylic acid-mediated oxidative damage requires H_2O_2). *Plant Physiology*, **115**, 137–149.

Rémus-Borel, W., Menzies, J.G. and Bélanger, R.R. (2009) Aconitate and methyl aconitate are modulated by silicon in powdery mildew-infected wheat plants. *Journal of Plant Physiology*, **166**, 1413–1422.

Restrepo-Diaz, H., Benlloch, M. and Fernández-Escobar, R. (2008) Plant water stress and K^+ starvation reduce absorption of foliar applied K^+ by olive leaves. *Scientia Horticulturae*, **116**, 409–413.

Řezanka, T. and Sigler, K. (2008) Biologically active compounds of semi-metals. In *Studies in Natural Products Chemistry*. Elsevier, pp. 835–921.

Rizza, A. and Jones, A.M. (2019) The makings of a gradient: spatiotemporal distribution of gibberellins in plant development. *Current Opinion in Plant Biology*, **47**, 9–15.

Rogalla, H. and Römheld, V. (2002) Role of leaf apoplast in silicon-mediated manganese tolerance of *Cucumis sativus L*. *Plant, Cell & Environment*, **25**, 549–555.

Rubio, F., Gassmann, W. and Schroeder, J.I. (1995) Sodium-driven potassium uptake by the plant potassium transporter HKT1 and mutations conferring salt tolerance. *Science*, **270**, 1660–1663.

Sanderson, J. (1983) Water uptake by different regions of the barley root. Pathways of radial flow in relation to development of the endodermis. *Journal of Experimental Botany*, **34**, 240–253.

Santa-María, G.E., Rubio, F., Dubcovsky, J. and Rodríguez-Navarro, A. (1997) The HAK1 gene of barley is a member of a large gene family and encodes a high-affinity potassium transporter. *The Plant Cell*, **9**, 2281–2289.

Saqib, M., Zörb, C. and Schubert, S. (2008) Silicon-mediated improvement in the salt resistance of wheat (*Triticum aestivum*) results from increased sodium exclusion and resistance to oxidative stress. *Functional Plant Biology*, **35**, 633–639.

Sauer, D., Saccone, L., Conley, D.J., Herrmann, L. and Sommer, M. (2006) Review of methodologies for extracting plant-available and amorphous Si from soils and aquatic sediments. *Biogeochemistry*, **80**, 89–108.

Schröppel-Meier, G. and Kaiser, W.M. (1988) Ion homeostasis in chloroplasts under salinity and mineral deficiency: I. Solute concentrations in leaves and chloroplasts from spinach plants under NaCl or $NaNO_3$ salinity. *Plant Physiology*, **87**, 822–827.

Seiler, C., Harshavardhan, V.T., Rajesh, K., Reddy, P.S., Strickert, M., Rolletschek, H., Scholz, U., Wobus, U. and Sreenivasulu, N. (2011) ABA biosynthesis and degradation contributing to ABA homeostasis during barley seed development under control and terminal drought-stress conditions. *Journal of Experimental Botany*, **62**, 2615–2632.

Seiler, C., Harshavardhan, V.T., Reddy, P.S., et al. (2014) Abscisic acid flux alterations result in differential abscisic acid signaling responses and impact assimilation efficiency in barley under terminal drought stress. *Plant Physiology*, **164**, 1677–1696.

Seki, M., Umezawa, T., Urano, K. and Shinozaki, K. (2007) Regulatory metabolic networks in drought stress responses. *Current Opinion in Plant Biology*, **10**, 296–302.

Seo, J.-S., Joo, J., Kim, M.-J., et al. (2011) OsbHLH148, a basic helix-loop-helix protein, interacts with OsJAZ proteins in a jasmonate signaling pathway leading to drought tolerance in rice. *The Plant Journal*, **65**, 907–921.

Shabbir, R.N., Waraich, E.A., Ali, H., et al. (2016) Supplemental exogenous NPK application alters biochemical processes to improve yield and drought tolerance in wheat (*Triticum aestivum L.*). *Environmental Science and Pollution Research*, **23**, 2651–2662.

Shakirova, F.M., Sakhabutdinova, A.R., Bezrukova, M.V., Fatkhutdinova, R.A. and Fatkhutdinova, D.R. (2003) Changes in the hormonal status of wheat seedlings induced by salicylic acid and salinity. *Plant Science*, **164**, 317–322.

Shi, X., Zhang, C., Wang, H. and Zhang, F. (2005) Effect of Si on the distribution of Cd in rice seedlings. *Plant and Soil*, **272**, 53–60.

Shi, Y., Zhang, Y., Han, W., Feng, R., Hu, Y., Guo, J. and Gong, H. (2016) Silicon enhances water stress tolerance by improving root hydraulic conductance in *Solanum lycopersicum L. Frontiers in Plant Science*, **7**, 196.

Shi, Y., Zhang, Y., Yao, H., Wu, J., Sun, H. and Gong, H. (2014) Silicon improves seed germination and alleviates oxidative stress of bud seedlings in tomato under water deficit stress. *Plant Physiology and Biochemistry*, **78**, 27–36.

Shin, R. and Schachtman, D.P. (2004) Hydrogen peroxide mediates plant root cell response to nutrient deprivation. *Proceedings of the National Academy of Sciences*, **101**, 8827–8832.

Silverstone, A.L., Ciampaglio, C.N. and Sun, T. (1998) The *Arabidopsis* RGA gene encodes a transcriptional regulator repressing the gibberellin signal transduction pathway. *The Plant Cell*, **10**, 155–169.

Šimura, J., Antoniadi, I., Široká, J., Tarkowská, D., Strnad, M., Ljung, K. and Novák, O. (2018) Plant hormonomics: Multiple phytohormone profiling by targeted metabolomics. *Plant Physiology*, **177**, 476–489.

Singh, B. and Usha, K. (2003) Salicylic acid induced physiological and biochemical changes in wheat seedlings under water stress. *Plant Growth Regulation*, **39**, 137–141.

Song, A., Li, P., Li, Z., Fan, F., Nikolic, M. and Liang, Y. (2011) The alleviation of zinc toxicity by silicon is related to zinc transport and antioxidative reactions in rice. *Plant and Soil*, **344**, 319–333.

Song, W., Liu, S., Meng, L., et al. (2015) Potassium deficiency inhibits lateral root development in tobacco seedlings by changing auxin distribution. *Plant and Soil*, **396**, 163–173.

Sonobe, K., Hattori, T., An, P., Tsuji, W., Eneji, A.E., Kobayashi, S., Kawamura, Y., Tanaka, K. and Inanaga, S. (2010) Effect of silicon application on sorghum root responses to water stress. *Journal of Plant Nutrition*, **34**, 71–82.

Sonobe, K., Hattori, T., An, P., Tsuji, W., Eneji, E., Tanaka, K. and Inanaga, S. (2009) Diurnal variations in photosynthesis, stomatal conductance and leaf water relation in sorghum grown with or without silicon under water stress. *Journal of Plant Nutrition*, **32**, 433–442.

Sreenivasulu, N., Sopory, S.K. and Kishor, P.K. (2007) Deciphering the regulatory mechanisms of abiotic stress tolerance in plants by genomic approaches. *Gene*, **388**, 1–13.

Stoll, M., Loveys, B. and Dry, P. (2000) Hormonal changes induced by partial rootzone drying of irrigated grapevine. *Journal of Experimental Botany*, **51**, 1627–1634.

Takahashi, E., Ma, J.F. and Miyake, Y. (1990) The possibility of silicon as an essential element for higher plants. *Comments on Agricultural and Food Chemistry*, **2**, 99–102.

Tang, R.-J., Zhao, F.-G., Yang, Y., Wang, C., Li, K., Kleist, T.J., Lemaux, P.G. and Luan, S. (2020) A calcium signalling network activates vacuolar K^+ remobilization to enable plant adaptation to low-K environments. *Nature Plants*, **6**, 384–393.

Tang, X., Gomes, A.M., Bhatia, A. and Woodson, W.R. (1994) Pistil-specific and ethylene-regulated expression of 1-aminocyclopropane-1-carboxylate oxidase genes in Petunia flowers. *The Plant Cell*, **6**, 1227–1239.

Tripathi, P., Tripathi, R.D., Singh, R.P., Dwivedi, S., Goutam, D., Shri, M., Trivedi, P.K. and Chakrabarty, D. (2013) Silicon mediates arsenic tolerance in rice (*Oryza sativa L.*) through lowering of arsenic uptake and improved antioxidant defence system. *Ecological Engineering*, **52**, 96–103.

Turner, N.C., Wright, G.C. and Siddique, K.H.M. (2001) Adaptation of grain legumes (pulses) to water-limited environments, 193-231.

Vandegeer, R.K., Zhao, C., Cibils-Stewart, X., Wuhrer, R., Hall, C.R., Hartley, S.E., Tissue, D.T. and Johnson, S.N. (2020) Silicon deposition on guard cells increases stomatal sensitivity as mediated by K^+ efflux and consequently reduces stomatal conductance. *Physiologia Plantarum*.

Vandesompele, J., De Preter, K., Pattyn, F., Poppe, B., Van Roy, N., De Paepe, A. and Speleman, F. (2002) Accurate normalization of real-time quantitative RT-PCR data by geometric averaging of multiple internal control genes. *Genome Biology*, **3**, research0034-1.

Verslues, P.E., Agarwal, M., Katiyar-Agarwal, S., Zhu, J. and Zhu, J.-K. (2006) Methods and concepts in quantifying resistance to drought, salt and freezing, abiotic stresses that affect plant water status. *The Plant Journal*, **45**, 523–539.

Voelker, C., Schmidt, D., Mueller-Roeber, B. and Czempinski, K. (2006) Members of the *Arabidopsis* AtTPK/KCO family form homomeric vacuolar channels in planta. *The Plant Journal*, **48**, 296–306.

Voisin, A.-S., Reidy, B., Parent, B., Rolland, G., Redondo, E., Gerentes, D., Tardieu, F. and Muller, B. (2006) Are ABA, ethylene or their interaction involved in the response of leaf growth to soil water deficit? An analysis using naturally occurring variation or genetic transformation of ABA production in maize. *Plant, Cell & Environment*, **29**, 1829–1840.

Walker, D.J., Leigh, R.A. and Miller, A.J. (1996) Potassium homeostasis in vacuolate plant cells. *Proceedings of the National Academy of Sciences*, **93**, 10510–10514.

Wang, C., Yang, A., Yin, H. and Zhang, J. (2008) Influence of water stress on endogenous hormone contents and cell damage of maize seedlings. *Journal of Integrative Plant Biology*, **50**, 427–434.

Wang, M., Zheng, Q., Shen, Q. and Guo, S. (2013) The critical role of potassium in plant stress response. *International Journal of Molecular Sciences*, **14**, 7370–7390.

Wang, T.-B., Gassmann, W., Rubio, F., Schroeder, J.I. and Glass, A.D. (1998) Rapid up-regulation of HKT1, a high-affinity potassium transporter gene, in roots of barley and wheat following withdrawal of potassium. *Plant Physiology*, **118**, 651–659.

Wang, X., Li, Q., Xie, J., Huang, M., Cai, J., Zhou, Q., Dai, T. and Jiang, D. (2020) Abscisic acid and jasmonic acid are involved in drought priming-induced tolerance to drought in wheat. *The Crop Journal*.

Wang, Y., Li, B., Du, M., Eneji, A.E., Wang, B., Duan, L., Li, Z. and Tian, X. (2012) Mechanism of phytohormone involvement in feedback regulation of cotton leaf senescence induced by potassium deficiency. *Journal of Experimental Botany*, **63**, 5887–5901.

Wang, Y., Li, L., Ye, T., Zhao, S., Liu, Z., Feng, Y.-Q. and Wu, Y. (2011) Cytokinin antagonizes ABA suppression to seed germination of *Arabidopsis* by downregulating ABI5 expression. *The Plant Journal*, **68**, 249–261.

Wang, Y., Stass, A. and Horst, W.J. (2004) Apoplastic binding of aluminum is involved in silicon-induced amelioration of aluminum toxicity in maize. *Plant Physiology*, **136**, 3762–3770.

Wang, Y. and Wu, W.-H. (2013) Potassium transport and signaling in higher plants. *Annual Review of Plant Biology*, **64**, 451–476.

Weast, R.C., Astle, M.J. and Beyer, W.H. (1983) CRC handbook of chemistry and physics. Florida. *CRC Press*, **198041981**, F4445.

Wei, J., Li, C., Li, Y., Jiang, G., Cheng, G. and Zheng, Y. (2013) Effects of external potassium (K) supply on drought tolerances of two contrasting winter wheat cultivars. *Plos One*, **8**, e69737.

Williams, L.J. and Abdi, H. (2010) Fisher's least significant difference (LSD) test. *Encyclopedia of Research Design*, **218**, 840–853.

Wong, Y.C., Heits, A. and Ville, J.D. (1972) Foliar symptoms of silicon deficiency in the sugarcane plant. *Proceedings, XXI Congress // International Society of Sugar Cane Technologists*, **14**, 766–776.

Wu, J., Geilfus, C.-M., Pitann, B. and Mühling, K.-H. (2016) Silicon-enhanced oxalate exudation contributes to alleviation of cadmium toxicity in wheat. *Environmental and Experimental Botany*, **131**, 10–18.

Wu, X., Yu, Y., Baerson, S.R., Song, Y., Liang, G., Ding, C., Niu, J., Pan, Z. and Zeng, R. (2017) Interactions between nitrogen and silicon in rice and their effects on resistance toward the brown planthopper *Nilaparvata lugens*. *Frontiers in Plant Science*, **8**, 28.

Xin, Z., Zhou, X. and Pilet, P.-E. (1997) Level changes of jasmonic, abscisic, and indole-3yl-acetic acids in maize under desiccation stress. *Journal of Plant Physiology*, **151**, 120–124.

Xu, L., Islam, F., Ali, B., Pei, Z., Li, J., Ghani, M.A. and Zhou, W. (2017) Silicon and water-deficit stress differentially modulate physiology and ultrastructure in wheat (*Triticum aestivum L.*). *3 Biotech*, **7**, 273.

Yamaji, N. and Ma, J.F. (2011) Further characterization of a rice silicon efflux transporter, Lsi2. *Soil Science and Plant Nutrition*, **57**, 259–264.

Yamaji, N. and Ma, J.F. (2007) Spatial distribution and temporal variation of the rice silicon transporter Lsi1. *Plant Physiology*, **143**, 1306–1313.

Yamaji, N., Sakurai, G., Mitani-Ueno, N. and Ma, J.F. (2015) Orchestration of three transporters and distinct vascular structures in node for intervascular transfer of silicon in rice. *Proceedings of the National Academy of Sciences*, **112**, 11401–11406.

Yasuda, M., Ishikawa, A., Jikumaru, Y., et al. (2008) Antagonistic interaction between systemic acquired resistance and the abscisic acid–mediated abiotic stress response in *Arabidopsis*. *The Plant Cell*, **20**, 1678–1692.

Yeo, A. (1998) Molecular biology of salt tolerance in the context of whole-plant physiology. *Journal of Experimental Botany*, **49**, 915–929.

Yin, L., Wang, S., Liu, P., Wang, W., Cao, D., Deng, X. and Zhang, S. (2014) Silicon-mediated changes in polyamine and 1-aminocyclopropane-1-carboxylic acid are involved in silicon-induced drought resistance in *Sorghum bicolor L*. *Plant Physiology and Biochemistry*, **80**, 268–277.

Yin, L., Wang, S., Tanaka, K., Fujihara, S., Itai, A., Den, X. and Zhang, S. (2016) Silicon-mediated changes in polyamines participate in silicon-induced salt tolerance in *Sorghum bicolor L*. *Plant, Cell & Environment*, **39**, 245–258.

Yoshida, S. (1965) Chemical aspects of the role of silicon in physiology of the rice plant. *Bull. Nat. Inst. Agr. Sci.*, **15**, 18–58.

Zeng, J., Quan, X., He, X., Cai, S., Ye, Z., Chen, G. and Zhang, G. (2018) Root and leaf metabolite profiles analysis reveals the adaptive strategies to low potassium stress in barley. *BMC Plant Biology*, **18**, 1–13.

ZHAO, X., YU, H., Jing, W.E.N., WANG, X., Qi, D.U., Jing, W. and Qiao, W. (2016) Response of root morphology, physiology and endogenous hormones in maize (*Zea mays L.*) to potassium deficiency. *Journal of Integrative Agriculture*, **15**, 785–794.

Zhu, Y. and Gong, H. (2014) Beneficial effects of silicon on salt and drought tolerance in plants. *Agronomy for Sustainable Development*, **34**, 455–472.

8 Annex

Table 1. List of primers used in the present study.

Gene	Forward primer	Reverse primer	Accession no.
HvLsi1	5'-TAGAGCGGTTGGTGAGTTGG-3'	5'-CCAGGAAGTAGAGCCAGAGG-3'	AB447482
HvLsi2	5'-GCTCTCCGTCATCATCCTCC-3'	5'-CCACCTCGTTCCCCATCAG-3'	AB447483
HvLsi6	5'-GCAGGGTTAGCAGTTGGTT-3'	5'-CGAAGCGGATGTAGGTGTAG-3'	AB447484
HvAKT1	5'-TGCTTCGTCTATGGCGTCTC-3'	5'-CGTTTCTTGTGGGTTCGGG-3'	DQ465922
HvAKT2	5'-CGACTCCAGATACAGGTGCT-3'	5'-GAAGAAGGTGAGGGCGATGT-3'	DQ465923
HvHAK1	5'-GTCCTCTCGCTCATCCTCT-3'	5'-CCACCATCTCCATTGTCGT-3'	AF025292
HvHAK4	5'-CCATTTGCTCTGTATTCGCTCC-3'	5'-TAACTCCTCATCCGCTGCTT-3'	DQ465924
HvSKOR	5'-CATGGCGACTGTTGGTTATG-3'	5'-TAAGCGCAGTCATGTTACCG-3'	HORVU7Hr1G040990.4
HvKCO1	5'-GCTTGTGTGTTCGTCTTCACA-3'	5'-TCCTGCTTCTCCACGAGATAA-3'	EU926490
HvCYC	5'-CTGTCGTGTCGTCGGTCTAA-3'	5'-CCAGCAGCCTAAAGAGTCCA-3'	AK253120
HvUBI	5'-CCAAGATCCAGGACAAGGAG-3'	5'-CGTCTTCTTCTTGCGCTTCT-3'	M60175.1

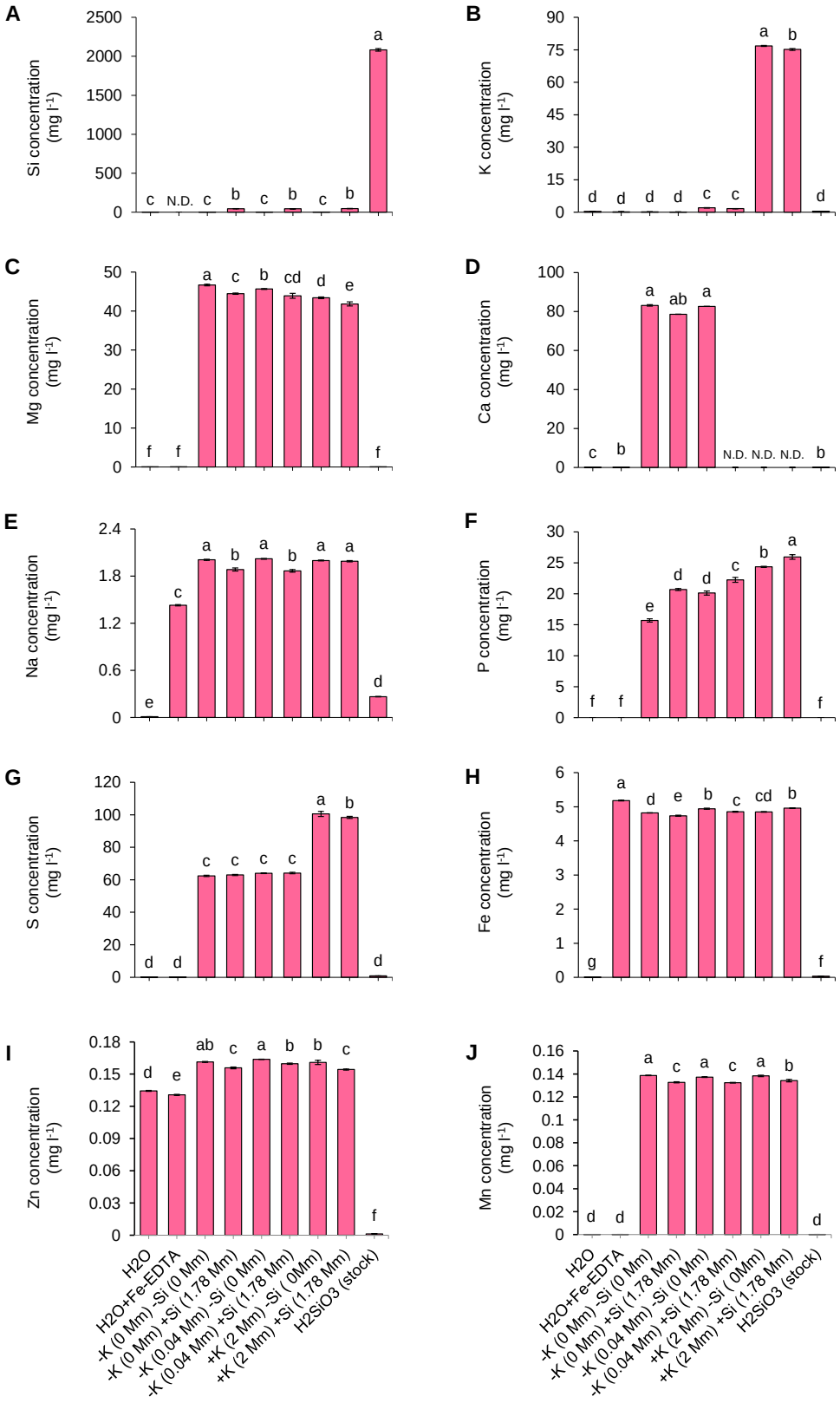

Figure 1. Concentration of macro- and micronutrients in water, water with iron, Hoagland solutions and stock solution of monosilicic acid H_2SiO_3. (A-J) Concentrations of silicon (Si; A), potassium (K; B), magnesium (Mg; C), calcium (Ca; D), sodium (Na; E), phosphorus (P; F), sulfur (S; G), iron (Fe; H), zinc (Zn; I), and manganese (Mn; J) in water (H_2O); water and iron (H_2O+Fe_EDTA); Hoagland solution without K, low K 0.04 Mm, or adequate K 2 mM, in the absence or presence of 1.78 mM Si; and stock solution of monosilicic acid H_2SiO_3. Bars indicate means ± SE. Different letters denote significant differences among solutions according to LSD test ($p < 0.05$; $n = 3$).

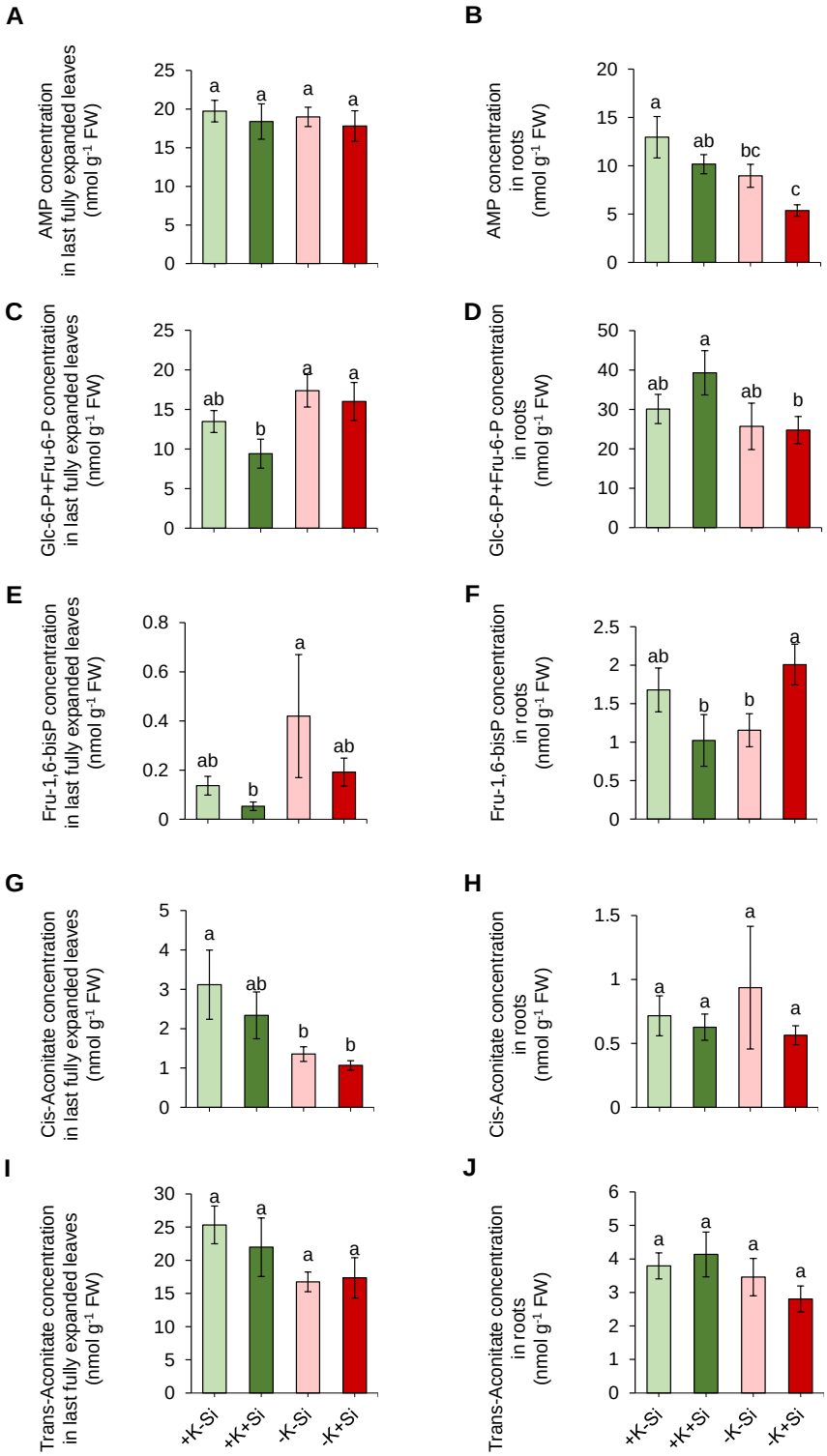

Figure 2. Influence of Si supply on concentrations of primary metabolites in leaves and roots of barley plants grown under adequate or low K supply. (A-J) Concentrations of adenosine monophosphate (AMP; A, B), glucose 6-phosphate+fructose 6-phosphate (Glc-6-P+Fru-6-P; C, D), fructose-1,6-bisphosphate (Fru-1,6-bisP; E, F), cis-aconitic acid (Cis-Aconitate; G, H), and trans-aconitic acid (Trans-Aconitate; I, J) in leaves (A, C, E, G, I) or in roots (B, D, F, H, J). After 7 days of germination, plants were grown under either adequate (2 mM) or low (0.04 mM) K for 24 days in the absence or presence of 1.78 mM Si. Leaf analysis is based on the last fully expanded leaf. Bars indicate means ± SE. Different letters denote significant differences among treatments according to LSD test ($p < 0.05$; $n = 8$).

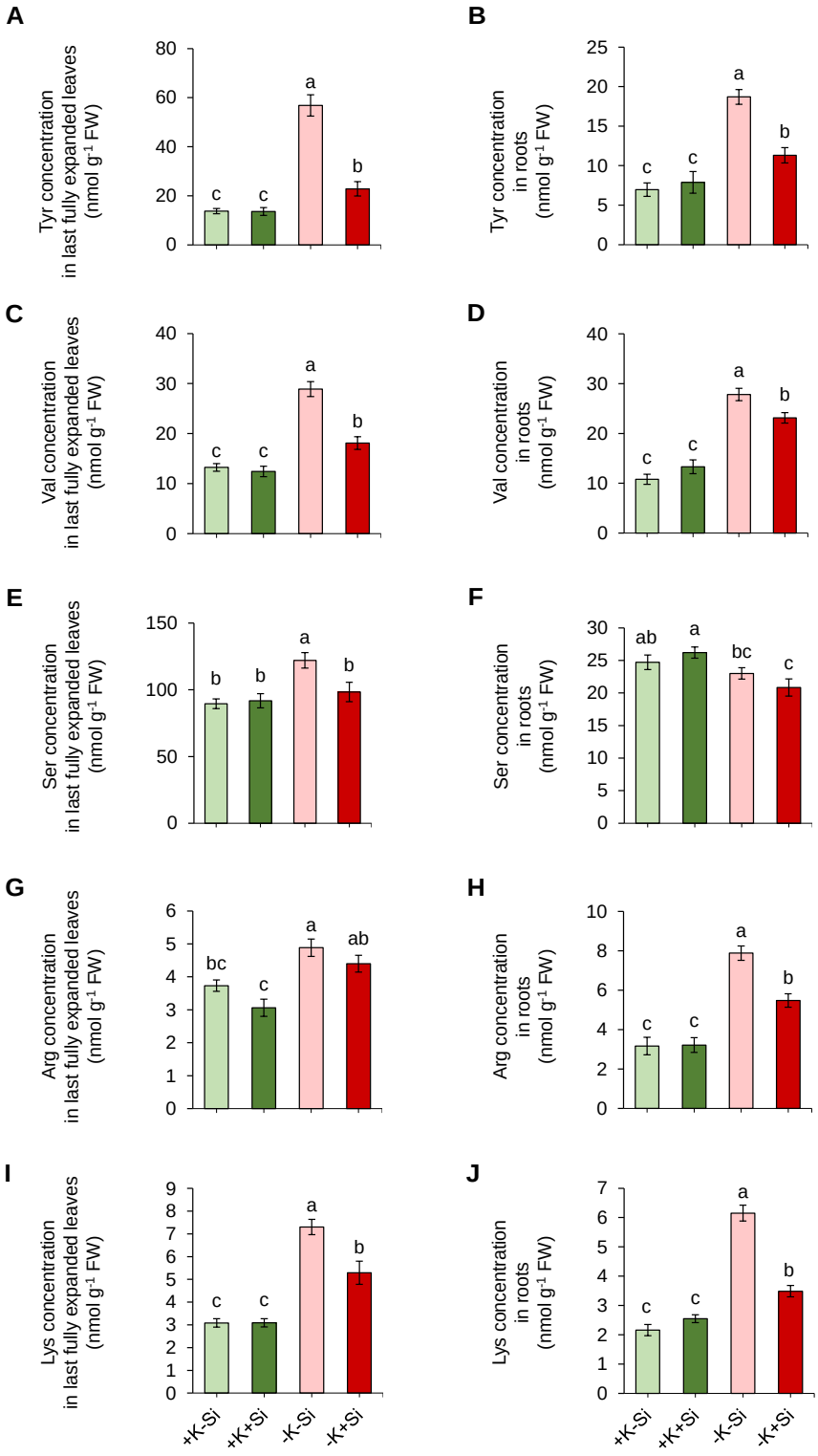

Figure 3. Influence of Si supply on concentrations of amino acids in leaves and roots of barley plants grown under adequate or low K supply. (A-J) Concentrations of tyrosine (Tyr; A, B), valine (Val; C, D), serine (Ser; E, F), arginine (Arg; G, H), and lysine (Lys; I, J) in leaves (A, C, E, G, I) or in roots (B, D, F, H, J). After 7 days of germination, plants were grown under either adequate (2 mM) or low (0.04 mM) K for 24 days in the absence or presence of 1.78 mM Si. Leaf analysis is based on the last fully expanded leaf. Bars indicate means ± SE. Different letters denote significant differences among treatments according to LSD test ($p < 0.05$; $n = 8$).

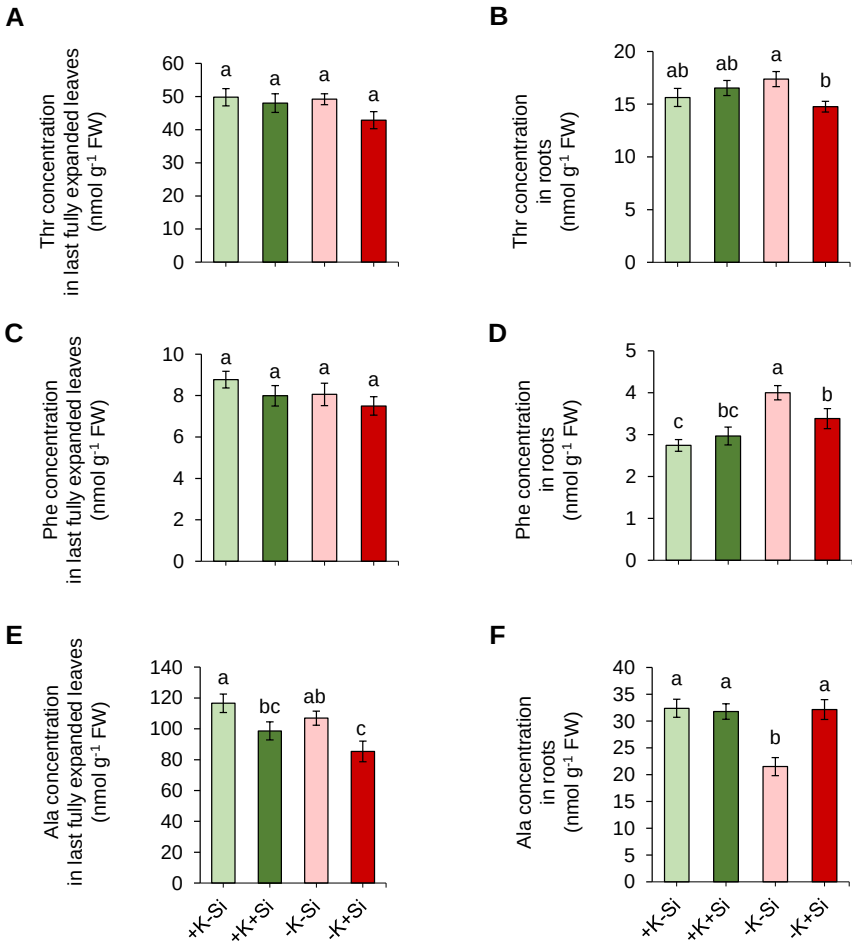

Figure 4. Influence of Si supply on concentrations of amino acids in leaves and roots of barley plants grown under adequate or low K supply. (A-F) Concentrations of threonine (Thr; A, B), phenylalanine (Phe; C, D), and alanine (Ala; E, F) in leaves (A, C, E) or in roots (B, D, F). After 7 days of germination, plants were grown under either adequate (2 mM) or low (0.04 mM) K for 24 days in the absence or presence of 1.78 mM Si. Leaf analysis is based on the last fully expanded leaf. Bars indicate means ± SE. Different letters denote significant differences among treatments according to LSD test ($p < 0.05$; $n = 8$).

9 Abbreviations

Abbreviation	Full name
3PGA	3-phosphoglycerate
ABA	Abscisic acid
ABAGlc	Aba-glucose ester
ACC	1-aminocyclopropane-1-carboxylic acid
ADP	Adenosine diphosphate
Al	Aluminum
Ala	Alanine
AMP	Adenosine monophosphate
Arg	Arginine
As	Arsenic
B	Boron
BP	Biological process
C	Carbon
Ca	Calcium
CC	Cellular component
Cd	Cadmium
CK	Cytokinin
Cl	Chloride
CNGC	Cyclic nucleotide gated channels
cZR	Cis-zeatin riboside
DPA	Dehydro-phaseic acid
DW	Dry weight
Fe	Iron
Fru	Fructose
Fru-1,6-bisP	Fructose-1,6-bisphosphate
FW	Fresh weight
GA	Gibberellin
GABA	Gamma-aminobutyric-acid
GID1	Gibberellin-insensitive dwarf 1
Glc	Glucose
Glc-6-P	Glucose-1-phosphate
Glc-6-P+Fru-6-P	Glucose 6-phosphate+fructose 6-phosphate
GlcA	Glucuronic acid
Gly	Glycine
IAA	Indole-3-acetic acid
IAAMe	Indole-3-acetic acid methyl ester
Ile	Isoleucine
IPR	Adenine riboside
JA	Jasmonic acid
JA-Ile	Ja-isoleucine
K	Potassium
Leu	Leucine

Abbreviation	Full name
Lys	Lysine
MF	Molecular function
Mg	Magnesium
Mn	Manganese
MRM	Multiple reactions monitoring
N	Nitrogen
NA	Nicotianamine
Na	Sodium
NCBI	National center for biotechnology information
oxIAA	2-oxindole-3-acetic acid
P	Phosphorus
PA	Phaseic acid
Pb	Lead
PCA	Principal component analysis
PEG	Poly ethylene glycol
Phe	Phenylalanine
PIP	Plasma-membrane intrinsic protein
PM	Plasmodesmata
Pro	Proline
Rb	Rubidium
ROS	Reactive oxygen species
RuBisCO	Ribulose-1,5-bisphosphat-carboxylase/-oxygenase
RWC	Relative water content
S	Sulfur
SA	Salicylic acid
Ser	Serine
Si	Silicon
Suc	Sucrose
Suc-6-P	Sucrose-6-phosphate
TCA	Tricarboxylic acid
Thr	Threonine
Tre-6-P	Trehalose-6-phosphate
TW	Turgid weight
Tyr	Tyrosine
tZ	Trans-zeatin
tZR	Trans-zeatin riboside
UDP	Uridine diphosphate
UDP-Glc	Uridine diphosphate glucose
UMP	Uridine monophosphate
Val	Valine
Zn	Zinc

10 Acknowledgements

I would like to express my deepest appreciation, first and foremost, to my supervisor, Prof. Dr. Nicolaus von Wirén, head of department of Physiology and Cell Biology at IPK, for providing me the opportunity to carry out my PhD in molecular plant nutrition group, and his immense knowledge, continuous support, patience and plentiful experience that encouraged me in all the aspects of my scientific career.
I would also like to give very special thanks to Dr. Seyed Abdollah Hosseini, project manager at Groupe Roullier company in France, who introduced me to Prof. Dr. Nicolaus von Wirén, and not only scientifically and continuously mentored the project but also kindly helped me to start a new life in Germany. Additionally, I would like to express gratitude to Dr. Jean-Claude Yvin, former research director of plant nutrition lab at Groupe Roullier company, who financially supported this project.
I am humbly grateful for the scientific and technical support that I received during my PhD from all the members in the Molecular Plant Nutrition (MPE) group at IPK, without whom I would not have been able to complete this research, especially Dr. Nara C. Marella for bioinformatic analysis, Dr. Yudelsy Antonia Tandron Moya and Barbara Kettig for element and hormone analysis, Dr. Mohammad Reza Hajirezaei for metabolite measurements and other colleagues: Vanessa Paffrath, Elis Fraust, Heike Nierig, Bijal Thakkar, Dagmar Boehmert, Nicole Schaefer, Elmarie Fischer, Dr. Suresh Tula, Annett Bieber, Melanie Ruff, Dr. Anja Hartmann, Dr. Ricardo Giehl, Dr. Kai Eggert and Jacqueline Fuge. I would also like to especially thank Dr. Britt Leps in International Office at IPK who very kindly and continuously helped me during my wonderful life in Germany.
Finally, I would like to extend my gratitude to my beloved parents and my sweet little sister, who always inspire me to have dreams and encourage me to fight for them. Also, my dear aunt and uncle, Mahnaz and Wolfgang, who kindly supported me to start my life in Germany. Last but not least, to love of my life, Sebastian, who guided me so positively and always made me feel confident in my abilities. Without his tremendous understanding and support in the past few years, it would be impossible for me to complete my study.
Thank you all!

Seyedeh Sara Beier

11 Publications related to the submitted thesis

Manuscripts under revision:

- Beier, S., Hosseini, S. A., Marella, N. C., Yvin, J.-C., von Wirén, N. Silicon nutrition improves the internal utilization efficiency of potassium by enhanced depletion and shoot allocation of root potassium pools.

- Beier, S., Hosseini, S. A., Yvin, J.-C., von Wirén, N. (2021). Impact of silicon nutrition on barley plants under drought stress.

12 Curriculum Vitae

12.1 Personal details

First Name	Seyedeh Sara
Last Name	Beier (Maiden name: Naseri Rad)
Nationality	Iranian

12.2 Educational backgrounds and working experiences

PhD
2016-2021

University: Martin Luther University, Halle, Germany.

- PhD thesis was performed at the Leibniz-Institute for Plant Genetics and Crop Plant Research (IPK) – Germany
- Major: Biology
- Thesis title: Impact of silicon nutrition on barley plants under potassium deficiency or drought stress: Insight into transcriptional, hormonal and metabolic regulation.
- Supervisor: Prof. Dr. Nicolaus von Wirén

Research Collaboration
2011-2016

Institute: Agricultural Biotechnology Research Institute of Iran (ABRII) – Iran

Project contributions:

- Screening phenotype-genotype correlations in two Iranian rice cultivars under drought stress
- Comparison of different gene identification programs in bread wheat
- Application of membrane separation technology in downstream processing of Bacillus thuringiensis biopesticide

Master of Science
2009-2011

University: University of Tehran – Iran

- Major: Agricultural Science-Biotechnology
- Thesis title: Identification and characterization of key genes in artemisinin production in Iranian Artemisia annua

Research Internship
2008-2009

Institute: Agricultural Biotechnology Research Institute of Iran (ABRII) – Iran

Project contributions:

- Detection of genetic diversity among citrus plants using amplified fragment length polymorphisms (AFLP) analysis

Bachelor of Science
2004-2008

University: Azad University of Karaj – Iran

- Major: Agricultural Science-Plant Breeding

12.3 Peer-reviewed publications

2020
- Soleimani, B., Lehnert, H., Keilwagen, J., Plieske, J., Ordon, F., Naseri Rad, S., Ganal, M., Beier, S. & Perovic, D. (2020). Comparison between core set selection methods using different Illumina marker platforms: a case study of assessment of diversity in wheat. Frontiers in Plant Science, 11, 1040.

2019
- Hosseini, S. A., Naseri Rad, S., Ali, N., & Yvin, J. C. (2019). The Ameliorative Effect of Silicon on Maize Plants Grown in Mg-Deficient Conditions. International journal of molecular sciences, 20(4), 969.

2016
- Naseri Rad, S., A Shirazi, M. M., Kargari, A., & Marzban, R. (2016). Application of membrane separation technology in downstream processing of Bacillus thuringiensis biopesticide: A review. Journal of Membrane Science and Research, 2(2), 66-77.

2013
- Nasiri, J., Naghavi, M., Naseri Rad, S., Yolmeh, T., Shirazi, M., Naderi, R., ... & Ahmadi, S. (2013). Gene identification programs in bread wheat: a comparison study. Nucleosides, Nucleotides and Nucleic Acids, 32(10), 529-554.

12.4 Conference contributions

2019
- Plant Science Student Conference (PSSC), Gatersleben, IPK, Germany; (Oral presentation). Naseri Rad, Sara; Hosseini, Seyed A.; Yvin, Jean-Claude.; von Wirén N. Impact of Silicon nutrition on plants under drought stress.

2018
- 2nd Global Conference on Plant Science & Molecular Biology, Rome, Italy; (Poster presentation). Naseri Rad, Sara; Hosseini, Seyed A.; Yvin, Jean-Claude.; von Wirén N. Effect of Silicon nutrition on Barley plants under potassium stress; Insight into transcriptional, hormonal and metabolic regulation.

2018
- Plant Science Student Conference (PSSC), Gatersleben, IPK, Germany; (Poster presentation). Naseri Rad, Sara; Hosseini, Seyed A.; Yvin, Jean-Claude.; von Wirén N. Effect of Silicon nutrition on Barley plants under potassium stress; Insight into transcriptional, hormonal and metabolic regulation.

12.5 Workshops

2019 ▪ International Spring School “Computational Biology Starter”. Leibniz-Institute for Plant Genetics and Crop Plant Research (IPK) – Germany.

2018 ▪ Practical Course in Fluorescence and Confocal Microscopy in Plant Science. Leibniz-Institute for Plant Genetics and Crop Plant Research (IPK) – Germany.

2017 ▪ Excel 01. Leibniz-Institute for Plant Genetics and Crop Plant Research (IPK) – Germany.

2017 ▪ Influence of nutrients on phytohormonal and architectural changes during adventitious root formation. Leibniz-Institute for Plant Genetics and Crop Plant Research (IPK) – Germany.

12.6 Honors and Awards

2018 ▪ Best poster award in Plant Science Student Conference (PSSC), Gatersleben, IPK, Germany. Naseri Rad, S., Hosseini, S. A., Marella, N. C., Yvin, J.-C., von Wirén, N. Effect of Silicon nutrition on Barley plants under potassium stress; Insight into transcriptional, hormonal and metabolic regulation.

2008 ▪ Ranked second among all Masters students of plant breeding in Azad University of Karaj – Iran.

13 Declaration under oath / Eidesstattliche Erklärung

I hereby declare that the submitted work has been completed by me, the undersigned, and that I have not used any other than permitted reference sources or materials or engaged any plagiarism. All the references and the other sources used in the presented work have been appropriately acknowledged in the work. I further declare that the work has not been previously submitted for the purpose of academic examination, either in its original or similar form, anywhere else.

Hiermit erkläre ich, dass ich diese Arbeit selbständig verfasst und keine anderen als die angegebenen Quellen und Hilfsmittel verwendet habe. Die den benutzten Hilfsmitteln wörtlich oder inhaltlich entnommenen Stellen habe ich unter Quellenangaben kenntlich gemacht. Die vorliegende Arbeit wurde in gleicher oder ähnlicher Form noch keiner anderen Institution oder Prüfungsbehörde vorgelegt.

_____

Seyedeh Sara Beier,

Gatersleben, Germany

14 Declaration concerning criminal record and pending investigations / Erklärung über bestehende vorstrafen und anhängige Ermittlungsverfahren

I hereby declare that I have no criminal record and that no preliminary investigations are pending against me.

Hiermit erkläre ich, dass ich weder vorbestraft bin noch, dass gegen mich Ermittlungsverfahren anhängig sind.

_____

Seyedeh Sara Beier,

Gatersleben, Germany.